

Electronic Thesis and Dissertation Repository

9-9-2015 12:00 AM

Biohydrogen Production from Cellulose by *Clostridium termitidis* and *Clostridium beijerinckii*.

Maritza Gomez-Flores
The University of Western Ontario

Supervisor
George Nakhla
The University of Western Ontario

Graduate Program in Chemical and Biochemical Engineering
A thesis submitted in partial fulfillment of the requirements for the degree in Master of
Engineering Science
© Maritza Gomez-Flores 2015

Follow this and additional works at: <https://ir.lib.uwo.ca/etd>

 Part of the [Biochemical and Biomolecular Engineering Commons](#)

Recommended Citation

Gomez-Flores, Maritza, "Biohydrogen Production from Cellulose by *Clostridium termitidis* and *Clostridium beijerinckii*." (2015). *Electronic Thesis and Dissertation Repository*. 3261.
<https://ir.lib.uwo.ca/etd/3261>

This Dissertation/Thesis is brought to you for free and open access by Scholarship@Western. It has been accepted for inclusion in Electronic Thesis and Dissertation Repository by an authorized administrator of Scholarship@Western. For more information, please contact wlsadmin@uwo.ca.

Biohydrogen Production from Cellulose by *Clostridium termitidis* and *Clostridium bejerinckii*

(Thesis format: Integrated Article)

by

Maritza Gomez-Flores

Graduate Program in Engineering Science
Department of Chemical and Biochemical Engineering

A thesis submitted in partial fulfillment
of the requirements for the degree of
Master of Engineering Science

The School of Graduate and Postdoctoral Studies
The University of Western Ontario
London, Ontario, Canada

© Maritza Gomez-Flores 2015

Abstract

The purpose of this study was to determine *Clostridium termitidis* microbial kinetics on glucose, cellobiose, and cellulose, and to assess its co-culture with *Clostridium beijerinckii* for hydrogen production. Microbial kinetics parameters of the mesophilic, cellulolytic, and hydrogen producer *C. termitidis* were determined on glucose and cellobiose using MATLAB for modelling biomass growth and substrate consumption. Hydrogen yields on these substrates were 1.99 and 1.11 mol H₂ mol⁻¹ hexose equivalent, respectively. *C. termitidis* microbial kinetics in mono-culture and in co-culture with mesophilic hydrogen producer *C. beijerinckii* were also investigated under agitated and non-agitated conditions, with hydrogen yields of 1.46 and 2.11 mol H₂ mol⁻¹ hexose equivalent_{added} for agitated mono-culture and co-culture, respectively, as compared with 1.45 and 1.92 mol H₂ mol⁻¹ hexose equivalent_{added} in unagitated cultures. Soluble metabolites were also included in the mathematical model. Moreover, co-culturing of *C. termitidis* and *C. beijerinckii* on cellulose was proven to enhance hydrogen production directly from a complex substrate like cellulose under mesophilic conditions.

Keywords

Biohydrogen production, cellulose, *Clostridium termitidis*, *Clostridium beijerinckii*, microbial kinetics, modeling.

Co-Authorship Statement

Chapter 3: Microbial kinetics of *Clostridium termitidis* on cellobiose and glucose for biohydrogen production.

Maritza Gomez-Flores, George Nakhla, Hisham Hafez

A version of this chapter has been published in *Biotechnology Letters*. 2015.

Maritza Gomez-Flores: experimental design, laboratory work, data analysis, development of the code in Matlab, modeling, and paper writing.

Dr. George Nakhla: supervision, critical and data interpretation, paper review, and corrections.

Dr. Hisham Hafez: paper review.

Chapter 4: Hydrogen production and microbial kinetics of *Clostridium termitidis* in mono-culture and co-culture with *Clostridium beijerinckii* on cellulose.

Maritza Gomez-Flores, George Nakhla, Hisham Hafez

To be submitted to *Biotechnology and Bioengineering*.

Maritza Gomez-Flores: experimental design, laboratory work, data analysis, development of the code in Matlab, modeling, and paper writing.

Dr. George Nakhla: supervision, critical and data interpretation, paper review, and corrections.

Dr. Hisham Hafez: paper review.

To my parents, Reyna and Raymundo, for their endless love and support.

To my best friend and sister, Reyna, for her everyday patience, love, care,
and lessons.

(A mis papás, Reyna y Raymundo, por su infinito amor y apoyo.

A mi mejor amiga y hermana, Reyna, por su paciencia, amor, cuidado y lecciones diarias)

Acknowledgments

I would like to begin by expressing my sincere gratitude to my supervisor, Dr. George Nakhla, for providing me the opportunity to be part of his research group, for all his support, guidance and mentorship throughout my graduate studies. I would also like to thank my co-supervisor, Dr. Hisham Hafez, for his support and helpful recommendations since the beginning of my studies.

My deepest gratitude to my advisory committee: Dr. Argyrios Margaritis for his thoughtful encouragement and support to undertake this journey, and facilitate the use of the equipment for aseptic microbiological conditions, and Dr. Dimitri Karamanev for his supportive guidance and knowledge regarding microbial kinetics and time provided for consulting.

I am very grateful to the past and current members of Dr. Nakhla's research group, specially to Medhavi Gupta and Noha Nasr, for their precious help, patience and friendship; Joseph Donohue, Kai Li, and August Wang, for their company since the start of our graduate studies; Kyriakos Manoli, for being an extraordinary classmate and friend; and Nan Yang, Chinaza Akobi, and Hyeongu Yeo, for their friendship and cheerful motivation.

I am indebted to Reyna Gomez-Flores, whose help in microbiology topics and techniques were of great benefit. I am deeply grateful to Dr. Salvador Escobedo-Salas for his help in the development of the Matlab code and to Thinesh Perantham for his advices in microbiology. Special appreciation to Dr. Ahmed Eldyasti for instructing me in the wastewater analyses and to Dr. Elsayed Elbeshbishy for his gracious encouragement and willingness to give advice at all times. I am truly thankful to Brian Dennis, Ashley Jokhu, Stephen Mallinson, Paul Sheller, and Nada Brkljac for their willingness to help and their encouragement. I am also grateful to Valerie Orr for the great experience to work together in the organization of the Graduate CBE Seminar Series. The financial support from Western Engineering, Consejo Nacional de Ciencia y Tecnologia de Mexico (CONACYT) and Alianza para la Formacion e Investigacion en Infraestructura para el Desarrollo de Mexico is gratefully acknowledged.

Particular praise is due to my parents, Reyna Flores Cuapio and Raymundo Arnulfo Gómez Herrera, who have been extremely supportive in completing this work through their invaluable love and encouragement at every stage of my life. There are not enough words to thank my sister Reyna Gomez-Flores for her teachings and support not only in research but also through all the ups and downs during this time, and most importantly for her endless love. You three were the pillars to make this possible. Also thanks to all my family, my grandmother, Petrita, my aunts, uncles, and cousins for their constant support and words of encouragement.

I wish to thank my friends in Mexico, specially to Areli Matias, Edith Aquino, Uriel Mendoza, Mildred López, Oscar Palma, and Handell Aguilar for their cheering calls, emails, and messages; and in Canada, specially to Isabela Reiniati for her sincere friendship, helpful advices and encouragement, and Sriram Vijayaraghavan for his priceless friendship.

Above all, I thank God, for making all things possible and for standing next to me in each step of this work.

Table of Contents

Abstract	ii
Co-Authorship Statement.....	iii
Acknowledgments.....	v
Table of Contents	vii
List of Tables	x
List of Figures	xii
List of Appendices	xv
Nomenclature	xvi
Abbreviations	xviii
Chapter 1	1
1 Introduction	1
1.1 Background.....	1
1.2 Problem Statement	2
1.3 Research Objectives.....	3
1.4 Thesis Organization	3
1.5 Research Contribution	4
1.6 References.....	5
Chapter 2.....	7
2 Literature Review.....	7
2.1 Introduction.....	7
2.2 Cellulose	7
2.2.1 Pure Cellulose	9
2.2.2 Lignocellulose.....	9
2.3 Hydrogen.....	13

2.3.1 Biohydrogen Production	14
2.4 Modeling Microbial Kinetics	30
2.5 Conclusions.....	33
2.6 References.....	33
Chapter 3.....	43
3 Microbial Kinetics of <i>Clostridium termitidis</i> on Cellobiose and Glucose for Biohydrogen Production	43
3.1 Introduction.....	43
3.2 Materials and Methods.....	44
3.2.1 Microbial Strain and Media	44
3.2.2 Experimental Conditions.....	45
3.2.3 Analytical Methods	45
3.2.4 Gas Measurements	45
3.2.5 Modeling.....	46
3.3 Results and Discussion	47
3.3.1 Statistical analysis	47
3.3.2 Monod Growth Kinetics and Substrate Utilization.....	47
3.3.3 Hydrogen Production	55
3.4 Conclusions.....	58
3.5 References.....	59
Chapter 4.....	61
4 Hydrogen Production and Microbial Kinetics of <i>Clostridium termitidis</i> in Mono-culture and Co-culture with <i>Clostridium beijerinckii</i> on Cellulose	61
4.1 Introduction.....	61
4.2 Materials and Methods.....	66
4.2.1 Microbial Strain and Media	66

4.2.2 Experimental Conditions.....	66
4.2.3 Analytical Methods	67
4.2.4 Gas Measurements	68
4.2.5 Kinetic Equations and Modeling.....	69
4.3 Results and Discussion	76
4.3.1 Statistical analysis	76
4.3.2 <i>C. beijerinckii</i> on Glucose Experiment.....	76
4.3.3 Hydrogen Production	77
4.3.4 Microbial Products	81
4.3.5 Microbial Kinetics.....	90
4.4 Conclusion	108
4.5 References.....	108
Chapter 5.....	115
5 Conclusions and Recommendations	115
5.1 Conclusions.....	115
5.2 Recommendations.....	116
Appendix A.....	117
Appendix B.....	118
Appendix C.....	120
Appendix D.....	130
Curriculum Vitae	131

List of Tables

Table 2.1: Cellulose, hemicellulose and lignin content in residues from the paper industry, agriculture, husbandry and others	12
Table 2.2 Operational and performance parameters of mesophilic mixed cultures experiments on cellulose and lignocellulose.....	19
Table 2.3: Operational and performance parameters of mesophilic pure cultures experiments on cellulose and lignocellulose.....	20
Table 2.4: Operational and performance parameters of thermophilic mixed cultures experiments on cellulose and lignocellulose.....	21
Table 2.5: Operational and performance parameters of thermophilic pure cultures experiments on cellulose and lignocellulose.....	22
Table 2.6: Operational and performance parameters of co-culture experiments under mesophilic and thermophilic conditions	29
Table 3.1: Monod kinetic parameters of <i>Clostridium termitidis</i> grown in glucose and cellobiose (2 g l ⁻¹) by linearization	48
Table 3.2: Monod kinetic parameters of <i>C. termitidis</i> grown in glucose and cellobiose (2 g l ⁻¹) obtained in MATLAB, APE, RMSE and H ₂ yields.....	52
Table 3.3: Monod kinetic parameters of <i>Clostridium</i> species grown on glucose and cellobiose.	54
Table 4.1: H ₂ yields and Gompertz parameters of <i>C. termitidis</i> mono-cultured on 2 g l ⁻¹ cellulose and co-cultured with <i>C. beijerinckii</i> on 2 g l ⁻¹ cellulose.....	80
Table 4.2: Metabolites production or consumption and theoretical H ₂ production of <i>C. termitidis</i> mono-cultured on 2 g l ⁻¹ cellulose and co-cultured with <i>C. beijerinckii</i> on 2 g l ⁻¹ cellulose	88

Table 4.3: COD balance of <i>C. termitidis</i> mono-cultured on 2 g l ⁻¹ cellulose and co-cultured with <i>C. beijerinckii</i> on 2 g l ⁻¹ cellulose	89
Table 4.4: Kinetic parameters obtained in MATLAB of <i>C. termitidis</i> mono-cultured on 2 g l ⁻¹ cellulose and co-cultured with <i>C. beijerinckii</i> on 2 g l ⁻¹ cellulose.	103
Table 4.5: APE and RMSE for biomass, substrate and metabolites of <i>C. termitidis</i> mono-cultured on 2 g l ⁻¹ cellulose and co-cultured with <i>C. beijerinckii</i> on 2 g l ⁻¹ cellulose	104
Table 4.6: Distribution of 1 g COD of substrate consumed expressed as yields for all metabolites, hydrogen and biomass from experimental and modeled data	107

List of Figures

Figure 2.1: a Primary structure of cellulose. b Structure of a cellulose fibril [Desvaux, 2005]
 8

Figure 3.1: Experimental and modeled growth kinetics of *C. termitidis*. a On glucose (2 g l⁻¹). Experimental (crosses) and modeled (dashed line) glucose concentration, experimental (diamonds) and modeled (solid line) dry weight. b On cellobiose (2 g l⁻¹). Experimental (crosses) and modeled (dashed line) cellobiose concentration, experimental (diamonds) and modeled (solid line) dry weight. Experimental data points represent mean values of duplicate experiments, lines above and below represent the actual duplicates. Modeled data was determined in MATLAB R2014a 49

Figure 3.2: Linear regression of experimental data against modeled data. a Glucose experiment. Glucose concentration (crosses) and glucose linear regression (dotted line). Dry weight (diamonds) and dry weight linear regression (solid line). b Cellobiose experiment. Cellobiose concentration (crosses) and cellobiose linear regression (dotted line). Dry weight (diamonds) and dry weight linear regression (solid line) 51

Figure 3.3: Cumulative H₂ production and pH. a *C. termitidis* on glucose (2 g l⁻¹). Cumulative H₂ profile (squares) and pH changes (triangles). b *C. termitidis* on cellobiose (2 g l⁻¹). Cumulative H₂ profile (squares) and pH changes (triangles). Data points represent the mean values of duplicate experiments, lines above and below represent the actual duplicates 56

Figure 3.4: μ vs pH. a *C. termitidis* on glucose. b *C. termitidis* on cellobiose. 57

Figure 4.1: *C. termitidis* speculative cell interaction with cellulose through its cellulosome based on *C. thermocellum*'s cellulosome model (left) and biochemical pathways from glucose based on Caspi et al. [2014] (right) 64

Figure 4.2: Non-cellulosome speculative interaction of *C. beijerinckii* sp. cell with cellulose (left) and biochemical pathways from glucose from Dürre [2005] (right) 65

Figure 4.3: Schematic representation of the steps involved in cellulose fermentation in mono-culture experiments	70
Figure 4.4: Schematic representation of the steps involved in cellulose fermentation in co-culture experiments.....	71
Figure 4.5: <i>C. beijerinckii</i> in 2 g l ⁻¹ glucose. a pH and cumulative H ₂ production profiles. b Dry weight and cellular protein content correlation. Data points represent the mean values of duplicate experiments, lines above, below and to the sides represent the actual duplicates	76
Figure 4.6: <i>C. termitidis</i> mono-cultured in 2 g l ⁻¹ cellulose and co-cultured with <i>C. beijerinckii</i> 2 g l ⁻¹ cellulose. a Cumulative H ₂ production profiles. b pH profiles. Data points are the averages of duplicates, lines above and below represent the actual duplicates	79
Figure 4.7: Metabolites production in non-agitated mono-culture of <i>C. termitidis</i> on 2 g l ⁻¹ cellulose. a Acetic acid and ethanol. b Lactic and formic acids. Data points are the averages of duplicates, lines above and below represent the actual duplicates	82
Figure 4.8: Metabolites production in agitated mono-culture of <i>C. termitidis</i> on 2 g l ⁻¹ cellulose. a Acetic acid and ethanol. b Lactic and formic acids. Data points are the averages of duplicates, lines above and below represent the actual to duplicates	83
Figure 4.9: Metabolites production or consumption in non-agitated co-culture of <i>C. termitidis</i> and <i>C. beijerinckii</i> on 2 g l ⁻¹ cellulose. a Butyric acid. b Ethanol, lactic, formic and acetic acids. Data points are the averages of duplicates, lines above and below represent the actual duplicates	85
Figure 4.10 Metabolites production or consumption in agitated co-culture of <i>C. termitidis</i> and <i>C. beijerinckii</i> on 2 g l ⁻¹ cellulose. a Butyric and acetic acids. b Ethanol, lactic and formic acids. Data points are the averages of duplicates, lines above and below represent the actual duplicates	86

Figure 4.11: Biomass and cellulose profiles in non-agitated bottles. Data points are the averages of duplicates, lines above and below represent the actual duplicates	90
Figure 4.12: Biomass (g dry weight l ⁻¹) – cumulative H ₂ (ml) correlation in agitated bottles. a Mono-culture of <i>C. termitidis</i> . b Co-culture of <i>C. termitidis</i> and <i>C. beijerinckii</i>	91
Figure 4.13: Experimental and modeled growth kinetics in non-agitated experiments. a Mono-culture. b Co-culture.....	93
Figure 4.14: Experimental and modeled PO/biomass profiles in non-agitated experiments. a Mono-culture. b Co-culture.....	94
Figure 4.15: Experimental and modeled growth kinetics in agitated experiments. a Mono-culture. b Cco-culture.....	95
Figure 4.16: Experimental and modeled PO/biomass profiles in agitated experiments. a Mono-culture. b Co-culture.....	96
Figure 4.17: Experimental and modeled profile of metabolites in non-agitated mono-culture. a Acetic acid and ethanol. b Lactic and formic acids	97
Figure 4.18: Experimental and modeled profile of metabolites in non-agitated co-culture. a Butyric acid. b Lactic, formic, acetic acids and ethanol	98
Figure 4.19: Experimental and modeled profile of metabolites in agitated mono-culture. a Acetic acid and ethanol. b Lactic and formic acids	99
Figure 4.20: Experimental and modeled profile of metabolites in agitated co-culture. a Butyric and acetic acids. b Lactic, formic acids, and ethanol	100
Figure 4.21: Experimental and modeled hydrogen profiles for: a Non-agitated mono-culture. b Non-agitated co-culture. c Agitated mono-culture. d Agitated co-culture	106

List of Appendices

Appendix A: Supplementary Figure 3.1 Correlation between dry weight and cellular protein content in <i>Clostridium termitidis</i>	117
Appendix B: Pictures from “Hydrogen production and Microbial Kinetics of <i>C. termitidis</i> in mono-culture and co-culture with <i>C. beijerinckii</i> ” experiment (Chapter 4).....	118
Appendix C: Data for duplicates and statistical analysis.....	120
Appendix D: <i>C. termitidis</i> on cellobiose under Optical and Electronic Microscopy	130

Nomenclature

$C_{H_2,i}$	Current fraction of H ₂ gas in the headspace of the reactor
$C_{H_2,i-1}$	Previous fraction of H ₂ gas in the headspace of the reactor
H	Cumulative H ₂ production (ml)
k_d	Decay coefficient (h ⁻¹)
K_L	Lactate consumption constant (l g ⁻¹ COD biomass d ⁻¹)
K_m	Substrate utilization rate (g substrate g ⁻¹ dry weight h ⁻¹ or g COD substrate g ⁻¹ COD biomass d ⁻¹)
K_s	Saturation constant or half-velocity constant (g l ⁻¹)
K_x	Half-velocity degradation coefficient (g COD substrate g ⁻¹ COD biomass)
P	H ₂ production potential (ml)
R_{max}	Maximum H ₂ production rate (ml d ⁻¹)
S_o	Non-biodegradable factor (g COD l ⁻¹)
$V_{G,i}$	Total biogas volume accumulated (ml)
$V_{H_2,i}$	Current cumulative H ₂ gas volume (ml)
$V_{H_2,i-1}$	Previous cumulative H ₂ gas volume (ml)
$V_{h,i}$	Total volume of the headspace of the reactor (ml)
$Y_{A/L}$	Acetate yield from lactate (g COD g ⁻¹ COD lactate)
$Y_{A/PO}$	Acetate yield from particulate organic (g COD g ⁻¹ COD PO)
$Y_{B/PO}$	Butyrate yield from particulate organic (g COD g ⁻¹ COD PO)

$Y_{E/PO}$	Ethanol yield from particulate organic (g COD g ⁻¹ COD PO)
$Y_{F/PO}$	Formate from particulate organic (g COD g ⁻¹ COD PO)
$Y_{L/PO}$	Lactate yield from particulate organic (g COD g ⁻¹ COD PO)
$Y_{X/S}$	Biomass yield from soluble substrate (g dry weight g ⁻¹ substrate)
$Y_{X/L}$	Biomass yield from lactate (g COD g ⁻¹ COD lactate)
$Y_{X/PO}$	Biomass yield from particulate organic (g COD biomass g ⁻¹ COD PO)
μ_{\max}	Maximum specific growth rate (h ⁻¹ or d ⁻¹)
λ	Lag phase (d)

Abbreviations

APE	Average Percentage Error
ARB	Anode-respiring Bacteria
ATCC	American Type Culture Collection
ATP	Adenosine Triphosphate
CBP	Consolidated Bioprocessing
COD	Chemical Oxygen Demand
CSBR	Continuously Stirred Bio-Reactor
CSTR	Continuous Stirred Tank Reactor
DSM	Deutsche Sammlung von Mikroorganismen und Zellkulturen (German Collection of Microorganisms and Cell Cultures)
MEC	Microbial Electrolysis Cell
MFC	Microbial Fuel Cell
PNS	Purple Non-sulfur
POM	Particulate Organic Matter
RCBC	Rumen Cellulose-degrading Bacteria Consortium
RID	Refractive Index Detector
RMSE	Root Mean Square Error
TCD	Thermal Conductivity Detector
VS	Volatile Solids

Chapter 1

1 Introduction

1.1 Background

Hydrogen is the most abundant element in the universe and mankind has harnessed its power indirectly, as the energy generated in the sun comes from the fusion of hydrogen nuclei resulting into helium nuclei and energy [NASA, 2007]. To produce hydrogen, a variety of process technologies can be used, including direct thermal, electrochemical, biological, photolytic and thermo-chemical [Rand et al., 2008; Azbar and Levin, 2012]. However, a real benefit for CO₂ reduction can only be achieved if hydrogen is produced without using energy from fossil fuels [Urbaniec and Bakker, 2015]. The main biohydrogen production technologies involve the use of MECs (microbial electrolysis cells) [Hallenbeck et al., 2012], direct water biophotolysis, indirect water biophotolysis, photofermentation, and anaerobic dark fermentation [Guo et al., 2010]. Lignocellulosic biomass is the most abundant renewable biological resource and it constitutes a major portion of agricultural wastes and industrial effluents from pulp and paper, and food industry [Saratale et al., 2008]. Dark fermentation has the advantage of potentially using many biomass residues and wastes as feedstocks [Hallenbeck et al., 2012; Urbaniec and Bakker, 2015]. Therefore, fermentative biological hydrogen production could provide a renewable-hydrogen stream [Hallenbeck, 2011]. Soluble sugars, mainly glucose, have served as model substrate to investigate biohydrogen production. However, real biomass residues contain complex substrates like cellulose. Therefore, great interest has been put towards consolidated bioprocessing (CBP) where cellulase production, cellulose hydrolysis, and fermentation are accomplished in one step [Carere et al., 2008].

Fermentative biohydrogen can be produced either by mixed cultures and pure cultures. The main advantage of natural mixed consortia is the ease of operation in a non-sterile environment and the broad choice of feedstock [Fang and Li, 2007]. Nevertheless, mixed consortia still need nutrients to be supplemented and the inoculum itself needs pretreatment to suppress hydrogen consuming bacteria [Fang and Li, 2007]. Comparable hydrogen

yields can be achieved from pure and mixed cultures with soluble substrates, like glucose. Nevertheless, on complex substrates like cellulose, pure cultures have achieved higher hydrogen yields. Even though thermophiles are primarily responsible for these high yields by pure cultures, the main disadvantage of thermophilic fermentative hydrogen production is the energy demand for heating and maintenance [Guo et al., 2010], and hence the importance to investigate hydrogen production at mesophilic temperatures.

Different strategies are proposed to increase hydrogen yields, and optimize bioprocess parameters, such as decreasing hydrogen partial pressure, metabolic engineering, two-stage systems [Hallenbeck et al., 2012; Hallenbeck, 2009], and defined mixed consortia. Co-cultures of a cellulolytic bacteria and a high hydrogen producing bacteria from soluble sugars have been reported to increase the hydrogen yields [Wang et al., 2008; Geng et al., 2010; Liu et al., 2008].

1.2 Problem Statement

Fermentative biohydrogen production has been under investigation for several years globally. Nevertheless, cellulose utilization by hydrogen producers remains an issue due to the low hydrogen yields reported. The pretreatment of cellulose prior to fermentation (to be converted to readily biodegradable substrate) requires complex and expensive steps such as chemical, thermochemical or enzymatic processes [Carere et al., 2008], making the conversion of cellulose to hydrogen in a single step very advantageous through the CBP.

The broad composition of mixed cultures increases the variation in hydrogen rates and yields even for a specific substrate, hence, the importance of utilizing defined strains. *Clostridium termitidis* is an anaerobic, mesophilic, cellulolytic and hydrogen producer isolated from the gut of a termite [Hethener et al., 1992], able to perform CBP due to its cellulosome (a multi-enzyme complex capable of hydrolyzing cellulose) [Munir et al., 2014]. On the other hand, *Clostridium beijerinckii* is a mesophilic hydrogen producer which is not able to degrade cellulose but is adept at hydrogen production from glucose [Masset et al., 2012].

Additionally, reasonably accurate mathematical models able to predict biochemical phenomena are essential since they provide the basis for design, control, optimization and scale-up of process systems [Huang and Wang, 2010].

1.3 Research Objectives

The main goal of this research was to investigate the microbial kinetics of *C. termitidis* for biohydrogen production. The specific objectives are as follows:

- Determine the microbial kinetics of *C. termitidis* on the soluble substrates, glucose and cellobiose, which are the hydrolysis products of cellulose.
- Determine the microbial kinetics of *C. termitidis* on cellulose considering metabolites production.
- Evaluate the effect of co-culturing *C. termitidis* and *C. beijerinckii* on hydrogen production and determine the microbial kinetics, also considering metabolites production.
- Evaluate the effect of agitation on *C. termitidis* mono-culture on cellulose and co-culture with *C. beijerinckii* on cellulose.

1.4 Thesis Organization

The present thesis comprises five chapters and conforms to the “integrated article” format as outlined in the Thesis Regulation Guide by the School of Graduate and Postdoctoral Studies (SGPS) of the University of Western Ontario. The five chapters are:

Chapter 1 presents the general introduction, as well as the research objectives and contribution.

Chapter 2 presents the literature review on biohydrogen production from cellulose.

- Chapter 3 describes the microbial kinetics of *C. termitidis* on glucose and cellobiose.
- Chapter 4 presents the hydrogen production and microbial kinetics of *C. termitidis* mono-cultured on cellulose and co-cultured with *C. beijerinckii* on cellulose.
- Chapter 5 summarizes the general conclusions and recommendations for future work based on the results of this research.

1.5 Research Contribution

Cellulose is the most important component of lignocellulosic biomass, which is a potential feedstock for fermentative biohydrogen production. Determination of microbial kinetics is crucial for scale-up and design of large scale bioreactors. Although different mixed consortia and specific strains have been tested for hydrogen production directly from cellulose, *C. termitidis* kinetics on cellulose and also from its soluble sugars have not been described. The main contributions of this research are:

- The microbial kinetics of *C. termitidis* growth on cellulose, cellobiose and glucose.
- The viability of a mesophilic co-culture and the actual hydrogen production enhancement from their interaction.
- The development of a mathematical model for cellulose utilization by *C. termitidis* in mono and co-culture with *C. beijerinckii*.

1.6 References

- Azbar N., Levin D.B. (2012) State of the art and progress in production of biohydrogen. Bentham Science Publishers, US
- Carere C.R., Sparling R., Cicek N., Levin D.B. (2008) Third generation biofuels via direct cellulose fermentation. *International Journal of Molecular Sciences* 9:1342-1360
- Elsharnouby O., Hafez H., Nakhla G., El Nagggar M.H. (2013) A critical literature review on biohydrogen production by pure cultures. *Int J Hydrogen Energy* 38:4945-4966
- Fang H., Li C. (2007) Fermentative Hydrogen Production From Wastewater and Solid Wastes by Mixed Cultures. *Crit Rev Environ Sci Technol* 37:1-39
- Geng A., He Y., Qian C., Yan X., Zhou Z. (2010) Effect of key factors on hydrogen production from cellulose in a co-culture of *Clostridium thermocellum* and *Clostridium thermopalmarium*. *Bioresour Technol* 101:4029-4033
- Guo X.M., Trably E., Latrille E., Carrère H., Steyer J.-P. (2010) Hydrogen production from agricultural waste by dark fermentation: A review. *Int J Hydrogen Energy* 35:10660-10673
- Hallenbeck P.C. (2009) Fermentative hydrogen production: Principles, progress, and prognosis. *Int J Hydrogen Energy* 34:7379-7389
- Hallenbeck P.C. (2011) Microbial paths to renewable hydrogen production. *Biofuels* 2:285-302
- Hallenbeck P.C., Abo-Hashesh M., Ghosh D. (2012) Strategies for improving biological hydrogen production. *Bioresour Technol* 110:1-9
- Hethener P., Brauman A., Garcia J.L. (1992) *Clostridium termitidis* sp. nov., a cellulolytic bacterium from the gut of the wood-feeding termite, *Nasutitermes lujae*. *Syst Appl Microbiol* 15:52-58

- Huang W.H., Wang F.S. (2010) Kinetic modeling of batch fermentation for mixed-sugar to ethanol production. *Journal of the Taiwan Institute of Chemical Engineers* 41:434-439
- Liu Y., Yu P., Song X., Qu Y. (2008) Hydrogen production from cellulose by co-culture of *Clostridium thermocellum* JN4 and *Thermoanaerobacterium thermosaccharolyticum* GD17. *Int J Hydrogen Energy* 33:2927-2933
- Masset J., Calusinska M., Hamilton C., Hiligsmann S., Joris B., Wilmotte A., Thonart P. (2012) Fermentative hydrogen production from glucose and starch using pure strains and artificial co-cultures of *Clostridium* spp. *Biotechnology for Biofuels* 5:1-15
- Munir R.I., Schellenberg J., Henrissat B., Verbeke T.J., Sparling R., Levin D.B. (2014) Comparative analysis of carbohydrate active enzymes in *Clostridium termitidis* CT1112 reveals complex carbohydrate degradation ability. *PLoS One* 9:e104260
- Nasa. 2007. *National Aeronautics and Space Administration. Technology through time. ISSUE #49: Solar energy* [Online]. Available: http://sunearthday.nasa.gov/2007/locations/ttt_solarenergy.php.
- Rand D.A.J., Dell R., Royal Society Of C. (2008) Hydrogen energy: challenges and prospects. Royal Society of Chemistry, Cambridge, UK
- Saratale G.D., Chen S.D., Lo Y.C., Saratale R.G., Chang J.S. (2008) Outlook of biohydrogen production from lignocellulosic feedstock using dark fermentation – a review. *Journal of Scientific & Industrial Research* 67:962-979
- Urbaniec K., Bakker R.R. (2015) Biomass residues as raw material for dark hydrogen fermentation - A review. *Int J Hydrogen Energy* 40:3648-3658
- Wang A.J., Ren N.Q., Shi Y.G., Lee D.J. (2008) Bioaugmented hydrogen production from microcrystalline cellulose using co-culture - *Clostridium acetobutylicum* X-9 and *Etilanoigenens harbinense* B-49. *Int J Hydrogen Energy* 33:912-917

Chapter 2

2 Literature Review

2.1 Introduction

Future energy demand growth will be dictated by: population growth and growth in per capita energy usage [Zannoni and De Philippis, 2014]. To meet future needs, interest is focused towards the use of carbon neutral fuels. Liquid (bioethanol, biodiesel, biobutanol) and gaseous (biohydrogen) biofuels are attractive alternatives [Carere et al., 2008]. Biohydrogen has numerous advantages and despite the several drawbacks related to its storage and utilization, there is an increasing activity in R&D in an effort to create a hydrogen economy [Hallenbeck and Ghosh, 2012]. Dark fermentation focusses on converting carbohydrates (monosaccharides, disaccharides or polysaccharides) into hydrogen, CO₂ and organic acids. Among carbohydrates, cellulose can be considered the most important because of its abundance on Earth [Fang, 2010] and its presence in wastes (lignocellulosic wastes) adds sustainable value to biohydrogen production.

2.2 Cellulose

Cellulose is the most common organic compound. It is an insoluble biopolymer represented by the molecular formula: (C₆H₁₀O₅)_n and consists of 7,000-15,000 glucose residue monomers in a linear array linked by β(1-4) glycosidic bonds where every other glucose residue is rotated approximately 180° [Kumar et al., 2008; Brown et al., 1996]. Consequently, as illustrated in Figure 2.1a, the structural repeating unit in cellulose is the disaccharide cellobiose, which is soluble in water [Brown et al., 1996]. As depicted in Figure 2.1b, cellulose is synthesized as individual molecules (linear chains of glucosyl residues) [Fang, 2010], and these linear molecules are strongly linked through inter and intramolecular hydrogen bonds and van der Waals forces with each other [Leschine, 1995]. About 30 cellulose molecules are assembled elementary fibrils (protofibrils), which are packed into microfibrils, and about 100 microfibrils are packed to form fibrils, and these

are in turn assembled into the familiar cellulose fibers [Lynd et al., 2002; Schwarz, 2001; Demain et al., 2005; Leschine, 1995]. Despite its simple chemical composition, cellulose exists in diverse crystalline and amorphous topologies [Schwarz, 2001], and unlike the other polysaccharides, cellulose crystalline structure involves a structural order tight enough to prevent penetration by enzymes [Lynd et al., 2002].

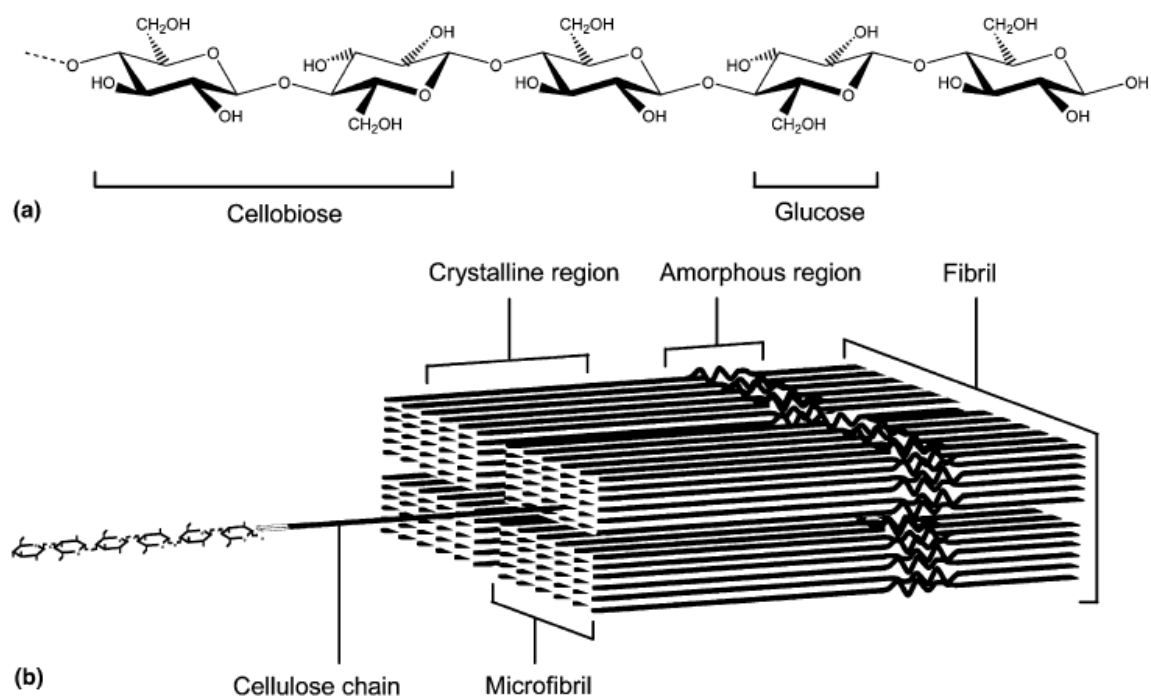


Figure 2.1: a Primary structure of cellulose. b Structure of a cellulose fibril
[Desvaux, 2005]

Cellulose, as organic substrate for anaerobic fermentation, can be broadly categorized as pure cellulose and cellulosic biomass or lignocellulose. The main characteristics of each are mentioned in the following sections.

2.2.1 Pure Cellulose

Pure cellulose is widely used in the food and pharmaceutical industries, as well as for laboratory purposes (microbial and hydrolysis studies). Purified cellulose could be powdered and microcrystalline cellulose, differing in particle size distribution. Powdered cellulose, like Solka Floc is produced by delignification of wood [Lynd et al., 2002], and microcrystalline cellulose, like Avicel and Sigmacell are produced by treating α -cellulose with dilute acid [Terinte et al., 2011; Lynd et al., 2002]. Microcrystalline cellulose is considered the purest cellulose since the more amorphous regions of the cellulose fibers are removed [Lynd et al., 2002]. On the other hand, biosynthesized crystalline cellulose can be produced by aerobic bacteria (i.e. *Acetobacter xylinum*), marine green algae (i.e. *Valonia* or *Mirasterias*) or by sea animals (i.e. *Halocynthia*) [Terinte et al., 2011].

2.2.2 Lignocellulose

Lignocellulose, lignocellulosic biomass, or lignocellulosic materials are composed primarily of cellulose, hemicellulose, and lignin. In a plant cell wall, rigid cellulose fibers are embedded in a cross-linked matrix of hemicellulose and lignin. It is considered that a typical cell wall contains of 35-50% cellulose, 20-35% hemicellulose, and 10-25% lignin [Lee and Shah, 2013]. The hemicellulose is amorphous due to its short and branched macromolecular structure, making it easier to hydrolyze to simple sugars. Hemicellulose contains six-carbon sugars (D-glucose, D- mannose and D-galactose) and five-carbon sugars (D-xylose and L-arabinose) as well as uronic acid [Lee and Shah, 2013]. In contrast, lignin is a complex cross-linked aromatic polymer covalently linked to hemicellulose which contributes to the stabilization of cell walls [Lee and Shah, 2013].

Some researchers consider the energy from lignocellulosic biomass as carbon neutral because biomass stores solar energy in carbohydrate chemical bonds through photosynthesis, and later the CO₂ emitted when they are burned or transformed can be considered equal to the CO₂ absorbed during growth [Martínez-Duart and Guerrero-Lemus, 2013]

2.2.2.1 Energy Crops

Energy crops are certain plants cultivated with the only purpose to exploit their biomass as feedstock for combustion or biotransformation to biofuels [Ntaikou et al., 2010]. Some of the most common energy crops are: woody energy crops (e.g. Miscanthus, switchgrass, SRC willow, poplar, eucalyptus, cardoon, sorghum, kenaf, prickly pear, whole crop maize, and reed canary grass), cellulose crops (e.g. straw, wood, short rotation coppice (SRC), etc.), starch and sugar crops (e.g. sugarcane, potato, sugar beet, Jerusalem artichoke), oil crops, and cereals (e.g. wheat, barley, maize, oats, and rye) [Monlau et al., 2011; Kumar et al., 2008; Sanderson et al., 2012; Sims et al., 2006; Ren et al., 2009]. Among the advantages of Miscanthus and switchgrass are: biomass yield is high, minimal fertilizer requirement, and planting is necessary only once, which lowers the costs for tillage and planting [Sanderson et al., 2012].

2.2.2.2 Lignocellulosic Wastes

Lignocellulosic wastes are derived from domestic, commercial, industrial, and agricultural activities. Among these wastes, there are: paper, cloth, garden debris, packing materials, textiles, demolition wood, etc. Unlike energy crops, lignocellulosic wastes have a very low or negative cost and their further use helps to divert materials from landfills [Duff and Murray, 1996].

Table 2.1 presents the cellulose, hemicellulose and lignin content in different residues. Cotton fibers and paper have the highest content of cellulose (80-99%), and newspaper has approximately half (40-55%) [Sun and Cheng, 2002]. Paper sludge has significant content of cellulose (54%) and very low content of lignin (7%), which makes it a potential feedstock for biofuels, as already demonstrated by Fan et al. [2003] and Moreau et al. [2015] when producing ethanol and hydrogen, respectively. Similarly, hardwood and softwood have almost 50% cellulose [McKendry, 2002]. In contrast, minimum cellulose content can be found in cattle manure and swine waste (1.6-6%) [Dewes and Hünsche, 1998; Boopathy, 1998]. Cellulose content in the most abundant lignocellulose agricultural wastes (i.e. corncobs, corn stover, switchgrass, and wheat, barley and rice straws) ranges

from 23 to 50%. In addition, with a hemicellulose content ranging from 18 to 40% [Fang, 2010; Sun and Cheng, 2002; Zhu et al., 2010; McKendry, 2002; Kaur et al., 1998], these agricultural wastes are rich in carbohydrates, hence, the importance to use them for biofuels production.

Table 2.1: Cellulose, hemicellulose and lignin content in residues from the paper industry, agriculture, husbandry and others

Residue or waste	Cellulose (%)	Hemicellulose (%)	Lignin (%)	Reference
Hardwood	45-50	20-25	20-25	[McKendry, 2002]
Softwood	35-40	25-30	27-30	[McKendry, 2002]
Nut shells	25-30	25-30	30-40	[Sun and Cheng, 2002]
Corn cobs	45	35	15	[Sun and Cheng, 2002]
Corn stover	41	23	22	[Zhu et al., 2010]
Grasses	25-40	35-50	10-30	[Sun and Cheng, 2002]
Wheat straw	33-40	20-25	15-20	[McKendry, 2002]
Rice straw	32-40	18	5.5-11.2	[Kaur et al., 1998]
Rice bran	35	25	17	[Fang, 2010]
Barley bran	23	32	21.4	[Fang, 2010]
Barley Straw	31-45	27-38	14-19	[Fang, 2010]
Leaves	15-20	80-85	0	[Sun and Cheng, 2002]
Sorted refuse	60	20	20	[Sun and Cheng, 2002]
Cotton seed hairs	80-95	5-20	0	[Sun and Cheng, 2002]
Switchgrass	30-50	10-40	5-20	[McKendry, 2002]
Solid cattle manure	1.6-4.7	1.4-3.3	2.7-5.7	[Dewes and Hünsche, 1998]
Swine waste	6.0	28		[Boopathy, 1998]
Primary wastewater solids	8-15	NA	24-29	[Cheung and Anderson, 1997]
Paper	85-99	0	0-15	[Sun and Cheng, 2002]
Newspaper	40-55	25-40	18-30	[Sun and Cheng, 2002]
Waste papers from chemical pulps	60-70	10-20	5-10	[Sun and Cheng, 2002]
Primary pulp and paper sludge	54	7	7	[Moreau et al., 2015]

2.3 Hydrogen

It is considered that hydrogen does not contribute to the greenhouse effect and has a high energy yield of 142 kJ g^{-1} , which is more than two times more than that of any hydrocarbon [Hafez et al., 2009]. Nevertheless, unlike most alternative liquid fuels that can be either blended with gasoline (or diesel) or used neat, hydrogen use needs further efforts to develop novel power-conversion infrastructure [Hallenbeck, 2011]. Despite this, the engineering of hydrogen storage and use have already placed prototype buses and cars on the streets through the use of fuel cells [Sørensen, 2012; Hallenbeck, 2009], a much more efficient technology than the combustion engines used with bioethanol or biodiesel [Hallenbeck and Ghosh, 2012]. While there are still challenges to produce, store, distribute and convert hydrogen to electric power [Hallenbeck, 2011], many scientists around the world are working towards solutions to use this almost inexhaustible energy carrier.

It is estimated that 50% of the hydrogen currently produced is used in the manufacture of ammonia (for fertilizers), 8% is dedicated to methanol production and the rest is principally used in the petrochemical industry [Martínez-Duart and Guerrero-Lemus, 2013]. Hydrogen production methods can be broadly categorized into: thermochemical, electrochemical and biological [Chaubey et al., 2013]. Ewan and Allen [2005] calculated that by 2005 hydrogen production was from methane steam reforming (48%), oil reforming (30%), coal gasification (18%), electrolysis of water (3.9%) and other sources (0.1%). Nevertheless, over 90% of global hydrogen is captive-produced, meaning that the production facility is built by the same industry that consumes hydrogen. Thus, approximately only 10% of the produced hydrogen reaches the open market [Martínez-Duart and Guerrero-Lemus, 2013].

The disadvantages of the aforementioned hydrogen production technologies are the high cost and large energy input needed [Azbar and Levin, 2012]. Although electrolysis of water can use renewable sources (wind, solar, hydro and photovoltaic cells), it is only approximately 65% efficient [Hallenbeck, 2011]. On the other hand, biological hydrogen production provides a sustainable mean to supply hydrogen [Chaubey et al., 2013], with low pollution and less energy demand.

2.3.1 Biohydrogen Production

Biohydrogen is the hydrogen produced by one of many biological processes, including: MECs (microbial electrolysis cell), biophotolysis, photofermentation and dark fermentation [Hallenbeck et al., 2012]. These technologies have diverse challenges to a profitable industrial scale-up and only the fermentation process is currently in industrial use, although not for hydrogen end production [Sørensen, 2012]. Hydrogen yields on dissolved organic material should be around 60%-80% for biohydrogen production to be economically viable [Hafez et al., 2014].

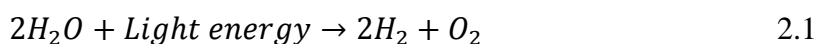
2.3.1.1 Microbial Electrolysis

Microbial electrolysis cells (MECs) are a variation of microbial fuel cell, which have been under research for decades. MECs have developed very rapidly in the last few years [Hallenbeck, 2011]. Anode-respiring bacteria (ARB), such as *Geobacter Shewanella*, *Clostridium*, *Pseudomonas*, *Desulfuromonas*, *Eseherichia*, and *Klebisella*, are able to transmit their electrons to a solid electron acceptor as part of their energy-generating respiration [Yang et al., 2015]. The energy in the electrons can be used to generate electricity in a microbial fuel cell (MFC) or for hydrogen production in a microbial electrolysis cell (MEC) [Torres et al., 2007]. The electrons reach the cathode and react with water to produce hydrogen [Yang et al., 2015], although external voltage needs to be supplemented in order for the hydrogen to be produced at the cathode [Liu et al., 2010]. MECs reach complete conversion of organic compounds, sugars and acid to hydrogen and CO₂ [Zannoni and De Philippis, 2014]. Nevertheless, improvements such as the search for inexpensive efficient cathode material and for a way to increase current densities (A/m²) and decrease voltage for high yields are desirable [Hallenbeck, 2011]. However, MECs could be advantageous when using the main fermentation products, acetate, butyrate and propionate to further produce hydrogen as recently published by Yang et al. [2015].

2.3.1.2 Light-driven Processes

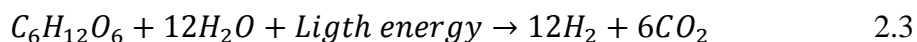
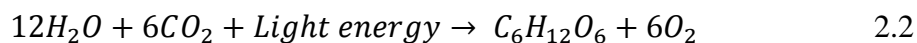
2.3.1.2.1 Biophotolysis

Photosynthesis in cyanobacteria and green microalgae can occur under oxygenic (oxygen producing) or hypoxic and anoxygenic conditions. Oxygenic photosynthesis occurs in algae, cyanobacteria, and vascular plants [Eroglu and Melis, 2011], which use solar energy to extract electrons and protons from water, producing oxygen [Azbar and Levin, 2012]. Biophotolysis is the direct production of hydrogen through water-splitting photosynthesis by certain green microalgae and cyanobacteria [Hallenbeck, 2011; Levin et al., 2004].



The main advantage is its abundant substrate (water) and simple products (hydrogen and O₂), but the low light conversion efficiencies, calculated as a maximum theoretical solar-to-hydrogen conversion efficiency of 12% in green microalgae [Eroglu and Melis, 2011], and oxygen inhibition of hydrogen production are problematic [Zannoni and De Philippis, 2014; Hallenbeck, 2011].

In indirect biophotolysis, water splitting (oxygenic photosynthesis) and hydrogen production reactions are separated in time or space, solving the oxygen inhibition for hydrogen production:



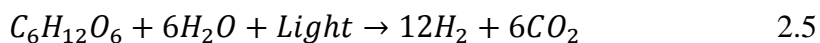
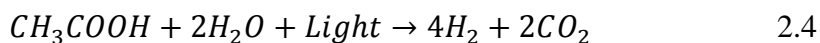
In the aerobic phase, solar energy and water are used to synthesize carbohydrates. Later, in the anaerobic phase low potential electrons are released in the carbohydrates catabolism necessary for hydrogen production [Azbar and Levin, 2012]. Filamentous cyanobacteria carry out the indirect biophotolysis and hydrogen production, this bacteria can be nitrogen fixing (i.e., the genus *Anabaena*, *Nostoc*, *Oscillatoria*, *Calothrix*, etc.), or non-nitrogen fixing (i.e., the genus *Synechococcus*, *Synechocystis*, *Gloebacter*, etc.) [Eroglu and Melis, 2011]. The involvement of multiple steps (synthesis, degradation of carbohydrates, anoxic

conditions) in indirect biophotolysis makes it less effective than the direct biophotolysis [Azbar and Levin, 2012].

The main disadvantage of both, direct and indirect biophotolysis, is that they do not use biowastes, whereas the next process (photofermentation) does [Hafez et al., 2014].

2.3.1.2.2 Photo Fermentation

Photofermentation is the conversion of exogenous organic substrates (usually organic acids) to hydrogen, by anoxygenic photosynthetic microbes like purple non-sulfur (PNS) bacteria (*Rhodobacter*, *Rhodopseudomonas*, *Rhodospirillum*, *Chromatium*) using solar energy to generate ATP (Adenosine triphosphate), which is needed to drive the nitrogenase-mediated hydrogen production under strict conditions of inorganic nitrogen limitation [Hallenbeck, 2011; Azbar and Levin, 2012].

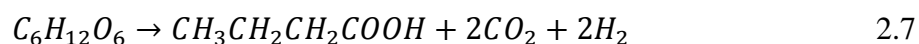
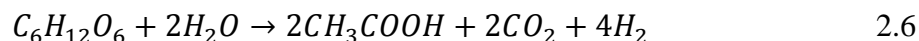


An advantage of photofermentation over biophotolysis is the higher substrate to hydrogen conversion efficiency [Zannoni and De Philippis, 2014]. Small-chain organics, like succinate, lactate, butyrate, malate, acetate, propionate, pyruvic acid, etc. can be used as electron sources for nitrogen fixation/hydrogen production. In addition, glucose and wastes like distillery effluents can be used as substrates [Azbar and Levin, 2012]. The rates of hydrogen production from these small organic acids have been reported to range from 1 to 36 ml H₂ l⁻¹ h⁻¹ [Eroglu and Melis, 2011]. *Rhodobacter sphaeroides* as wild type strain achieved the highest rate from malate (36 ml H₂ l⁻¹ h⁻¹) [Eroglu and Melis, 2011]. The drawbacks that preclude the practical application of photofermentation are the low light-conversion efficiencies, with a maximum theoretical solar-to-hydrogen energy conversion efficiency of 10% [Eroglu and Melis, 2011], and the excess energy demand by nitrogenase, as well as the need for low cost transparent hydrogen-impermeable photobioreactors covering inordinately large surface areas [Hallenbeck, 2011; Zannoni and De Philippis,

2014]. In conclusion, the rate and efficiency of photobiological hydrogen production are not economically viable [Hafez et al., 2014].

2.3.1.3 Anaerobic Dark Fermentation

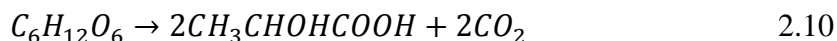
Fermentative hydrogen production is the anaerobic production of hydrogen from organic substrates [Hallenbeck, 2011]. Carbohydrate-rich substrates are preferable, since only a few amino acids contribute to hydrogen through fermentation, and lipids conversion to hydrogen is only possible at very low hydrogen partial pressures [Hallenbeck, 2011]. Therefore, cellulosic wastes are potential feedstocks for this process [Carere et al., 2008]. Using glucose as a model substrate, among the several reactions that take place in anaerobic fermentation, the most widely used are represented by the stoichiometric Equations 2.6-2.10. Acetate and butyrate pathways involve hydrogen production and according to Equations 2.6 and 2.7, respectively, a maximum of 4 mol H₂ mol⁻¹ glucose is obtained when acetate is produced. Whereas butyrate pathway involves only 2 mol H₂ mol⁻¹ glucose [Guo et al., 2010]:



Hydrogen is consumed by the propionate pathway, as follows [Vavilin et al., 1995]:



Ethanol and lactate are involved in a zero-H₂ balance pathway according to Equations 2.9 and 2.10, respectively [Guo et al., 2010]:



Unlike other biofuels, this technology is often considered as carbon negative, since the CO₂ produced together with hydrogen could be captured or sequestered [Hallenbeck and Ghosh,

2012]. Among the barriers to overcome in fermentative biohydrogen production are the low yields due to metabolic restrictions, incomplete substrate conversion and the production of unwanted side products [Hallenbeck, 2011]. However, bioreactor configuration and operation, do not seem to present a particular technical challenge [Hallenbeck and Ghosh, 2012]. Fermentative hydrogen production is influenced by several factors, including pH by affecting the end product formation, and hydrogen partial pressure since hydrogen synthesis pathways are sensitive to hydrogen concentration causing end-product inhibition.

Many studies have been carried out on dark fermentative hydrogen production with either pure substrates (synthetic) or a variety of wastes. A comparison on studies on fermentative biohydrogen production from synthetic cellulose and from lignocellulose using mixed and pure cultures is addressed in the following sections. Tables 2.2 and 2.3 present studies under mesophilic conditions using mixed cultures and pure cultures, respectively, and Tables 2.4 and 2.5 contain the studies under thermophilic conditions using mixed and pure cultures, respectively.

Table 2.2 Operational and performance parameters of mesophilic mixed cultures experiments on cellulose and lignocellulose

	Culture(s)	Reactor	T (°C)	Substrate (g l ⁻¹)	Pre-treatment	pH	H ₂ yield (mol H ₂ mol ⁻¹ hexose _{eq.})	H ₂ production rate (l l ⁻¹ d ⁻¹)	Initial cellulose % in substrate	Substrate removal efficiency (%)	Substrate degradation rate ^a (g l ⁻¹ d ⁻¹)	Ref.
Cellulose	Rumen liquor from cattle	Batch	38	Avicel (10)	NP	ND	0.29	ND	NA	30	0.45	Wang et al., 2010
	Rumen cellulose-degrading bacterial consortium						0.25			35	0.53	Wang et al., 2010
	Anaerobically Digested Sludge	Batch	37	α-cellulose (11.5)	NP	5.5	0.13	0.12	NA	ND	ND	Gupta et al., 2014
Lignocellulose	Anaerobic Digested Activated Sludge	Batch	35	Wheat stalk (60)	Milled to 40-mesh screen (powder)	6.5 ^b	0.92 ^c	5.56 ^d	43.9	46.6	1.44	Chu et al., 2011
	Anaerobic Digested Dairy Manure						1.46 ^c	7.97 ^d	43.9	75.2	2.33	
	Pretreated Lesser Panda Manure	CSBR	36	Corn stalk (15)	Biotreatment (Anaerobic microbes for 15 days)	5.5	ND	0.43	35.39	ND	ND	Fan et al., 2008

^a: No kinetics data, zero order assumed.

^b: pH controlled

^c: mmol H₂ g⁻¹ VS

^d: ml H₂ g⁻¹ VS d⁻¹

NP: No Pretreatment. Pretreatments presented belong only to lignocellulosic substrates

ND: Not Defined

NA: Not applicable. Cellulose percentage in substrate only applies to lignocellulosic substrates

CSBR: Continuously Stirred Bio-Reactor

Table 2.3: Operational and performance parameters of mesophilic pure cultures experiments on cellulose and lignocellulose

	Culture(s)	T (°C)	Substrate (g l ⁻¹)	pH	H ₂ yield (mol H ₂ mol ⁻¹ hexose _{eq.})	H ₂ production rate (l l ⁻¹ d ⁻¹)	Substrate removal efficiency (%)	Substrate degradation rate ^a (g l ⁻¹ d ⁻¹)	Ref.
Cellulose	<i>Clostridium acetobutylicum</i> X9	37	Cellulose (25)	7	0.58	21.33	68.3	10.56	Wang et al., 2008
	<i>Clostridium termitidis</i> CT1112	37	α-celullose (2)	7.2	0.62	0.085	100	0.51	Ramachandran et al., 2008
	<i>Enterococcus gallinarum</i> G1	37	Avicel (5)	6.5	0.13	0.63	42.6	0.51	Wang et al., 2009
	<i>Clostridium cellulolyticum</i> ATCC 35319	35	Avicel (5)	6.5	1.6	ND	46	0.16	Ren et al., 2007
	<i>Clostridium populeti</i> DSM 5832	35	Avicel (5)	6.5	1.4	ND	52	0.18	Ren et al., 2007
	<i>Ruminococcus albus</i> 7 ^d	37	Avicel (10.9)	6.7-6.8	1.58	16.52	70	1.18 ^b	Pavlostathis et al., 1988a
Ligno-cellulose	<i>Clostridium acetobutylicum</i> X9 ^e	37	Corn stalk powder	5	3.4 ^c	ND	47	ND	Ren et al., 2008

All experiments are reported as batch tests, unless specified the contrary.

^a: No kinetics data, zero order assumed. Only where specified the contrary

^b: d⁻¹. First order kinetics

^c: mmol/ g substrate

^d CSTR: Continuous stirred-tank reactor

^e Initial cellulose content in substrate was not defined by the authors. Pretreatment: steam explosion H₂SO₄ (1%, 121°C, 15psi, 2h)

ND: Not Defined

Table 2.4: Operational and performance parameters of thermophilic mixed cultures experiments on cellulose and lignocellulose

	Culture (s)	T (°C)	Substrate (g l ⁻¹)	Pretreatment	pH	H ₂ yield (mol H ₂ mol ⁻¹ hexose _{eq.})	H ₂ production rate (l l ⁻¹ d ⁻¹)	Initial cellulose % in substrate	Substrate removal efficiency (%)	Substrate degradation rate ^a (g l ⁻¹ d ⁻¹)	Ref.
Cellulose	Heat shocked mesophilic Anaerobically Digested Sludge	60	Cellulose (11.8)	NP	5.5	0.42	ND	NA	ND	ND	Gupta et al., 2015
Lignocellulose	Anaerobic Digested Sludge	55	Milled Corn stover (13.33)	Milled to powder	7	ND	0.11	36.5	46.8	0.62	Liu and Cheng 2010
				Microwave-assisted Water (90 min)			0.15	37.8	52.5	0.68	
				Microwave-assisted Acid (0.3N H ₂ SO ₄ , 45 min)			0.16	37.2	54.8	0.69	
				Thermal Acid (0.2N H ₂ SO ₄ , 90 min)		1.53	0.2	39.4	59	0.71	

Experiments are reported as batch tests

^a: No kinetics data, zero order assumed.

NP: No Pretreatment. Pretreatments presented belong only to lignocellulosic substrates

ND: Not Defined

NA: Not applicable. Cellulose percentage in substrate only applies to lignocellulosic substrates

Table 2.5: Operational and performance parameters of thermophilic pure cultures experiments on cellulose and lignocellulose

	Culture (s)	Reactor	T (°C)	Substrate (g l ⁻¹)	Pre-treatment	pH	H ₂ yield (mol H ₂ mol ⁻¹ hexose _{eq})	H ₂ production rate (l l ⁻¹ d ⁻¹)	Initial cellulose % in substrate	Substrate removal efficiency (%)	Substrate degradation rate ^a (g l ⁻¹ d ⁻¹)	Ref.
Cellulose	<i>Clostridium thermocellum</i> ATCC 27405	Batch	60	α-cellulose (1)	NP	7.2	1.9	0.18	NA	52	0.17	Islam et al., 2009
				α-cellulose (5)			1.28	0.16		24	0.38	
	<i>Thermotoga maritima</i> DSM 3109	Batch	80	Cellulose (5)	NP	6.5-7	0.04	ND	NA	28.6	ND	Nguyen et al., 2008
	<i>Thermotoga neapolitana</i> DSM 4359	Batch	75	Cellulose (5)	NP	6.5-7	0.056	ND	NA	33	ND	Nguyen et al., 2008
	<i>Clostridium thermocellum</i> ATCC 27405	CSTR	60	α-cellulose (1.5)	NP	7	0.98	0.2	NA	78	ND	Magnusson et al., 2009
α-cellulose (2)				1.65			0.4	69				
α-cellulose (3)				1.53			0.5	64				
α-cellulose (4)				1.29			0.66	76				
Lignocellulose	<i>Clostridium thermocellum</i> 7072	Batch	55	Corn stalk (30)	Milled to ≤ 1 mm	7.4	1.25	4.8	24	52.7	7.9	Cheng and Liu 2011
		CSTR 10 L					1.46	18.42		61.5	9.22	
		CSTR 100 L					1.54	17.75		63.5	9.52	
	<i>Clostridium thermocellum</i> 27405	Batch	60	Delignified wood fiber (0.1)	Not described	7	2.32	ND	ND	ND	ND	Levin et al., 2006
	<i>Clostridium thermocellum</i> DSMZ 1237	Batch	60	Pulp and Paper sludge (5)	None	7.2	0.67	ND	54	100	ND	Moreau et al., 2015

^a: No kinetics data, zero order assumed. NP: No Pretreatment. Pretreatments presented belong only to lignocellulosic substrates. ND: Not Defined. NA: Not applicable. Cellulose percentage in substrate only applies to lignocellulosic substrates. CSTR: Continuous Stirred Tank-Reactor. *C. thermocellum* DSMZ 1237 is the same strain *C. thermocellum* ATCC 27405

2.3.1.3.1 Use of Mixed Cultures and Pure Cultures

Hydrogen yield is highly influenced by the type of inoculum used, since the bacterial metabolism impacts the fermentation end products [Elsharnouby et al., 2013]. In natural cultures (mixed cultures) the metabolic flexibility of the mixed consortia is beneficial to use different substrates and tolerate environmental conditions [Masset et al., 2012]. Nevertheless, for the purpose of hydrogen production this may be at the same time a disadvantage by supporting other pathways different than acetate and butyrate, or even hydrogen consuming pathways like propionate. Moreover, as part of the variety of bacteria found in a mixed culture, methanogens (hydrogen consuming bacteria) are a big drawback for biohydrogen production [Wang et al., 2010]. The main advantage, however, is the non-dependency on aseptic conditions [Monlau et al., 2011].

Generally speaking, pure cultures have better hydrogen yields than mixed cultures using pure cellulose as substrate. As shown in Tables 2.2 and 2.4, mixed consortia that have been used to produce hydrogen from cellulose have achieved very low hydrogen yields, ranging from 0.13-0.42 mol H₂ mol⁻¹ hexose equivalent, as well as low substrate removal efficiencies (30-35%). Rumen liquor from cattle, anaerobically digested sludge (ADS) and rumen-cellulose degrading bacterial consortium are among them [Wang et al., 2010; Gupta et al., 2014; Gupta et al., 2015]. Efforts to improve hydrogen production are pretreatment of the inoculum at 70°C for 30 min to inhibit methanogens [Gupta et al., 2014], initial pH of 5.5 since it favors acidogenic bacteria and also inhibits methanogens [Gupta et al., 2015] (pH higher than 6 favours methanogens [Fang and Liu, 2002]), and enrichment by serially diluting the original mixed culture to obtain a functional consortium by Wang et al. [2010].

Wang et al. [2010] utilized rumen liquor from cattle to produce hydrogen at 38°C in a batch reactor. The authors obtained a hydrogen yield of 0.29 mol H₂ mol⁻¹ hexose and a 30% substrate removal efficiency in 50 hours of fermentation test. There was no apparent time lag but the gradual consumption of 27% of the hydrogen produced in the next 110 hours, indicated the possible presence of methanogens. The aforementioned authors performed the enrichment strategy consisting of serial dilutions to obtain the functional consortium of the original mixed culture called “rumen cellulose-degrading bacterial consortium”

(RCBC). RCBC DNA sequence was studied. The composition was *Ruminococcus* sp. as cellulose degrader and *Butyrivibrio* and/or *Succinivibrio* sp. as the hydrogen producers. RCBC yielded $0.25 \text{ mol H}_2 \text{ mol}^{-1}$ hexose and achieved 35% substrate removal efficiency. Although RCBC enhanced cellulose degradation, it did not enhance hydrogen production, hence the main advantage was that there was no consumption of hydrogen indicating no presence of methanogens.

Cellulolytic (cellulose-degrading) and non-cellulolytic bacteria coexist in natural environments. Cellulolytic strains, however, play a vital role in the ecosystem as the predominant polymer-degrading species [Bayer et al., 1994]. From Tables 2.3 and 2.5, it can be seen that hydrogen yields from pure cultures on cellulose have a wider range than mixed cultures, varying from $0.04 \text{ mol H}_2 \text{ mol}^{-1}$ hexose equivalent *Thermotoga maritima* to $1.9 \text{ mol H}_2 \text{ mol}^{-1}$ hexose equivalent by *Clostridium thermocellum*. Similarly, substrate removal efficiencies varied broadly, from 29% by *Thermotoga maritima* to 78 and 100% by *C. thermocellum* and *Clostridium termitidis*.

After the thermophilic *C. thermocellum*, the best cellulolytic bacteria appear to be the mesophilic *Clostridium cellulolyticum*, *Clostridium populeti* and *Ruminococcus albus* with hydrogen yields of 1.6, 1.4 and $1.58 \text{ mol H}_2 \text{ mol}^{-1}$ hexose equivalent, respectively, achieving a 46%, 52% and 70% substrate removal efficiency, respectively [Islam et al., 2009; Pavlostathis et al., 1988a; Ren et al., 2007]. In contrast, the hyperthermophilic *Thermotoga maritima* and *Thermotoga neapolitana*, and the mesophilic *Enterococcus gallinarum* achieved hydrogen yields as low as 0.04, 0.056 and $0.13 \text{ mol H}_2 \text{ mol}^{-1}$ hexose equivalent, respectively, with substrate removal efficiencies of 29, 33 and 43%, making evident their low cellulolytic capabilities and lack of suitability for CBP.

Lignocellulosic wastes have also been tested in both, pure and mixed cultures. For example, Fan et al. [2008] pretreated lesser panda manure by continuous aeration with forced-air pumping in order to inhibit hydrogen consumers and isolate the predominant hydrogen producing bacteria, which was subsequently used for fermentation of pretreated corn stalk, with 35% cellulose content, in a 5 liters continuously stirred bioreactor (CSBR) at 36°C and pH of 5.5, and achieved a hydrogen production rate of $0.43 \text{ l H}_2 \text{ g}^{-1} \text{ TS per}$

day. On the other hand, Ren et al. [2008] pretreated the same substrate, i.e. corn stalk, by steam explosion (1% H₂SO₄, 121°C, 15psi, 2h), to be used by *Clostridium acetobutylicum* X9 at 37°C and pH of 5 in a batch reactor and reached a hydrogen yield of 3.4 mmol H₂ g⁻¹ substrate.

2.3.1.3.2 Mesophilic and Thermophilic Conditions

Microbial cellulose utilization is affected by physical and chemical conditions in the environment and the effect of temperature is particularly important [Lynd et al., 2002]. Fermentations can be performed at mesophilic (25-40°C), thermophilic (40-65 °C) or hyperthermophilic (>80°C) temperatures [Sinha and Pandey, 2011].

Gupta et al. [2015] compared hydrogen production under mesophilic (37°C) and thermophilic (60°C) conditions using mesophilic anaerobic digester sludge and cellulose as substrates in batch fermentations. The hydrogen yields obtained were 0.13 and 0.42 mol H₂ mol⁻¹ hexose equivalent, respectively. This demonstrated the capability of mesophilic mixed cultures to withstand temperature changes.

With pure cultures, Islam et al. [2009] treated 5 g l⁻¹ α-cellulose with *Clostridium thermocellum* strain 27405 at pH 7.2 in a batch reactor yielding 1.28 mol H₂ mol⁻¹ hexose_{consumed}, hydrogen production rate of and 0.16 l l⁻¹ per day and a substrate removal efficiency of 24%. Ren et al. [2007] obtained a hydrogen yield of 1.6 mol H₂ mol⁻¹ hexose_{consumed} and a substrate removal efficiency of 68% with *Clostridium cellulolyticum* at 35°C and pH 6.5 from 5 g l⁻¹ of Avicel.

2.3.1.3.3 Bioreactor Type

Normally, in order to have a reference, experiments are performed in batch mode first since it is easier to manipulate the initial parameters and improvement can be done exactly where needed. The second step involves scaling up to a continuous flow system, since this is the closest imitation of industrial scale. It has been observed that continuous fermentation

significantly increases hydrogen production [Magnusson et al., 2009] but obstacles due to end-product inhibition, system stability, and methanogens contamination must be overcome [Kobayashi et al., 2012].

Initial substrate concentrations have been reported to affect the hydrogen yield and metabolic pathways. [Islam et al., 2009] compared the assimilation of α -cellulose by *C. thermocellum* ATCC 27405 in low (1 g l^{-1}) and high (5 g l^{-1}) initial substrate concentrations in batches at 60°C and pH of 7.2, and obtained 1.9 and $1.28 \text{ mol H}_2 \text{ mol}^{-1} \text{ hexose}_{\text{consumed}}$, respectively. The aforementioned authors observed higher substrate removal efficiency (52%) at low substrate concentration compared to 24% substrate removal at high concentrations. Also, formate and ethanol pathways were favored at low substrate concentration, explaining the lower hydrogen yield than at low substrate concentration. Likewise, Magnusson et al. [2009] produced hydrogen continuously using the same substrate and bacterial strain. Four experiments were run at similar conditions (5 liters working volume fermentor, 60°C , pH 7) with different carbon-loading concentrations (1.5, 2, 3 and 4 g l^{-1} of substrate), at an HRT of 24 h. Hydrogen yields were 0.98, 1.65, 1.53 and $1.29 \text{ mol H}_2 \text{ mol}^{-1} \text{ hexose consumed}$ and substrate removal efficiencies of 78, 69, 64 and 76%, respectively. It is worth to mention that both experiments observed less hydrogen production as substrate concentration increased, substrate removal efficiencies are higher in CSTR and carbon-loading of 2 g l^{-1} of cellulose appears to be optimum in a CSTR. Some problems were encountered when using cellulose in continuous flow bioreactors, such as temperature failures due to power outage, non-homogeneous mixing of the suspension of insoluble cellulose and clogging of the delivery line from feed reservoir to the bioreactor [Magnusson et al., 2009].

Cheng and Liu [2011] performed a successful scale-up of hydrogen fermentation from corn stalk by *C. thermocellum* at 55°C and pH of 7.4 from 125 ml bottles to a 10 l CSTR (6.5 l working volume), and then to a 100 l CSTR (60 l working volume). Corn stalk was milled to $\leq 1 \text{ mm}$ and used directly as substrate at 30 g l^{-1} . Hydrogen yields, hydrogen production rates and substrate removal efficiencies improved as the bioreactor size increased. The aforementioned authors reported hydrogen yields of 1.25, 1.46 and $1.54 \text{ mol H}_2 \text{ mol}^{-1} \text{ hexose}_{\text{consumed}}$ for 125 ml, 10 l and 100 l bioreactors respectively. More importantly, pilot-

scale hydrogen production with a working volume of 60 l from lignocellulose by pure cultures was proved.

2.3.1.3.4 Substrate

The use of lignocellulosic wastes has been used as substrates for fermentative biohydrogen production. Because lignocellulose has a more complex structure than pure cellulose, pretreatment is often required. Some experiments comparing the use of both substrates (cellulose and lignocellulose) by the same inoculum are discussed below.

C. thermocellum has been proved to be able to utilize wastes like corn stalk, delignified wood fibers and pulp and paper sludge. Levin et al. [2006] used delignified wood fibers as substrate for *C. thermocellum* ATCC 27405 at concentrations of 0.1, 1.1 and 4.5 g l⁻¹, obtaining hydrogen yields of 2.31, 1.47 and 0.99 mol H₂ mol⁻¹ hexose_{consumed}, respectively at 0.1 g l⁻¹, 60°C and pH 7. Moreau et al. [2015] investigated the use of pulp and paper sludge as substrate (5 g l⁻¹) by the same strain at 60°C and pH 7.2 and achieved a hydrogen yield of 0.67 mol H₂ mol⁻¹ hexose_{consumed} and 100% substrate removal efficiency.

Cheng and Liu [2011] used *Clostridium thermocellum* 7072 to produce hydrogen from microcrystalline cellulose and corn stalk without pretreatment (only milled). Both experiments were executed at 55°C, and a pH of 7.4 in 125 ml anaerobic bottles. The main difference lied in the concentration of substrate added, 30g l⁻¹ for corn stalk and 5 g l⁻¹ for microcrystalline cellulose. Corn stalk yielded 1.25 mol H₂ mol⁻¹ hexose_{consumed} and microcrystalline cellulose 1.2 mol H₂ mol⁻¹ hexose. These practically equal hydrogen yields from pure cellulose and lignocellulosic biomass were potentially caused because the corn stalk composition included 13% total soluble sugar which are easier to degrade than cellulose, and cellulose removal efficiency was less in lignocellulosic biomass (52.7 compared to >95%).

Inhibitors such as furan derivatives and phenolic compounds from the pretreatment of lignocellulose negatively affect hydrogen production. According to Quéméneur et al. (2012), furans exert a more negative effect than that induced by phenolic compounds.

These authors found that *Clostridium beijerinckii* strains resisted these inhibitors better than other Clostridial and non-clostridial bacteria did. Thus, *C. beijerinckii* is a promising microorganism for hydrogen production from lignocellulosic hydrolysates [Reginatto and Antonio, 2015].

2.3.1.3.5 Co-cultures

A deeper comparison of pure cultures can be done when using mono- and co-cultures. Specifically, for a complex substrate like cellulose it has been found that the use of cellulose degrading bacteria and high hydrogen producing from monosaccharides bacteria makes an improvement together [Wang et al., 2008; Geng et al., 2010; Li and Liu, 2012; Liu et al., 2008]. Table 2.6 shows the comparison of mono-cultures against co-cultures experiments for biohydrogen production from cellulose. For example, Liu et al. [2008] demonstrated the synergy between the thermophiles *Clostridium thermocellum* JN4 and *Thermoanaerobacterium thermosaccharolyticum* GD17 when microcrystalline cellulose was used as substrate in a batch reactor at 60°C and pH of 4.4. Hydrogen yield and hydrogen production rate increased from 0.8 to 1.8 mol H₂ mol⁻¹ hexose_{consumed} and from 0.08 to 0.34 l l⁻¹ per day, respectively. Substrate removal efficiencies were 100%, corresponding to a substrate degradation rate of 1.14 g l⁻¹ per day in both experiments. The aforementioned tests were performed with corn stalk powder and corn cob powder as feedstocks. Co-cultures also showed an improvement in degrading cellulose and producing hydrogen compared with JN4 monoculture. Both strains could utilize cellulosic biomass, however, not as efficiently as microcrystalline cellulose.

The best pure cellulose degradation rate reported in the literature was achieved by the co-culture *Clostridium acetobutylicum* X9 (cellulose degrader and hydrogen producer) and *Ethanoigenes harbinense* B49 (hydrogen producer from simple sugars). At 37°C and pH of 7 in a batch reactor, the degradation rate was 25.86 g cellulose l⁻¹ per day [Wang et al., 2008].

Table 2.6: Operational and performance parameters of co-culture experiments under mesophilic and thermophilic conditions

	Culture(s)	T (°C)	Reactor	Substrate (g l ⁻¹)	pH	H ₂ yield (mol H ₂ mol ⁻¹ hexose _{eq.})	H ₂ production rate (l l ⁻¹ d ⁻¹)	Substrate removal efficiency (%)	Substrate degradation rate ^a (g l ⁻¹ d ⁻¹)	Ref.
Mesophilic	<i>Clostridium acetobutylicum</i> X9	37	Batch	Cellulose (25)	7	0.58	21.33	68.3	10.56	Wang et al., 2008
	<i>Clostridium acetobutylicum</i> X9 + <i>Ethanoigenens harbinense</i> B49					1.31	11.08	77.6	25.86	
	<i>Enterococcus gallinarum</i> G1	37	Batch	Avicel (5)	6.5	0.13	0.63	42.6	0.51	Wang et al., 2009
	<i>Enterococcus gallinarum</i> G1 + <i>Ethanoigenens harbinense</i> B49					0.23	1.22	53.8	0.64	
Thermophilic	<i>C. thermocellum</i> DSM 1237 + <i>Clostridium thermopalmarium</i> DSM 5974	55	Batch	Filter paper (α -cellulose) (9)	6.92	1.36	0.42	90	2.45	Geng et al., 2010
	<i>Clostridium thermocellum</i> JN4	60	Batch	Microcrystalline cellulose (5)	4.4	0.8	0.08	100	1.14	Liu et al., 2008
	<i>C. thermocellum</i> JN4 + <i>Thermoanaerobacterium thermosaccharolyticum</i> GD17					1.8	0.34			
	<i>C. thermocellum</i> DSM 7072 + <i>Clostridium thermosaccharolyticum</i> DSM 869	55	Batch	Milled to 1 mm powder corn stalk (10). 31.5% cellulose	7.2	ND	0.34	41.6	0.26	Li and Liu 2012
CSTR			0.44				43.7	0.27		

^a: No kinetics data, zero order assumed.

ND: Not Defined

CSTR: Continuous Stirred Tank-Reactor

Li and Liu [2012] performed a comparative study in continuous-flow production of hydrogen with a batch experiment as its counterpart, using corn stalk without pretreatment but milled to 1 mm powder. The co-culture used was *Clostridium thermocellum* and *Clostridium thermosaccharolyticum*. Conditions were the same in both reactors (temperature 55°C, substrate concentration of 10 g l⁻¹ and a pH of 7.2). Both hydrogen production and cellulose degradation rates in the continuous-flow system of 0.44 l H₂ l⁻¹ per day and 43.71 g l⁻¹ per day were significantly higher than the 0.34 l H₂ l⁻¹ per day and 0.26 g l⁻¹ per day observed in batches. The success of co-culturing in batch tests is very promising for continuous flow system.

Ramachandran et al. [2008] reported the hydrogen production by *Clostridium termitidis* from α -cellulose, achieving a relatively low hydrogen yield of 0.62 mol H₂ mol⁻¹ hexose equivalent compared to the other mesophilic cellulolytic bacteria. Nevertheless, it is worth to mention that this strain achieved the highest substrate removal efficiency (100%) at mesophilic temperatures, emphasizing its cellulolytic activity and potential use for co-culture.

2.4 Modeling Microbial Kinetics

Models are mathematical relationships between variables, regularly built from “theoretical” relationships that gives the structure and experimental observations and sets a numerical value to the coefficients [Doran, 2013]. Mathematical modeling is a demonstrated tool in the quantitative analysis of complex processes such as fermentations [Huang and Wang, 2010].

Temperature has a great influence on metabolic rates since it can change the arrangement of cell components, mainly membrane constituents and proteins [Doran, 2013], hence the importance of maintaining a stable temperature when determining microbial kinetics. Although growth rates depends on medium pH, the maximum growth rate is generally keep unchanged over 1 to 2 pH units but declines with further variation [Doran, 2013].

Models are broadly classified as structured and unstructured [Shuler and Kargı, 2002]. Structure models describe growth-associated changes in microbial cell composition, which means including mass-balance equations for all intracellular components [Panikov, 2002]. In contrast, unstructured models describe the simplest manifestation of growth [Panikov, 2002]. The degree of complexity of the model depends on what is needed to be described, prioritizing the simplest model that can adequately describe the desired phenomena is the goal [Shuler and Kargı, 2002]. Monod model is an empirical and unstructured model [Panikov, 2002], and is the most common model relating microbial growth rate and substrate concentration [Doran, 2013]. Equations 2.11 and 2.12 describe microbial growth and substrate consumption by Monod, respectively.

$$\frac{dX}{dt} = \frac{\mu_{max}SX}{K_s+S} - k_dX \quad 2.11$$

$$\frac{dS}{dt} = \frac{-\mu_{max}SX}{Y_{X/S}(K_s+S)} \quad 2.12$$

where μ_{max} (h^{-1}) is the maximum specific growth rate, K_s ($g\ l^{-1}$) is the saturation constant or half-velocity constant and is equal to the concentration of the rate-limiting substrate when the specific growth rate is equal to one half of the maximum, k_d (h^{-1}) is the decay coefficient, and $Y_{X/S}$ (g dry weight g^{-1} substrate consumed) is the biomass yield [Shuler and Kargı, 2002]. Monod model considers a growth-limiting substrate found in excess and its complete utilization. This is the case for soluble substrates like glucose and cellobiose. Nevertheless, when using insoluble substrates like cellulose, Monod approach cannot be used since only 1 in 3,000 β -glucosidic bonds is accessible [Lynd et al., 2002]. Other approaches have been investigated. For example, Holwerda and Lynd [2013] tested three alternative kinetic models for cellulose utilization by *C. thermocellum*:

1. Constant specific growth rate. First order in cells:

$$\frac{dX}{dt} = \mu X \quad 2.13$$

$$\frac{dS}{dt} = -\frac{1}{Y_{X/S}} \frac{dX}{dt} \quad 2.14$$

Equations 2.13 and 2.14 were able to fit experimental data well in the early stage of the fermentation, but not during the later stages.

2. Substrate utilization first order in substrate:

$$\frac{dS}{dt} = -k_1 S \quad 2.15$$

$$\frac{dX}{dt} = -Y_{X/S} \frac{dS}{dt} \quad 2.16$$

where k_1 is the reaction rate constant (h^{-1}). Equations 2.15 and 2.16 were able to fit the experimental substrate data well only during the late but failed to fit the biomass growth.

3. Substrate utilization first order in substrate and first order in cells, second order overall:

$$\frac{dS}{dt} = -k_2 SX \quad 2.17$$

$$\frac{dX}{dt} = -Y_{X/S} \frac{dS}{dt} - k_e X \quad 2.18$$

where k_2 is the reaction constant ($1 \text{ g}^{-1} \text{ biomass h}^{-1}$), k_e is the endogenous metabolism constant (h^{-1}). Equations 2.17 and 2.18 fit the data very well, but over-predicted biomass growth. Holwerda and Lynd [2013] corrected the discrepancy by adding an endogenous metabolism term and claimed this descriptive model could also be applied for lignocellulosic substrates.

2.5 Conclusions

Biohydrogen production from cellulose by pure cultures has shown higher hydrogen yields than by mixed cultures. Moreover, among the strategies to improve hydrogen production, the use of co-cultures has shown promise compared to the use of the cellulolytic strains alone. Nevertheless, the highest hydrogen yields have been achieved by thermophiles. Since thermophilic operation is considered to be technically unfavorable [Hawkes et al., 2007], investigation on hydrogen production at mesophilic conditions by co-cultures is of interest.

This study provides fundamental kinetic information and product yields that can be used for the design and optimization of bioreactor systems with pure cultures of *Clostridium termitidis* and *Clostridium beijerinckii*.

2.6 References

- Azbar N., Levin D.B. (2012) State of the art and progress in production of biohydrogen. Bentham Science Publishers, US
- Bayer E.A., Morag E., Lamed R. (1994) The cellulosome — A treasure-trove for biotechnology. ENGLAND: Elsevier Ltd
- Boopathy R. (1998) Biological treatment of swine waste using anaerobic baffled reactors. Bioresour Technol 64:1-6
- Brown R.M., Saxena I.M., Kudlicka K. (1996) Cellulose biosynthesis in higher plants. Trends Plant Sci 1:149-156
- Carere C.R., Sparling R., Cicek N., Levin D.B. (2008) Third generation biofuels via direct cellulose fermentation. International Journal of Molecular Sciences 9:1342-1360
- Chaubey R., Sahu S., James O.O., Maity S. (2013) A review on development of industrial processes and emerging techniques for production of hydrogen from renewable and sustainable sources. Renewable and Sustainable Energy Reviews 23:443-462

- Cheng X.-Y., Liu C.-Z. (2011) Hydrogen production via thermophilic fermentation of cornstalk by *Clostridium thermocellum*. *Energy Fuels* 25:1714-1720
- Cheung S.W., Anderson B.C. (1997) Laboratory investigation of ethanol production from municipal primary wastewater solids. *Bioresour Technol* 59:81-96
- Chu Y., Wei Y., Yuan X., Shi X. (2011) Bioconversion of wheat stalk to hydrogen by dark fermentation: Effect of different mixed microflora on hydrogen yield and cellulose solubilisation. *Bioresour Technol* 102:3805-3809
- Demain A.L., Newcomb M., Wu J. (2005) Cellulase, clostridia, and ethanol. *Microbiology and Molecular Biology Reviews* 69:124
- Desvaux M. (2005) *Clostridium cellulolyticum*: model organism of mesophilic cellulolytic clostridia. *FEMS Microbiol Rev* 29:741-764
- Dewes T., Hünsche E. (1998) Composition and Microbial Degradability in the Soil of Farmyard Manure from Ecologically-Managed Farms. *Biological Agriculture & Horticulture* 16:251-268
- Doran P.M. (2013) *Bioprocess engineering principles*. Academic Press, Waltham, MA
- Duff S.J.B., Murray W.D. (1996) Bioconversion of forest products industry waste cellulose to fuel ethanol: a review. *Bioresource Technology* 55:1-33
- Elsharnouby O., Hafez H., Nakhla G., El Naggar M.H. (2013) A critical literature review on biohydrogen production by pure cultures. *Int J Hydrogen Energy* 38:4945-4966
- Eroglu E., Melis A. (2011) Photobiological hydrogen production: Recent advances and state of the art. *Bioresour Technol* 102:8403-8413
- Ewan B.C.R., Allen R.W.K. (2005) A figure of merit assessment of the routes to hydrogen. *Int J Hydrogen Energy* 30:809-819

- Fan Y.-T., Xing Y., Ma H.-C., Pan C.-M., Hou H.-W. (2008) Enhanced cellulose-hydrogen production from corn stalk by lesser panda manure. *Int J Hydrogen Energy* 33:6058-6065
- Fan Z., South C., Lyford K., Munsie J., Van walsum P., Lynd L. (2003) Conversion of paper sludge to ethanol in a semicontinuous solids-fed reactor. *Bioprocess Biosystems Eng* 26:93-101
- Fang H.H.P. (2010) Environmental anaerobic technology: applications and new developments. Imperial College Press, Hackensack, NJ; London; Singapore
- Fang H.H.P., Liu H. (2002) Effect of pH on hydrogen production from glucose by a mixed culture. *Bioresour Technol* 82:87-93
- Geng A., He Y., Qian C., Yan X., Zhou Z. (2010) Effect of key factors on hydrogen production from cellulose in a co-culture of *Clostridium thermocellum* and *Clostridium thermopalmarium*. *Bioresour Technol* 101:4029-4033
- Guo X.M., Trably E., Latrille E., Carrère H., Steyer J.P. (2010) Hydrogen production from agricultural waste by dark fermentation: A review. *Int J Hydrogen Energy* 35:10660-10673
- Gupta M., Gomez-Flores M., Nasr N., Elbeshbishy E., Hafez H., Hesham El Naggar M., Nakhla G. (2015) Performance of mesophilic biohydrogen-producing cultures at thermophilic conditions. *Bioresour Technol* 192:741
- Gupta M., Velayutham P., Elbeshbishy E., Hafez H., Khafipour E., Derakhshani H., El Naggar M.H., Levin D.B., Nakhla G. (2014) Co-fermentation of glucose, starch, and cellulose for mesophilic biohydrogen production. *Int J Hydrogen Energy* 39:20958-20967
- Hafez H., Nakhla G., Naggar H.E. (2009) Biological Hydrogen Production from Corn-Syrup Waste Using a Novel System. *Energies* 2:445-455

- Hafez H., Nakhla G., El Naggar H., Ibrahim G., Said S.E.H.E. (2014) Biological Hydrogen Production:: Light-Driven Processes. Handbook of Hydrogen Energy. CRC Press,
- Hallenbeck P.C. (2009) Fermentative hydrogen production: Principles, progress, and prognosis. *Int J Hydrogen Energy* 34:7379-7389
- Hallenbeck P.C. (2011) Microbial paths to renewable hydrogen production. *Biofuels* 2:285-302
- Hallenbeck P.C., Abo-Hashesh M., Ghosh D. (2012) Strategies for improving biological hydrogen production. *Bioresour Technol* 110:1-9
- Hallenbeck P.C., Ghosh D. (2012) Improvements in fermentative biological hydrogen production through metabolic engineering. *J Environ Manage* 95, Supplement:S360-S364
- Hawkes D.L., Hawkes F.R., Hussy I., Kyazze G., Dinsdale R. (2007) Continuous dark fermentative hydrogen production by mesophilic microflora: Principles and progress. *Int J Hydrogen Energy* 32:172-184
- Holwerda E.K., Lynd L.R. (2013) Testing alternative kinetic models for utilization of crystalline cellulose (Avicel) by batch cultures of *Clostridium thermocellum*. *Biotechnol Bioeng* 110:2389-2394
- Huang W.-H., Wang F.-S. (2010) Kinetic modeling of batch fermentation for mixed-sugar to ethanol production. *Journal of the Taiwan Institute of Chemical Engineers* 41:434-439
- Islam R., Cicek N., Sparling R., Levin D. (2009) Influence of initial cellulose concentration on the carbon flow distribution during batch fermentation by *Clostridium thermocellum* ATCC 27405. *Appl Microbiol Biotechnol* 82:141-148
- Junghare M., Subudhi S., Lal B. (2012) Improvement of hydrogen production under decreased partial pressure by newly isolated alkaline tolerant anaerobe, *Clostridium*

- butyricum TM-9A: Optimization of process parameters. *Int J Hydrogen Energy* 37:3160-3168
- Kaur P.P., Arneja J.S., Singh J. (1998) Enzymic hydrolysis of rice straw by crude cellulase from *Trichoderma reesei*. *Bioresour Technol* 66:267-269
- Kobayashi T., Xu K.-Q., Li Y.-Y., Inamori Y. (2012) Evaluation of hydrogen and methane production from municipal solid wastes with different compositions of fat, protein, cellulosic materials and the other carbohydrates. *International Journal of Hydrogen Energy* 37:15711-15718
- Kumar N., Das D. (2000) Enhancement of hydrogen production by *Enterobacter cloacae* IIT-BT 08. *Process Biochem* 35:589-593
- Kumar R., Singh S., Singh O. (2008) Bioconversion of lignocellulosic biomass: biochemical and molecular perspectives. *Journal of Industrial Microbiology & Biotechnology* 35:377-391
- Kvesitadze G., Sadunishvili T., Dudauro T., Zakariashvili N., Partskhaladze G., Ugrekhelidze V., Tsiklauri G., Metreveli B., Jobava M. (2012) Two-stage anaerobic process for bio-hydrogen and bio-methane combined production from biodegradable solid wastes. *Energy* 37:94-102
- Lee S., Shah Y.T. (2013) *Biofuels and Bioenergy: Processes and Technologies*. Taylor and Francis Group CRC Press, Boca Raton, Florida
- Leschine S.B. (1995) Cellulose Degradation in Anaerobic Environments. *Annual Review of Microbiology* 49:399-426
- Levin D.B., Islam R., Cicek N., Sparling R. (2006) Hydrogen production by *Clostridium thermocellum* 27405 from cellulosic biomass substrates. *Int J Hydrogen Energy* 31:1496-1503
- Levin D.B., Pitt L., Love M. (2004) Biohydrogen production: prospects and limitations to practical application. *Int J Hydrogen Energy* 29:173-185

- Li Q., Liu C.-Z. (2012) Co-culture of *Clostridium thermocellum* and *Clostridium thermosaccharolyticum* for enhancing hydrogen production via thermophilic fermentation of cornstalk waste. *Int J Hydrogen Energy* 37:10648-10654
- Liu C.-z., Cheng X.-y. (2010) Improved hydrogen production via thermophilic fermentation of corn stover by microwave-assisted acid pretreatment. *Int J Hydrogen Energy* 35:8945-8952
- Liu H., Hu H., Chignell J., Fan Y. (2010) Microbial electrolysis: novel technology for hydrogen production from biomass. *Biofuels* 1:129-142
- Liu Y., Yu P., Song X., Qu Y. (2008) Hydrogen production from cellulose by co-culture of *Clostridium thermocellum* JN4 and *Thermoanaerobacterium thermosaccharolyticum* GD17. *Int J Hydrogen Energy* 33:2927-2933
- Logan B.E., Oh S.E., Kim I.S., Van Ginkel S. (2002) Biological hydrogen production measured in batch anaerobic respirometers. *Environ Sci Technol* 36:2530-2535
- Lynd L.R., Weimer P.J., Van Zyl W.H., Pretorius I.S. (2002) Microbial Cellulose Utilization: Fundamentals and Biotechnology. *Microbiology and Molecular Biology Reviews* 66
- Magnusson L., Cicek N., Sparling R., Levin D. (2009) Continuous hydrogen production during fermentation of [alpha]- cellulose by the thermophilic bacterium *Clostridium thermocellum*. *Biotechnol Bioeng* 102:759
- Magnusson L., Islam R., Sparling R., Levin D., Cicek N. (2008) Direct hydrogen production from cellulosic waste materials with a single-step dark fermentation process. *Int J Hydrogen Energy* 33:5398-5403
- Martínez-Duart J.M., Guerrero-Lemus R. (2013) Renewable Energies and CO₂: Cost Analysis, Environmental Impacts and Technological Trends (2012 Edition). Springer London,

- Masset J., Calusinska M., Hamilton C., Hiligsmann S., Joris B., Wilmotte A., Thonart P. (2012) Fermentative hydrogen production from glucose and starch using pure strains and artificial co-cultures of *Clostridium* spp. *Biotechnology for Biofuels* 5:1-15
- Mckendry P. (2002) *Energy production from biomass (part 1): overview of biomass*. England: Elsevier Ltd
- Monlau F., Barakat A., Trably E., Dumas C., Steyer J.-P., Carrère H. (2011) Lignocellulosic Materials Into Biohydrogen and Biomethane: Impact of Structural Features and Pretreatment. *Critical Reviews in Environmental Science and Technology* 43:260-322
- Moreau A., Montplaisir D., Sparling R., Barnabé S. (2015) Hydrogen, ethanol and cellulase production from pulp and paper primary sludge by fermentation with *Clostridium thermocellum*. *Biomass Bioenergy* 72:256-262
- Nguyen T.-A.D., Kim K.-R., Kim M.S., Sim S.J. (2010) Thermophilic hydrogen fermentation from Korean rice straw by *Thermotoga neapolitana*. *Int J Hydrogen Energy* 35:13392-13398
- Nguyen T.A.D., Pyo Kim J., Sun Kim M., Kwan Oh Y., Sim S.J. (2008) Optimization of hydrogen production by hyperthermophilic eubacteria, *Thermotoga maritima* and *Thermotoga neapolitana* in batch fermentation. *Int J Hydrogen Energy* 33:1483-1488
- Ntaikou I., Antonopoulou G., Lyberatos G. (2010) Biohydrogen Production from Biomass and Wastes via Dark Fermentation: A Review. *Waste and Biomass Valorization* 1:21-39
- Panikov N.S. (2002) *Kinetics, Microbial Growth*. *Encyclopedia of Bioprocess Technology*. John Wiley & Sons, Inc.,

- Pavlostathis S.G., Miller T.L., Wolin M.J. (1988a) Fermentation of Insoluble Cellulose by Continuous Cultures of *Ruminococcus albus*. *Appl Environ Microbiol* 54:2655-2659
- Pavlostathis S.G., Miller T.L., Wolin M.J. (1988b) Kinetics of insoluble cellulose fermentation by continuous cultures of *Ruminococcus albus*. *Appl Environ Microbiol* 54:2660-2663
- Ramachandran U., Wrana N., Cicek N., Sparling R., Levin D.B. (2008) Hydrogen production and end-product synthesis patterns by *Clostridium termitidis* strain CT1112 in batch fermentation cultures with cellobiose or α -cellulose. *Int J Hydrogen Energy* 33:7006-7012
- Reginatto V., Antonio R.V. (2015) Fermentative hydrogen production from agroindustrial lignocellulosic substrates. *Braz J Microbiol* 46:323-335
- Ren N., Wang A., Cao G., Xu J., Gao L. (2009) Bioconversion of lignocellulosic biomass to hydrogen: Potential and challenges. *Biotechnology Advances* 27:1051-1060
- Ren N., Wang A., Gao L., Xin L., Lee D.-J., Su A. (2008) Bioaugmented hydrogen production from carboxymethyl cellulose and partially delignified corn stalks using isolated cultures. *Int J Hydrogen Energy* 33:5250-5255
- Ren Z., Ward T.E., Logan B.E., Regan J.M. (2007) Characterization of the cellulolytic and hydrogen-producing activities of six mesophilic *Clostridium* species. *Journal of Applied Microbiology* 103:2258-2266
- Sanderson M.A., Schmer M., Owens V., Keyser P., Elbersen W. (2012) Crop Management of Switchgrass. *In: Monti, A. (ed.) Switchgrass: Valuable Biomass Crop for Energy*. London: Springer-Verlag
- Schwarz W.H. (2001) The cellulosome and cellulose degradation by anaerobic bacteria. *Appl Microbiol Biotechnol* 56:634-649

- Shuler M.L., Kargi F. (2002) Bioprocess engineering: basic concepts. Second ed. Prentice Hall PTR, Upper Saddle River, NJ
- Sims R.E.H., Hastings A., Schlamadinger B., Taylor G., Smith P. (2006) Energy crops: current status and future prospects. *Global Change Biology* 12:2054-2076
- Sinha P., Pandey A. (2011) An evaluative report and challenges for fermentative biohydrogen production. *Int J Hydrogen Energy* 36:7460-7478
- Sørensen B. (2012) Hydrogen and fuel cells: emerging technologies and applications. Academic Press, Amsterdam; Boston, MA
- Sun Y., Cheng J. (2002) Hydrolysis of lignocellulosic materials for ethanol production: a review. England: Elsevier Ltd
- Terinte N., Ibbett R., Schuster K.C. (2011) Overview on native cellulose and microcrystalline cellulose I structure studied by X-ray diffraction (WAXD): Comparison between measurement techniques. *Lenzinger Berichte* 89:118-131
- Torres C.I., Kato Marcus A., Rittmann B.E. (2007) Kinetics of consumption of fermentation products by anode-respiring bacteria. *Appl Microbiol Biotechnol* 77:689-697
- Ueno Y., Kawai T., Sato S., Otsuka S., Morimoto M. (1995) Biological production of hydrogen from cellulose by natural anaerobic microflora. *J Ferment Bioeng* 79:395-397
- Vavilin V.A., Rytow S.V., Lokshina L.Y. (1995) Modelling hydrogen partial pressure change as a result of competition between the butyric and propionic groups of acidogenic bacteria. *Bioresour Technol* 54:171-177
- Wang A., Gao L., Ren N., Xu J., Liu C. (2009) Bio-hydrogen production from cellulose by sequential co-culture of cellulosic hydrogen bacteria of *Enterococcus gallinarum* G1 and *Ethanoigenens harbinense* B49. *Biotechnol Lett* 31:1321-1326

- Wang A., Gao L., Ren N., Xu J., Liu C., Lee D.-J. (2010) Enrichment strategy to select functional consortium from mixed cultures: Consortium from rumen liquor for simultaneous cellulose degradation and hydrogen production. *Int J Hydrogen Energy* 35:13413-13418
- Wang A.J., Ren N.Q., Shi Y.G., Lee D.J. (2008) Bioaugmented hydrogen production from microcrystalline cellulose using co-culture - *Clostridium acetobutylicum* X-9 and *Etilanoigenens harbinense* B-49. *Int J Hydrogen Energy* 33:912-917
- Yang N., Hafez H., Nakhla G. (2015) Impact of volatile fatty acids on microbial electrolysis cell performance. *Bioresour Technol* 193:449-455
- Zannoni D., De Philippis R. (2014) *Microbial bioenergy: hydrogen production*. Springer, Dordrecht; New York
- Zhu J., Wan C., Li Y. (2010) Enhanced solid-state anaerobic digestion of corn stover by alkaline pretreatment. *Bioresour Technol* 101:7523-7528

Chapter 3

3 Microbial Kinetics of *Clostridium termitidis* on Cellobiose and Glucose for Biohydrogen Production¹

3.1 Introduction

Fermentative H₂ production from carbohydrate-rich wastes is attracting the attention due to its environmental impact and high energy content. Among carbohydrates, cellulose is the most abundant [Fang, 2010] and biohydrogen production from lignocellulosic wastes would be sustainable. The primary hydrolysis product of cellulose is cellobiose, which comprises two glucose molecules [Levin et al., 2009].

The most complex and best investigated cellulosome (a multi-enzyme complex capable of hydrolyzing cellulose) is that of the thermophilic bacterium *Clostridium thermocellum* [Schwarz, 2001]. A number of anaerobic, mesophilic, cellulolytic bacteria have been isolated and described. These include *Clostridium cellulolyticum*, *C. cellulovorans*, *C. phytofermentans*, and *C. termitidis* [Levin et al., 2009]. All utilize cellulose, cellobiose and glucose as carbon sources [Giallo et al., 1985; Hethener et al., 1992; Sleat et al., 1984; Warnick et al., 2002].

Hethener et al. [1992] reported the isolation of the mesophile, *Clostridium termitidis*, from the gut of a wood-feeding termite, *Nasutitermes lujae*, and described it as an anaerobic, spore-forming, cellulolytic bacterium able to utilize cellulose, cellobiose, glucose, fructose, etc. to produce acetate, ethanol, H₂ and CO₂.

There are only 4 publications focused on *Clostridium termitidis* strain CT1112. Ramachandran et al. [2008] studied the end-product synthesis and H₂ production from cellobiose and cellulose adding lactate and formate to the previously reported end-products [Hethener et al., 1992] and obtained maximum yields of acetate, ethanol, H₂ and formate from cellobiose of 5.9, 3.7, 4.6 and 4.2 mmol l⁻¹ culture, respectively, with respective yields

¹ Published in Biotechnology Letters. Gomez-Flores M., Nakhla G., Hafez H. (2015) Microbial kinetics of *Clostridium termitidis* on cellobiose and glucose for biohydrogen production. Biotechnol Lett:1-7

from cellulose of 7.2, 3.1, 7.7 and 2.9 mmol l⁻¹ culture, respectively. Lal et al. [2013] reported the draft genome sequence of *Clostridium termitidis*, while recently, Munir et al. [2014] analyzed *Clostridium termitidis* for carbohydrate-active enzymes (CAZymes) and cellulosomal components, identifying significantly higher 355 CAZymes sequences than other Clostridial species.

Growth kinetics of the various mesophilic cellulose-degrading microorganisms excluding *Clostridium termitidis* have been studied [Alalayah et al., 2010; Lin et al., 2007; Srivastava and Volesky, 1990; Yang and Tsao, 1994], Thus, the aim of this study was to obtain the Monod kinetic parameters (μ_{\max} , K_s , k_d and $Y_{X/S}$) of *C. termitidis* to facilitate the engineering design of bioreactors.

3.2 Materials and Methods

3.2.1 Microbial Strain and Media

The strain used was *Clostridium termitidis* ATCC 51846. All chemicals for media and substrates were obtained from Sigma-Aldrich Co. Fresh cells were maintained by successively transferring 10% (v/v) of inoculum to ATCC 1191 medium containing filter-sterilized glucose or cellobiose at 2 g l⁻¹. This medium contained (per liter of distilled water): KH₂PO₄, 1.5 g; Na₂HPO₄, 3.35 g; NH₄Cl, 0.5 g; MgCl₂.6H₂O, 0.18 g; yeast extract, 2 g; 0.25 ml 1 g resazurin l⁻¹; mineral solution, 1 ml; vitamin solution, 0.5 ml, and L-cysteine, as reducing agent, 1 g. The mineral solution contained (g per 500 ml): trisodium nitrilotriacetate 10.1; FeCl₃.6H₂O, 1.05; CoCl₂.6. H₂O, 1; MnCl₂.4H₂O, 0.5; ZnCl₂, 0.5; NiCl₂.6H₂O, 0.5; CaCl₂.2H₂O, 0.25; CuSO₄.5H₂O, 0.32; and Na₂MoO₄.2H₂O, 0.25. The vitamin solution contained (mg per 500 ml): pyridoxine-HCl, 50; riboflavin, 25; thiamine, 25; nicotinic acid, 25; *p*-aminobenzoic acid, 25; lipoic acid (thioctic acid), 25; biotin, 10; folic acid, 10; and cyanocobalamin, 5. The initial pH was 7.2 but was not controlled during growth.

3.2.2 Experimental Conditions

Batch anaerobic fermentations were performed in serum bottles (Wheaton) with a working volume of 400 ml and 310 ml of headspace. Bottles containing 344 ml of ATCC 1191 medium were tightly capped with rubber stoppers, degassed by applying vacuum and sparged with high purity N₂ gas, and autoclaved. Duplicate bottles were inoculated with 10% (v/v) of fresh cultures. Bottles were incubated at 37°C and 90 rpm for 48 h when grown with glucose and 58 h when grown with cellobiose.

3.2.3 Analytical Methods

Cell growth was monitored by measuring the OD₆₀₀ value, cellular protein content, and dry weight. Duplicates using the 1191 Media with the same concentration of glucose or cellobiose without the culture subjected to the same procedure as the fermentation bottles, served as controls. To measure proteins, samples were placed in microcentrifuge tubes and centrifuged at 10,000×g for 15 min. Supernatants were discarded and pellets re-suspended with 0.9% (w/v) NaCl and centrifuged at the same aforementioned conditions. Supernatants were discarded; 1 ml 0.2 M NaOH was added to microcentrifuge tubes and vortexed to re-suspend the pellet. Microcentrifuge tubes were held at 100°C for 10 min. When cool, samples were analyzed following the Bradford method. Soluble samples (filtered through 0.45 µm) were used to analyze for glucose and cellobiose. Glucose was measured using a UV-test kit and cellobiose was measured by the phenol sulfuric acid method. Chemical Oxygen Demand (COD) was measured using a standard kit (Hach Co.).

3.2.4 Gas Measurements

Gas volume was measured by releasing the gas pressure in the bottles using appropriately sized glass syringes in the range of 5-100 ml to equilibrate with the ambient pressure [Owen et al., 1979]. H₂ analysis was conducted by employing a gas chromatograph equipped with a thermal conductivity detector (TCD) and a molecular sieve column (Mole sieve 5A, mesh

80/100, 1.83 m x 0.32 cm). The temperatures of the column and the TCD detector were 90 and 105 °C, respectively. Argon was used as the carrier gas at a flow rate of 30 ml/min.

H₂ gas production was calculated from headspace measurements of gas composition and the total volume of biogas produced, at each time interval, using the mass balance equation.

$$V_{H_2,i} = V_{H_2,i-1} + C_{H_2,i} * V_{G,i} + V_{h,i}(C_{H_2,i} - C_{H_2,i-1}) \quad 3.1$$

where $V_{H_2,i}$ and $V_{H_2,i-1}$ are cumulative H₂ gas volumes at the current (i) and previous (i - 1) time intervals. $V_{G,i}$ is the total biogas volume accumulated between the previous and current time intervals. $C_{H_2,i}$ and $C_{H_2,i-1}$ are the fractions of H₂ gas in the headspace of the reactor in the current and previous intervals, and $V_{h,i}$ is the total volume of the headspace of the reactor in the current interval [López et al., 2007].

3.2.5 Modeling

Monod kinetics parameters (μ_{max} , K_s , k_d and $Y_{X/S}$) were determined by using MATLAB R2014a. The objective function employed was *lsqcurvefit*, a non-linear least square fit. The solver function used to estimate numerical integration of the ordinary differential equations (Equations 3.2 and 3.3) was *Ode45*, which implements fourth/fifth order Runge-Kutta methods. A first approximation for the Monod kinetics parameters was obtained by linearization with Lineweaver-Burk plots in Excel; these results were used as the initial conditions in MATLAB.

$$\frac{dX}{dt} = \frac{\mu_{max}SX}{K_s+S} - k_dX \quad 3.2$$

$$\frac{dS}{dt} = \frac{-\mu_{max}SX}{Y_{X/S}(K_s+S)} \quad 3.3$$

where μ_{max} (h⁻¹) is the maximum specific growth rate, K_s (g l⁻¹) is the saturation constant or half-velocity constant and is equal to the concentration of the rate-limiting substrate when the specific growth rate is equal to one half of the maximum, k_d (h⁻¹) is the decay coefficient, and $Y_{X/S}$ (g dry weight g⁻¹ substrate consumed) is the biomass yield [Shuler

and Kargı, 2002]. Average percentage errors (APE), root mean square errors (RMSE) and ANOVA analysis of the modeled data with experimental data were calculated.

3.3 Results and Discussion

3.3.1 Statistical analysis

Statistical analysis based on the correlation coefficients (R^2) of duplicates data were performed for all measurements, with the detailed data presented in Appendix C.

3.3.2 Monod Growth Kinetics and Substrate Utilization

Biomass growth kinetics were determined using cellular protein content and assuming 100% viability of the cells. As shown in the Supplementary Figure 3.1 (Appendix A), the correlation between dry weight and cellular protein content was calculated, resulting in a 19% protein content per gram of dry weight. Atkinson and Mavituna [1991] reported that the protein content of bacterium typically varied from 40-50% of dry weight, while Giallo et al. [1985] observed that the protein content of *Clostridium cellulolyticum* was 62% of dry weight. The relatively low protein content measured here reflects the low protein extraction efficiency estimated at 33% - 48%. It must be asserted however that this extraction efficiency does not impact the estimation of biokinetic constants.

Monod kinetic parameters were first calculated by linearization using Lineweaver-Burk plots and these values were used as initial conditions for modeling in MATLAB (Table 3.1).

Table 3.1: Monod kinetic parameters of *Clostridium termitidis* grown in glucose and cellobiose (2 g l⁻¹) by linearization

Substrate	μ_{max} (h ⁻¹)	K_S (g l ⁻¹)	k_d (h ⁻¹)	$Y_{x/s}$ ^a	R ² (1/ μ vs 1/S)
Glucose	0.3	0.87	0.003	0.21	0.9
Cellobiose	0.34	0.37	0.0041	0.3	0.93

^a g dry weight g⁻¹ substrate

Figure 3.1 shows the change of substrate and biomass concentrations with time in both glucose and cellobiose experiments. Glucose and cellobiose were completely depleted after 20 and 35 hours, respectively. To determine Monod kinetics, the data after the lag phase until the decay phase was taken into account. An initial lag phase of 10 hours was observed with cellobiose. For glucose, the experimental data used for modeling was from 0 to 48 hours whereas for cellobiose the experimental data from 10 to 58 hours was considered.

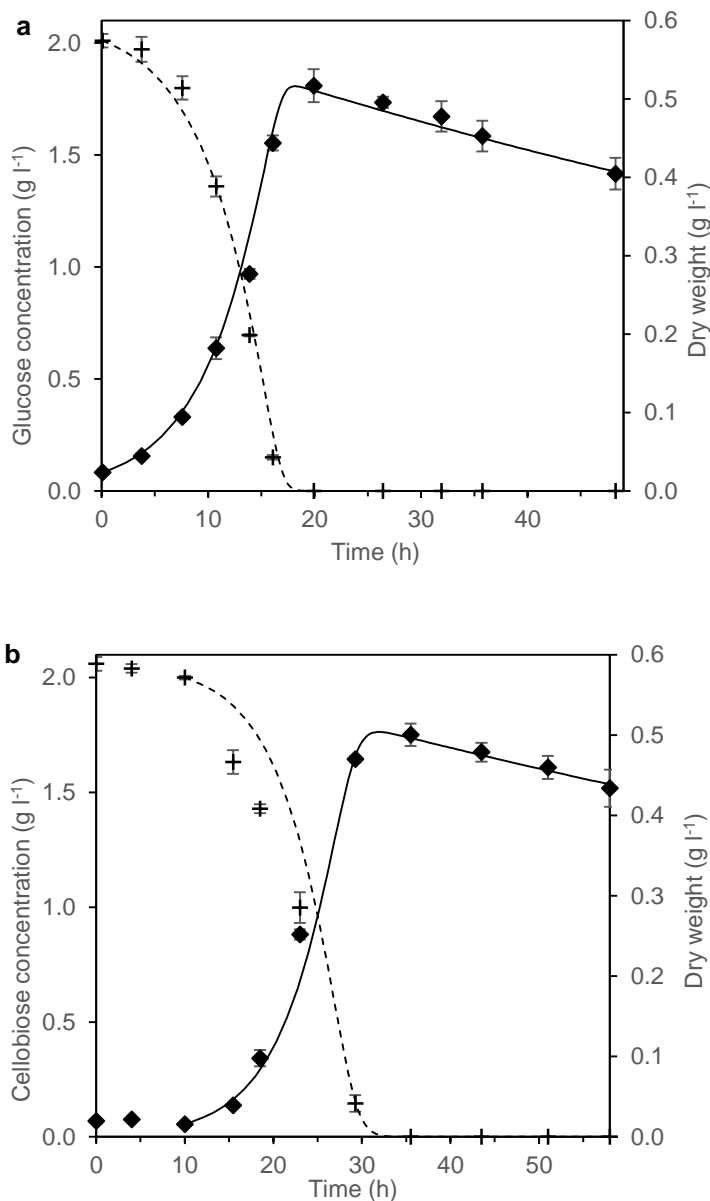


Figure 3.1: Experimental and modeled growth kinetics of *C. termitidis*. a On glucose (2 g l⁻¹). Experimental (crosses) and modeled (dashed line) glucose concentration, experimental (diamonds) and modeled (solid line) dry weight. b On cellobiose (2 g l⁻¹). Experimental (crosses) and modeled (dashed line) cellobiose concentration, experimental (diamonds) and modeled (solid line) dry weight. Experimental data points represent mean values of duplicate experiments, lines above and below represent the actual duplicates. Modeled data was determined in MATLAB R2014a

Linearization is not the best option to determine kinetic parameters because of the low R^2 value and the clear cluster of points. Experimental data can be visually compared with the modeled data from MATLAB in Figure 3.1. In order to evaluate the modeling, average percentage errors (APE) and root mean square errors (RMSE) values were calculated with the results shown in Table 3.2. Furthermore a correlation between the experimental data and the modeled data is illustrated in Figure 3.2 together with the correlation coefficient. All R^2 values were greater than 0.98, and RMSE values were low, between 0.021 g l^{-1} and 0.16 g l^{-1} . The highest APE was for cellobiose (8.6%) and the lowest APE is for dry weight in the same experiment (4.17%). As shown in Figure 3.2, the modelled dry weight and glucose concentrations deviated from the experimental values by 0.47% and 1.5%, respectively. Similarly the modelled dry weight and cellobiose concentrations differed from the experimental observations by 1.5% and 12%, respectively.

In order to determine the goodness of fit for the modeling, linear regression (Figure 3.2) and ANOVA analysis (data not shown) were performed for both experiments. All p-values obtained from the F-Distribution were lower than 0.01, concluding there is evidence to suggest a good fit for the linear relationship with $\alpha=0.05$. Similarly, all p-values obtained from the t-Distribution were greater than $\alpha=0.05$, inferring slope=1 and intercept=0 in all cases. In conclusion, Monod kinetics modelled in MATLAB for the *Clostridium termitidis* were statistically proven to be a good fit.

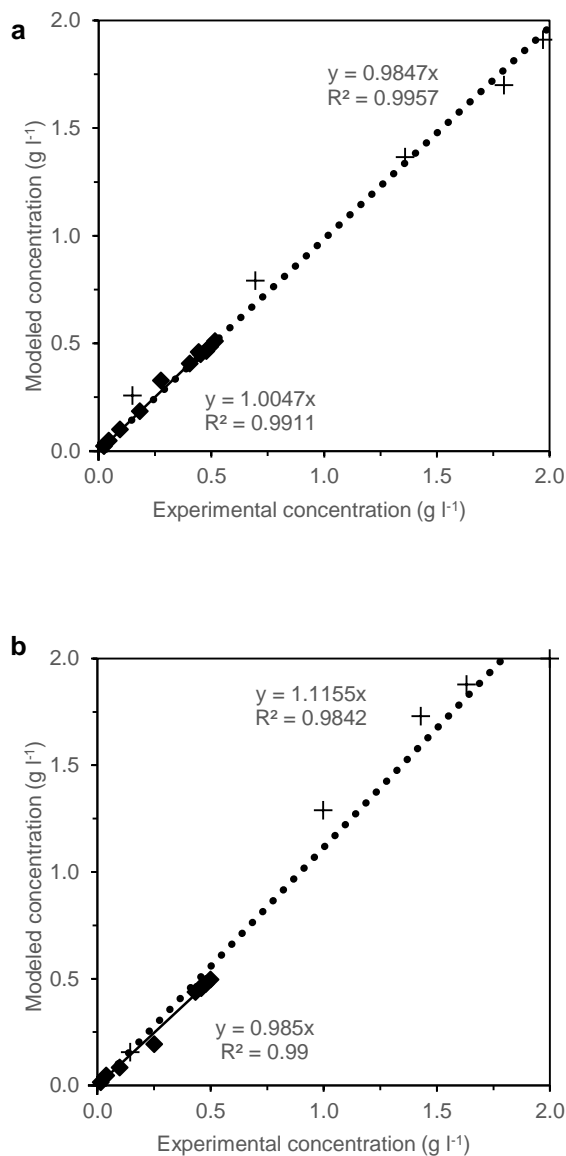


Figure 3.2: Linear regression of experimental data against modeled data. a Glucose experiment. Glucose concentration (crosses) and glucose linear regression (dotted line). Dry weight (diamonds) and dry weight linear regression (solid line). b Cellobiose experiment. Cellobiose concentration (crosses) and cellobiose linear regression (dotted line). Dry weight (diamonds) and dry weight linear regression (solid line)

Table 3.2: Monod kinetic parameters of *C. termitidis* grown in glucose and cellobiose (2 g l⁻¹) obtained in MATLAB, APE, RMSE and H₂ yields.

		Glucose	Cellobiose
Monod kinetic parameters	μ_{max} (h ⁻¹)	0.22	0.24
	K_S (g l ⁻¹)	0.17	0.38
	k_d (h ⁻¹)	0.008	0.0055
	$Y_{x/s}$ ^a	0.26	0.257
	K_m ^b	0.84	0.93
APE ^c (%)	Dry weight	6.7	4.17
	Substrate	8.11	8.6
RMSE ^d (g l ⁻¹)	Dry weight	0.025	0.021
	Substrate	0.036	0.16
H ₂ yield (mol H ₂ mol ⁻¹ hexose equivalent)		1.99	1.11

^a g dry weight g⁻¹ substrate

^b g substrate g⁻¹ dry weight h⁻¹

^c Average Percentage Error

^d Root Mean Square Error

Table 3.2 shows that the Monod kinetic parameters obtained for *C. termitidis* in this study. i.e. μ_{\max} and $Y_{x/s}$ values for both experiments were very similar whereas K_s for cellobiose was more than two times than for glucose. Upon comparing the growth biokinetic coefficients for cellobiose based on linearization (Table 3.1) and nonlinear modeling (Table 3.2), it is evident the biomass yield and K_s were relatively close within 14% and 2% of the larger values while μ_{\max} differed by 29%. It must be asserted however that the accuracy of determining K_s from a single batch test is not high, as generally several batches at a wide range of initial substrate concentrations are employed to ensure accurate delineation of K_s . The discrepancy between the biokinetic constants for glucose using linear and nonlinear methods are even larger (19% - 80%) than for cellobiose except for the biomass yield, thus emphasizing the limitations of linearization techniques. As *C. termitidis* Monod kinetic parameters have not been reported in the literature before, other *Clostridium* species kinetic parameters were reviewed and are shown in Table 3.3 [Alalayah et al., 2010; Lin et al., 2007; Linville et al., 2013; Srivastava and Volesky, 1990; Yang and Tsao, 1994].

Table 3.3: Monod kinetic parameters of *Clostridium* species grown on glucose and cellobiose.

Culture	Substrate	Temp (°C)	pH	μ_{max} (h ⁻¹)	K_S (g l ⁻¹)	$Y_{x/s}$ ^a	K_m ^b	Method	Ref.
<i>C. acetobutylicum</i> M121	Glucose	35	7.2	-	0.18	0.2 ^c	-	AQUASIM	Lin et al. 2007
<i>C. butyricum</i> ATCC 19398	Glucose	35	7.2	-	0.78	0.34 ^c	-	AQUASIM	Lin et al. 2007
<i>C. tyrobutyricum</i> FYa102	Glucose	35	7.2	-	0.72	0.46 ^c	-	AQUASIM	Lin et al. 2007
<i>C. beijerinckii</i> L9	Glucose	35	7.2	-	0.47	0.23 ^c	-	AQUASIM	Lin et al. 2007
<i>C. saccharoperbutylacetonicum</i> N1-4	Glucose	37	ND	0.4	5.51	-	-	Box-Wilson Statistica 7.0	Alalayah et al. 2010
<i>C. acetobutylicum</i>	Glucose	-	6.4	0.58	0.64	-	-	Linear regression	Yang and Tsao 1994
<i>C. acetobutylicum</i>	Glucose	-	6	0.48	10.69	-	-	Linear regression	Srivastava and Volesky 1990
<i>C. thermocellum</i> wild type	Cellobiose	58	7	0.57	0.92	0.23	2.48	Matlab 7.10.0 (R2010a)	Linville et al. 2013
<i>C. thermocellum</i> mutant	Cellobiose	58	7	1.22	2.22	0.24	5.1	Matlab 7.10.0 (R2010a)	Linville et al. 2013

^a g dry weight g⁻¹ substrate

^b g substrate g⁻¹ dry weight h⁻¹

^c g VSS g⁻¹ substrate

ND: Not Defined

Notwithstanding the accuracy of K_s determination from the single batch tests used here, the K_s value for glucose observed in this study of 0.17 g l^{-1} is very similar to the 0.18 g l^{-1} reported for the mesophile *C. acetobutylicum* [Lin et al., 2007] while that obtained for cellobiose, 0.38 g l^{-1} , is lower than for the thermophile *C. thermocellum*, 0.92 g l^{-1} . The μ_{\max} values for *C. termitidis* on glucose and cellobiose are lower than those reported in the literature ($0.39\text{-}0.58 \text{ h}^{-1}$ for glucose and $0.57\text{-}1.22 \text{ h}^{-1}$ for cellobiose). However, the biomass yields for *C. termitidis* of 0.26, and $0.257 \text{ g dry weight g}^{-1}$ substrate are consistent with the yields reported in Table 3.3. It is important to note that the maximum cellobiose utilization rate (K_m) for the mesophilic *Clostridium termitidis* is 10% greater than the maximum glucose utilization rate. Although k_d was significantly lower than μ_{\max} , k_d for glucose was atypically 45% higher than for cellobiose clearly highlighting the low determination accuracy.

3.3.3 Hydrogen Production

Figure 3.3 shows the cumulative H_2 production after 20 and 30 hours from glucose and cellobiose respectively, along with the changes in pH. *C. termitidis* stopped H_2 production the same time glucose was depleted and biomass concentration reached its maximum, with pH decreasing to its minimum value of 5.8, while on cellobiose, *C. termitidis* reached the complete substrate utilization at 30 hours and pH decreased to 6.1. It must be emphasized, however, that the added alkalinity was consistent with the recommended growth media.

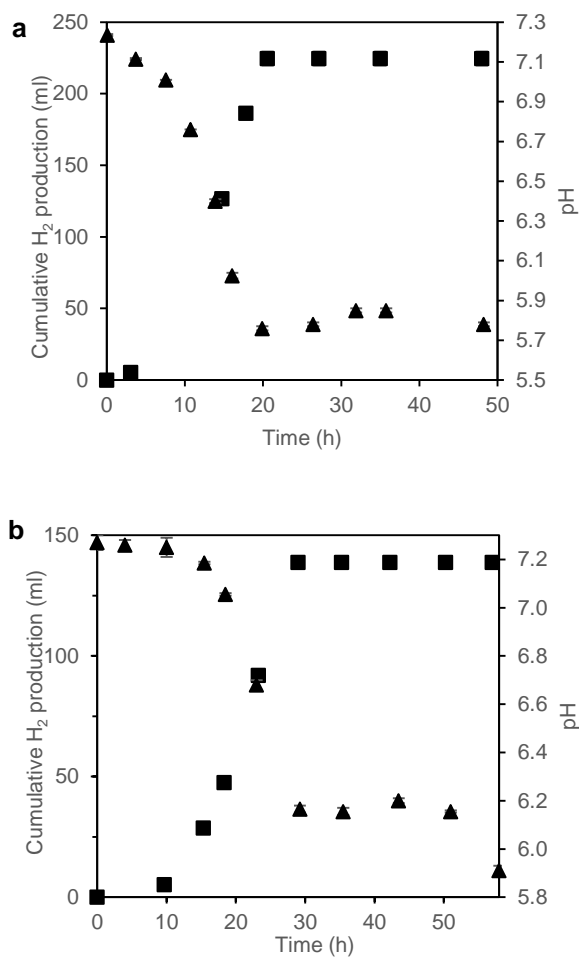


Figure 3.3: Cumulative H₂ production and pH. a *C. termitidis* on glucose (2 g l⁻¹). Cumulative H₂ profile (squares) and pH changes (triangles). b *C. termitidis* on cellobiose (2 g l⁻¹). Cumulative H₂ profile (squares) and pH changes (triangles). Data points represent the mean values of duplicate experiments, lines above and below represent the actual duplicates

As the pH range for *C. termitidis* growth has been reported to be >5.0 and <8.2 [Hethener et al., 1992], the pH changes observed in this study were assumed not to affect the determination of the microbial kinetics. Figure 3.4 shows the specific growth rates (μ) at the different pH values during glucose and cellobiose fermentations. It is noteworthy that within the pH experimental range of 6-7.2, μ values were 60-96% of μ_{\max} on glucose and >46% on cellobiose.

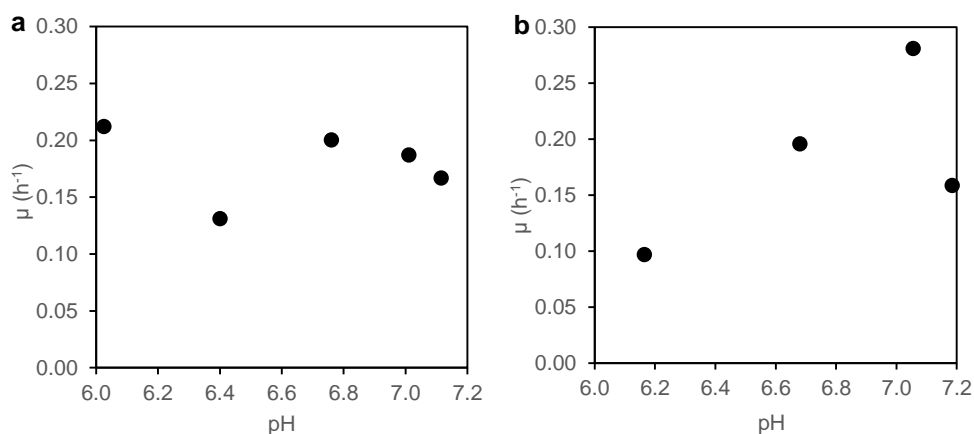


Figure 3.4: μ vs pH. a *C. termitidis* on glucose. b *C. termitidis* on cellobiose.

The H_2 yields presented in Table 3.2 indicate that the yield was higher for glucose (1.99 $\text{mol H}_2 \text{ mol}^{-1}$ hexose equivalent) than cellobiose (1.11 $\text{mol H}_2 \text{ mol}^{-1}$ hexose equivalent). Nevertheless, H_2 yield by *C. termitidis* in cellobiose was more than two times higher than the 0.39 $\text{mol H}_2 \text{ mol}^{-1}$ hexose equivalent previously reported by Ramachandran et al. [2008]. Both experiments were run in batches but the main difference was the reactor size, 10 ml working volume compared to 400 ml used in this study. The same authors [Ramachandran et al., 2008] obtained a higher H_2 yield of 0.62 $\text{mol H}_2 \text{ mol}^{-1}$ hexose equivalent when *C. termitidis* was fed with cellulose, as compared to the cellobiose yield of 0.39 $\text{mol H}_2 \text{ mol}^{-1}$ hexose equivalent, which is not plausible since cellobiose is the product of hydrolysis of cellulose.

The closures of COD balances at $99 \pm 1\%$ verifies the reliability of the data. Based on the final COD measurements in the glucose experiment, the biomass yield was $0.15 \text{ g dry weight g}^{-1}$ glucose. This agrees with the biomass yield of $0.18 \text{ g dry weight g}^{-1}$ glucose considering the Monod theoretical yield and decay coefficient. In the case of cellobiose, the observed biomass yield at the end of the fermentation was $0.24 \text{ g dry weight g}^{-1}$ cellobiose, as compared with $0.2 \text{ g dry weight g}^{-1}$ cellobiose based on the Monod model kinetics.

3.4 Conclusions

Clostridium termitidis CT1112, isolated from the gut of a wood feeding termite, *Nasutitermes lujae*, has become of great scientific interest because of its ability to degrade cellulose at mesophilic temperatures and to produce H_2 .

Growth kinetics on glucose and cellobiose were modeled in MATLAB by fitting the data to experimental results and Monod kinetic parameters (μ_{\max} , K_s , k_d and $Y_{X/S}$) were determined. In glucose μ_{\max} was 0.22 h^{-1} and 0.24 h^{-1} for cellobiose, K_s was 0.17 and 0.38 g l^{-1} respectively and finally biomass yield was 0.26 and $0.257 \text{ g dry weight g}^{-1}$ substrate. H_2 yields of 1.99 and $1.11 \text{ mol H}_2 \text{ mol}^{-1}$ hexose equivalent were also determined for glucose and cellobiose respectively. *C. termitidis* exhibited a higher biomass yield and a lower H_2 yield when grown in cellobiose than in glucose.

This study has provided valuable insights into the fermentation of mono and disaccharides by *C. termitidis*. The microbial kinetics of this model microorganism will enhance engineering biofuel production applications. Furthermore, studies of substrate consumption and microbial growth will provide an understanding of microbial metabolism under specific fermentation conditions.

3.5 References

- Alalayah W.M., Kalil M.S., Kadhum A.A.H., Jahim J., Zaharim A., Alauj N.M., El-Shafie A. (2010) Applications of the box-wilson design model for bio-hydrogen production using *Clostridium saccharoperbutylacetonicum* N1-4 (ATCC 13564). Pak J Biol Sci 13:674-682
- Atkinson B., Mavituna F. (1991) Biochemical engineering and biotechnology handbook. Stockton Press, New York
- Fang H.H.P. (2010) Environmental anaerobic technology: applications and new developments. Imperial College Press, Hackensack, NJ; London; Singapore
- Giallo J., Gaudin C., Belaich J.P. (1985) Metabolism and solubilization of cellulose by *Clostridium cellulolyticum* H10. Appl Environ Microbiol 49:1216-1221
- Hethener P., Brauman A., Garcia J.L. (1992) *Clostridium termitidis* sp. nov., a cellulolytic bacterium from the gut of the wood-feeding termite, *Nasutitermes lujae*. Syst Appl Microbiol 15:52-58
- Lal S., Ramachandran U., Zhang X., Munir R., Sparling R., Levin D.B. (2013) Draft genome sequence of the cellulolytic, mesophilic, anaerobic bacterium *Clostridium termitidis* strain CT1112 (DSM 5398). Genome Announc 1:e00281-13
- Levin D.B., Carere C.R., Cicek N., Sparling R. (2009) Challenges for biohydrogen production via direct lignocellulose fermentation. Int J Hydrogen Energy 34:7390-7403
- Lin P.Y., Whang L.M., Wu Y.R., Ren W.J., Hsiao C.J., Chang S.L.L.S. (2007) Biological hydrogen production of the genus *Clostridium*: metabolic study and mathematical model simulation. Int J Hydrogen Energy 32:1728-1735
- Linville J.L., Rodriguez M., Mielenz J.R., Cox C.D. (2013) Kinetic modeling of batch fermentation for *Populus* hydrolysate tolerant mutant and wild type strains of *Clostridium thermocellum*. Bioresour Technol 147:605-613

- López S., Dhanoa M.S., Dijkstra J., Bannink A., Kebreab E., France J. (2007) Some methodological and analytical considerations regarding application of the gas production technique. *Anim Feed Sci Technol* 135:139-156
- Munir R.I., Schellenberg J., Henrissat B., Verbeke T.J., Sparling R., Levin D.B. (2014) Comparative analysis of carbohydrate active enzymes in *Clostridium termitidis* CT1112 reveals complex carbohydrate degradation ability. *PLoS One* 9:e104260
- Owen W.F., Stuckey D.C., Healy J.B., Young L.Y., Mccarty P.L. (1979) Bioassay for monitoring biochemical methane potential and anaerobic toxicity. *Water Res* 13:485-492
- Ramachandran U., Wrana N., Cicek N., Sparling R., Levin D.B. (2008) Hydrogen production and end-product synthesis patterns by *Clostridium termitidis* strain CT1112 in batch fermentation cultures with cellobiose or α -cellulose. *Int J Hydrogen Energy* 33:7006-7012
- Schwarz W.H. (2001) The cellulosome and cellulose degradation by anaerobic bacteria. *Appl Microbiol Biotechnol* 56:634-649
- Shuler M.L., Kargi F. (2002) *Bioprocess engineering: basic concepts*. Second ed. Prentice Hall PTR, Upper Saddle River, NJ
- Sleat R., Mah R.A., Robinson R. (1984) Isolation and characterization of an anaerobic, cellulolytic bacterium, *Clostridium cellulovorans* sp. nov. *Appl Environ Microbiol* 48:88-93
- Srivastava A.K., Volesky B. (1990) Updated model of the batch acetone-butanol fermentation. *Biotechnol Lett* 12:693-698
- Warnick T.A., Methé B.A., Leschine S.B. (2002) *Clostridium phytofermentans* sp. nov., a cellulolytic mesophile from forest soil. *Int J Syst Evol Microbiol* 52:1155-1160
- Yang X.P., Tsao G.T. (1994) Mathematical-modelling of inhibition-kinetics in acetone-butanol fermentation by *Clostridium acetobutylicum*. *Biotechnol Prog* 10:532-538

Chapter 4

4 Hydrogen Production and Microbial Kinetics of *Clostridium termitidis* in Mono-culture and Co-culture with *Clostridium beijerinckii* on Cellulose

4.1 Introduction

The eco-friendly and sustainable nature of biofuels makes them an important and promising alternative energy source for fossil fuels. Hydrogen (H₂) is considered a clean and renewable energy resource that does not contribute to the greenhouse effect. For global environmental considerations, microbial H₂ production represents an important area of bioenergy production [Kuo et al., 2014]. The main source of H₂ production from fermentation is carbohydrates, in the form of either oligosaccharides or polymers (e.g., cellulose, hemicellulose, and starch). Among the polymeric forms, cellulose is not only the predominant constituent that is widely available in agricultural wastes and industrial effluents such as pulp/paper and food industries; but also a very promising feedstock for biohydrogen production [Kuo et al., 2014]. In comparison to the use of natural mixed consortia, pure cultures have achieved higher H₂ yields [Masset et al., 2012], with more detectable metabolic shifts [Elsharnouby et al., 2013].

Artificial microbial co-cultures and consortia has attracted attention for biohydrogen production because of the complex functions they can perform [Masset et al., 2012], for example, simultaneous hexose and pentose consumption [Eiteman et al., 2008], can help conserve anaerobic conditions for obligate H₂ producers, eliminating at the same time the need for a reducing agent, improve the hydrolysis of complex sugars, provide a wider range of pH for bacteria to ferment H₂ [Elsharnouby et al., 2013], and be more robust to changes in environmental conditions since co-cultures can resist periods of nutrient limitation better [Brenner et al., 2008].

Temperature is a very important operational parameter in fermentative H₂ production. Although, thermophiles have shown higher H₂ production yields than mesophiles in the literature [Munro et al., 2009; Lu et al., 2007; Ngo et al., 2012; Kumar and Das, 2000; Lin

et al., 2007; O-Thong et al., 2008; Xu et al., 2008], the improved yield has been also substrate dependent [Elsharnouby et al., 2013]. For example, mesophilic *Pantoea agglomerans* had roughly the same H₂ yield (3.8 mol H₂ mol⁻¹ glucose) [Zhu et al., 2008] as thermophilic *Thermotoga neapolitana* with glucose [d'Ippolito et al., 2010]. Similarly, the thermophilic *Caldicellulosiruptor saccharolyticus* and mesophilic *E. cloacae* on sucrose, attaining 2.96 and 3.1 mol H₂ mol⁻¹ hexose, respectively [van Niel et al., 2002; Kumar and Das, 2000]. However, mesophilic H₂ production is more economical and reliable than thermophilic and hyperthermophilic production. Four co-culture experiments for biohydrogen production from pure cellulose, two at mesophilic and two at thermophilic conditions [Wang et al., 2008; Geng et al., 2010; Liu et al., 2008; Wang et al., 2009] have been reported. All of these studies have shown enhancement of H₂ production, with the highest H₂ yield of 1.8 mol H₂ mol⁻¹ hexose achieved by the co-culture of *Clostridium thermocellum* JN4 and *Thermoanaerobacterium thermosaccharolyticum* GD17 at 60°C [Liu et al., 2008].

Clostridium termitidis ATCC 51846 is an anaerobic, mesophilic, cellulolytic bacterium isolated from the gut of a termite [Hethener et al., 1992], with reported H₂ yields of 1.99 mol H₂ mol⁻¹ hexose from glucose, of 1.11 mol H₂ mol⁻¹ hexose equivalent from cellobiose [Gomez-Flores et al., 2015] and of 0.62 mol H₂ mol⁻¹ hexose equivalent from cellulose [Ramachandran et al., 2008]. On the other hand, *Clostridium beijerinckii* is a mesophilic H₂ producer which is not able to degrade cellulose but is adept at H₂ production from glucose [Masset et al., 2012]. *C. beijerinckii* H₂ yields on glucose have been reported to be 1.88, 2.81, 2.52, 2 mol H₂ mol⁻¹ hexose [Masset et al., 2012; Lin et al., 2007; Pan et al., 2008; Taguchi et al., 1992].

Many cellulolytic bacteria have their cellulases (cellulose degrading enzymes) organized into a discrete multi-enzyme complex, called cellulosome [Bayer et al., 1994]. The cellulosome subunits are composed of several functional domains that interact with each other and with the insoluble substrate by promoting adhesion [Bayer and Lamed, 1992; Shoham et al., 1999]. In this regard, the cellulosome controls the binding of the bacterial cell to the substrate and its extracellular hydrolysis to soluble sugars [Bayer et al., 1998].

For example, in the anaerobic thermophilic *Clostridium thermocellum* bacterium, in the absence of cellulose, the cellulosome forms bulbous protuberances on the surface of the cell [Bayer et al., 1998]. However, when cellulose is present, the cellulosome forms extended filamentous protrusions that anchor the cell to its substrate [Bayer et al., 1998]. The cellulosome was first elucidated in *C. thermocellum* and has served as a model [Bayer and Lamed, 1992]. Currently, cellulosomes of many cellulolytic bacteria are under investigation and some have been described, e.g. *Acetivibrio cellulolyticus*, *Bacteroides cellulosolvens*, *Clostridium cellulolyticum*, *C. cellulovorans*, *C. Josui*, *C. Papyrosolvens*, *Ruminococcus albus*, *R. flavefaciens*, among others [Wall et al., 2008]. It is important to note that not all cellulolytic bacteria have cellulosomes, some like *Clostridium stercorarium* and *C. phytofermentans*, only secrete free enzymes [Munir et al., 2014]. Conversely, it is intriguing that *C. acetobutylicum* can produce a cellulosome, but this bacterium is not able to hydrolyze cellulose [Sabathé et al., 2002]. Hence, the importance of an active cellulosome machinery.

Munir et al. [2014] recently reported the presence of a putative cellulosome assembly in *C. termitidis*. Based on a simple representation of *C. thermocellum*'s cellulosome, Figure 4.1 shows the speculative interaction of *C. termitidis* bacterial cells with cellulose, where the Cellulose Binding Module (CBM) in dark cherry color, is responsible to anchor the scaffoldin to the cellulose. The scaffoldin is a scaffolding protein, represented with the same color as the CBM (dark cherry), which contains varying number of enzyme binding domains called cohesins (Cohesin I domain), connected to the catalytic subunits (different colors) through docking domains called Dockerins (Dockerin I domain) [Bayer et al., 1994]. The cellulosome is usually connected to the bacterial cell via a Type II Dockerin and Cohesin domains, nevertheless, Munir et al. [2014] were not able to detect an anchoring protein (light gray). Therefore, the authors suggested the idea of a putative cellulosome adherence mechanism or putative cell free cellulosome production [Munir et al., 2014]. Also, Munir et al. [2015] found S-layer proteins in *C. termitidis*, shown in orange ovals in Figure 4.1. The S-layer serves as a coat to protect the organism from extreme environmental conditions in addition to promote adhesion to the substrate [Munir et al., 2015]. In contrast, *C. beijerinckii* has not been reported to have a cellulosome structure [Bayer et al., 2007] and there is limited evidence that this bacterium may be able to release

extracellular cellulolytic enzymes in order to hydrolyze cellulose into soluble sugars [Shoham et al., 1999]. Therefore, co-culture of *C. termitidis* and *C. beijerinckii* could lead to an efficient substrate utilization and H₂ production improvement. Figure 4.2 shows the non-cellulosome speculative interaction of *C. beijerinckii* bacterial cell with cellulose.

Additionally, Figures 4.1 and 4.2 show the theoretical biochemical pathways from glucose for *C. termitidis* ATCC 51846 and *C. beijerinckii* sp., respectively. In Figure 4.2, although formic acid is not included, there is experimental evidence of its production by *C. beijerinckii* DSM 1820 [Masset et al., 2012], also, acetone and butanol pathways (dotted orange rectangles) are expressed only in certain *C. beijerinckii* spp. [Dürre, 2005].

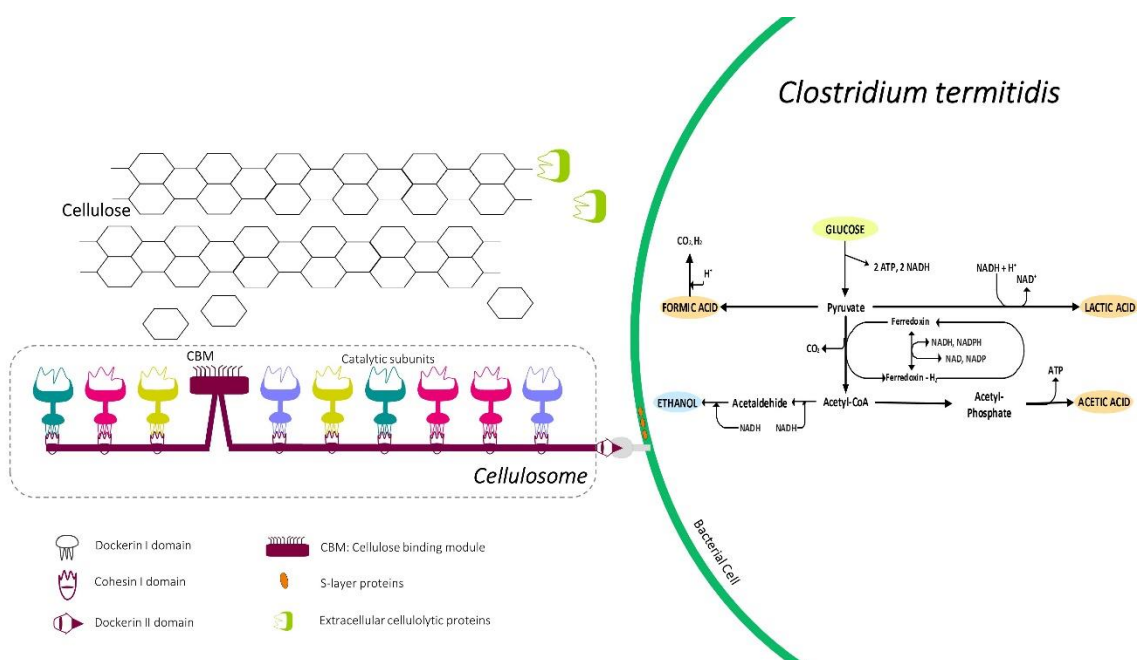


Figure 4.1: *C. termitidis* speculative cell interaction with cellulose through its cellulosome based on *C. thermocellum*'s cellulosome model (left) and biochemical pathways from glucose based on Caspi et al. [2014] (right)

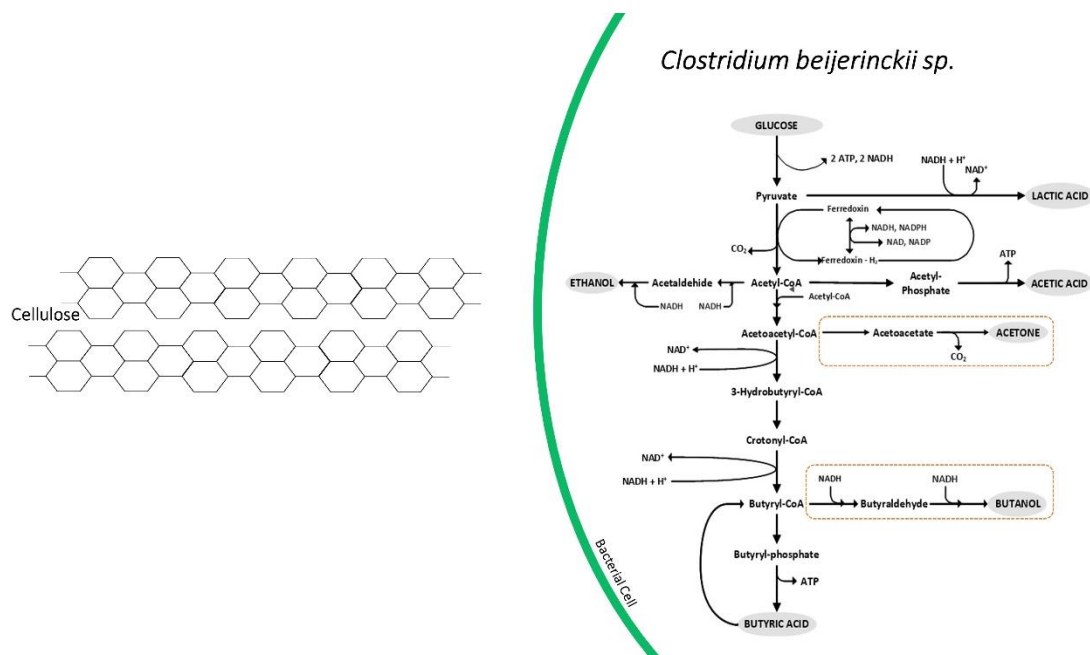


Figure 4.2: Non-cellulosome speculative interaction of *C. beijerinckii* sp. cell with cellulose (left) and biochemical pathways from glucose from Dürre [2005] (right)

Furthermore, agitation has been reported to negatively affect the growth on cellulose of *Clostridium thermocellum* ATCC 31549 [Freier et al., 1988]. Freier et al. [1988] tested different agitation rates and found that at 200 strokes per minute, only few cells were attached to cellulose fibers, inhibiting *C. thermocellum* growth on cellulose.

Since non-shaking conditions are closer to the conditions in the natural environment of *C. termitidis* and because the agitation effect on *C. termitidis* grown on cellulose has never been investigated, this study has two goals. The first is to evaluate the effect of co-culture of *C. termitidis* and *C. beijerinckii* in biohydrogen production and microbial kinetics and the second is to evaluate the effect of agitation in pure cultures grown in cellulose.

4.2 Materials and Methods

4.2.1 Microbial Strain and Media

The strains used were *Clostridium termitidis* ATCC 51846 and *Clostridium beijerinckii* DSM 1820. All chemicals for media and substrates were obtained from Sigma-Aldrich Co. Fresh cells of *C. termitidis* were maintained by successively transferring 10% (v/v) of inoculum to ATCC 1191 medium containing 2 g l⁻¹ of cellulose, whereas fresh cells of *C. beijerinckii* were maintained by successively transferring 10% (v/v) of inoculum to ATCC 1191 medium containing 2 g l⁻¹ of cellobiose. This medium contained (per liter of distilled water): KH₂PO₄, 1.5 g; Na₂HPO₄, 3.35 g; NH₄Cl, 0.5 g; MgCl₂·6H₂O, 0.18 g; yeast extract, 2 g; 0.25 ml 1 g resazurin l⁻¹; mineral solution, 1 ml; vitamin solution, 0.5 ml, and L-cysteine, as reducing agent, 1 g. The mineral solution contained (g per 500 ml): trisodium nitrilotriacetate 10.1; FeCl₃·6H₂O, 1.05; CoCl₂·6H₂O, 1; MnCl₂·4H₂O, 0.5; ZnCl₂, 0.5; NiCl₂·6H₂O, 0.05; CaCl₂·2H₂O, 0.25; CuSO₄·5H₂O, 0.32; and Na₂MoO₄·2H₂O, 0.25. The vitamin solution contained (mg per 500 ml): pyridoxine-HCl, 50; riboflavin, 25; thiamine, 25; nicotinic acid, 25; *p*-aminobenzoic acid, 25; lipoic acid (thioctic acid), 25; biotin, 10; folic acid, 10; and cyanocobalamin, 5.

4.2.2 Experimental Conditions

Batch fermentations were performed in media bottles (Wheaton) with a working volume of 500 ml and 210 ml of headspace. For co-culture experiment, bottles containing 450 ml of ATCC 1191 medium and 1 g cellulose were tightly capped with screw caps with butyl septum, degassed by applying vacuum and sparged with high purity N₂ gas, and autoclaved. Mono-culture bottles were inoculated with 10% (v/v) of *C. termitidis* cultures, while co-culture bottles were inoculated with 10% (v/v) of *C. termitidis* and *C. beijerinckii* cultures in a ratio of 1:1. All bottles were incubated at 37°C in shakers (Max Q4000, Thermo Scientific, CA) and they were divided into two sets, mono and co-culture under continuous agitation at 100 rpm (and completely mixed at each liquid sampling point) and mono and co-culture without agitation. For agitated batches, three (3) ml homogeneous liquid samples were taken at specific times for pH, metabolite, cellular protein content and

cellulose analyses. For unagitated batches three (3) ml liquid samples of the supernatant were taken with 6 in long needles (Hamilton Company, Reno, NV) at specific times for pH measurements and metabolite analysis. Fermentations ran for 45 days except for the non-agitated co-culture which lasted 40 days. pH was initially set to 7.2 but it was not controlled. Data shown is the average of duplicate experiments. Additionally, microbial kinetics of *C. beijerinckii* on glucose 2 g l^{-1} was performed in serum bottles (Wheaton) with a working volume of 500 ml and 210 ml of headspace. Bottles containing 430 ml of ATCC 1191 medium were tightly capped with rubber stoppers, degassed by applying vacuum and sparged with high purity N_2 gas, and autoclaved. Duplicate bottles were inoculated with 10 % (v/v) of fresh cultures. Bottles were incubated at 37°C and 100 rpm for 48 h. Initial pH was set to 7.2 but was not controlled.

4.2.3 Analytical Methods

Cell growth was monitored by measuring cellular protein content, samples (1 ml) were placed in microcentrifuge tubes (VWR®, Polypropylene) and centrifuged (Corning® LSE™, NY, US) at $10,000\times g$ for 15 min. Supernatants were used for soluble product analysis by transferring to new microcentrifuge tubes and freezing if not used immediately. The pellets were re-suspended with 0.9% (w/v) NaCl and centrifuged at the same aforementioned conditions. Supernatants were discarded, and 1 ml of 0.2 M NaOH was added to microcentrifuge tubes and vortexed to re-suspend the pellet. Microcentrifuge tubes were placed in a water bath at 100°C for 10 min. After cooling for 30 min at room temperature, tubes were centrifuged and supernatants were collected for Bradford assay using bovine serum albumin (BSA) as standard and a UV-visible spectrophotometer (Cary 50 Bio, Varian) at 595 nm. The cellulose pellet was quantified gravimetrically after being dried overnight at 100°C [Liu et al., 2008]. pH was measured using a B10P SympHony pH meter (VWR®). Lactic acid, formic acid, acetic acid, ethanol, butyric acid, glucose and cellobiose, were measured as follows: supernatants for metabolites analysis were filtered through $0.2 \mu\text{m}$ and measured using an HPLC, consisting of a Dionex GP50 Gradient pump and a Dionex LC25 Chromatography oven equipped with an Aminex HPX-87H column (Bio-Rad) at 30°C and 9 mM H_2SO_4 at 0.6 ml/min as mobile phase, connected to a Perkin

Elmer 200 series refractive index detector (RID). Standard curves of metabolites, glucose and cellobiose were performed on ATCC 1191 medium. Cellular protein content was then converted to dry weight using the correlation dry weight (g l^{-1}) = $0.0051 \times \text{protein} (\mu\text{g ml}^{-1})$ [Gomez-Flores et al., 2015]. For the estimation of the COD equivalents for the biomass dry weight, it was assumed that the empirical formula of the organic fraction of the biomass was $\text{C}_5\text{H}_7\text{O}_2\text{N}$ [Metcalf and Eddy, 2003], and that the organic fraction was 90% of the cell dry weight [Pavlostathis et al., 1988]. For *C. beijerinckii* on glucose experiment, pH and cellular protein content were measured over time in like manner as previously described, glucose was measured using a UV-test kit (Sekisui Diagnostics).

4.2.4 Gas Measurements

Gas volume was measured by releasing the gas pressure in the bottles using appropriately sized glass syringes in the range of 5-100 ml to equilibrate with the ambient pressure [Owen et al., 1979]. H_2 analysis was conducted by employing a gas chromatograph (Model 310, SRI Instruments, Torrance, CA) equipped with a thermal conductivity detector (TCD) and a molecular sieve column (Mole sieve 5A, mesh 80/100, 1.83 m x 0.32 cm). The temperatures of the column and the TCD detector were 90 and 105 °C, respectively. Argon was used as the carrier gas at a flow rate of 30 ml/min.

H_2 gas production was calculated from headspace measurements of gas composition and the total volume of biogas produced, at each time interval, using the mass balance equation.

$$V_{\text{H}_2,i} = V_{\text{H}_2,i-1} + C_{\text{H}_2,i} * V_{\text{G},i} + V_{\text{h},i}(C_{\text{H}_2,i} - C_{\text{H}_2,i-1}) \quad 4.1$$

where $V_{\text{H}_2,i}$ and $V_{\text{H}_2,i-1}$ are cumulative H_2 gas volumes at the current (i) and previous (i - 1) time intervals. $V_{\text{G},i}$ is the total biogas volume accumulated between the previous and current time intervals. $C_{\text{H}_2,i}$ and $C_{\text{H}_2,i-1}$ are the fractions of H_2 gas in the headspace of the reactor in the current and previous intervals, and $V_{\text{h},i}$ is the total volume of the headspace of the reactor in the current interval [López et al., 2007].

4.2.5 Kinetic Equations and Modeling

Figures 4.3 and 4.4 are the schematic representations of the mono and co-culture experiments. There are mainly 2 steps: hydrolysis of cellulose and fermentation of soluble sugars (glucose). *C. termitidis* cellulosome is responsible for cellulose hydrolysis in both, mono and co-culture. In mono-culture, *C. termitidis* is responsible for the fermentation of soluble sugars from cellulose, whereas in co-culture both, *C. termitidis* and *C. beijerinckii* ferment the soluble sugars from cellulose.

As shown in Figure 4.3, the soluble products in mono-culture are acetate, ethanol, lactate and formate. Additionally in co-culture, initial lactate carried from *C. beijerinckii* inoculum acted as substrate, and butyrate was also part of the soluble products due to *C. beijerinckii* metabolism, as illustrated in Figure 4.4.

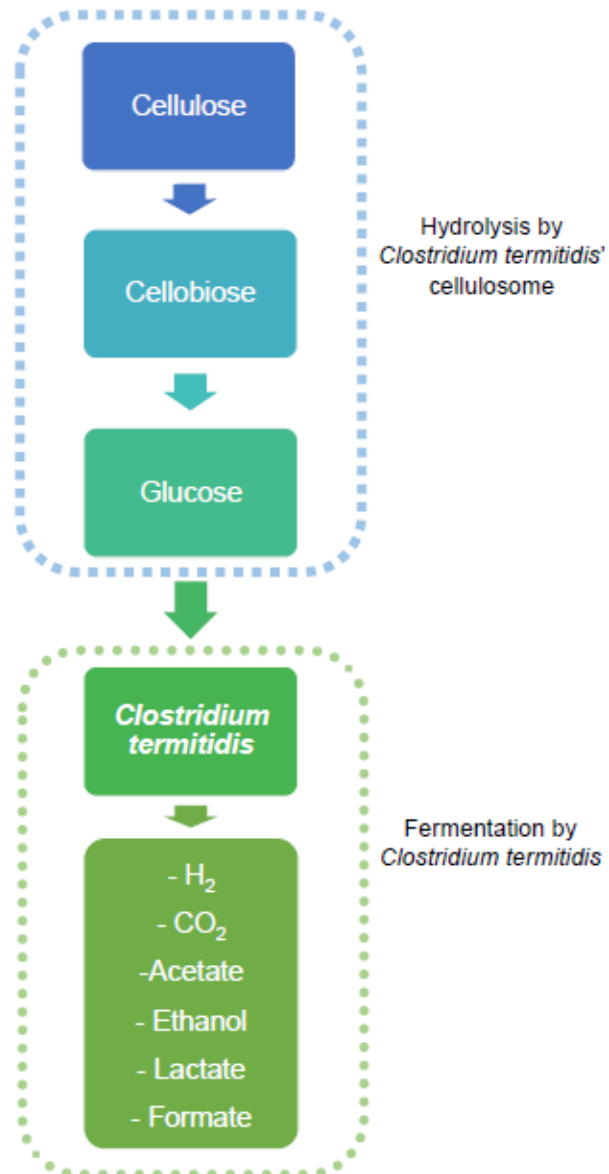


Figure 4.3: Schematic representation of the steps involved in cellulose fermentation in mono-culture experiments

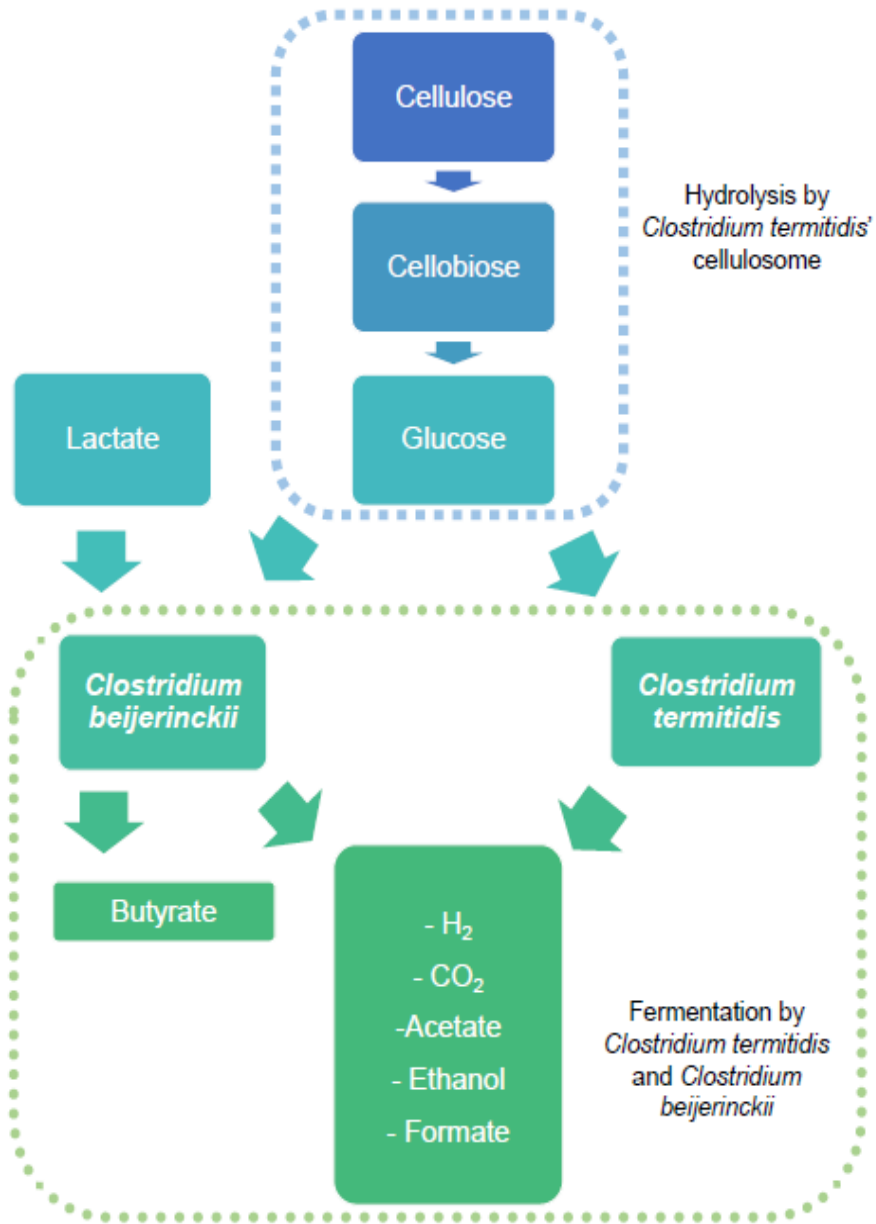
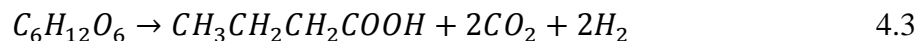
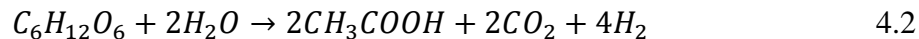
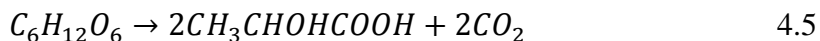


Figure 4.4: Schematic representation of the steps involved in cellulose fermentation in co-culture experiments

During glucose fermentation, several reactions take place. Among them, acetate and butyrate pathways involve H₂ production according to Equations 4.2 and 4.3, respectively [Guo et al., 2010]:



On the other hand, ethanol and lactate are involved in a zero-H₂ balance pathway according to Equations 4.4 and 4.5, respectively [Guo et al., 2010]:



Lactate utilization is represented by Equation 4.6 [Thauer et al., 1977; Costello et al., 1991; Grause et al., 2012], where 1 mol of lactate produces 1 mol of acetate and 2 moles of H₂.



Based on the schematic representations of mono and co-culture experiments (Figures 4.3 and 4.4) two mathematical models describing bacterial growth, substrate consumption and product formation were developed. These mathematical models imply a complete substrate utilization. Because cellulose is not completely biodegraded, the use of a non-biodegradable factor S_o (g COD l⁻¹) was needed as presented in Equation 4.7.

$$S = \int \frac{dS}{dt} + S_o \quad 4.7$$

where S is cellulose concentration (g COD l⁻¹) and S_o is the cellulose concentration at the end of the fermentation. Soluble sugars from cellulose hydrolysis (cellobiose and glucose) were not detected in any of the fermentations, meaning cellulose hydrolysis is the rate limiting factor and no intermediate production/consumption rate was considered. Nevertheless, cellulose is an insoluble substrate and Monod model cannot be used. Therefore, a modified Monod approach, incorporating Particulate Organic Matter (POM) [Metcalf and Eddy, 2003] was used (Equation 4.8).

$$\mu = \frac{\mu_{max} \left(\frac{PO}{X} \right)}{K_X + \left(\frac{PO}{X} \right)} \quad 4.8$$

where μ_{max} (d^{-1}) is the maximum specific growth rate, K_X is the half-velocity degradation coefficient (g COD substrate g^{-1} COD biomass), PO is the particulate organic (cellulose) concentration (g COD l^{-1}) and X is biomass concentration (g COD l^{-1}) [Metcalf and Eddy, 2003]. For simplicity, all concentrations were expressed as g COD; for biomass the factor of 1.42 g COD g^{-1} biomass based on the empirical formula of $C_5H_7O_2N$ was used [Metcalf and Eddy, 2003].

The two models are described as follows:

- a. **Mono-culture** (*C. termitidis* only). Biomass growth and PO consumption are described in Equations 4.9 and 4.10, respectively.

$$\frac{dX}{dt} = \mu X = \frac{\mu_{max} \left(\frac{PO}{X} \right) X}{\left[K_X + \left(\frac{PO}{X} \right) \right]} \quad 4.9$$

$$\frac{dPO}{dt} = - \frac{1}{Y_{X/PO}} \frac{dX}{dt} = - \frac{\mu_{max} \left(\frac{PO}{X} \right) X}{Y_{X/PO} \left[K_X + \left(\frac{PO}{X} \right) \right]} \quad 4.10$$

where $Y_{X/PO}$ (g COD biomass g^{-1} COD substrate consumed) is the biomass yield [Shuler and Kargi, 2002]. The decay coefficient, k_d , was not included due to lack of sufficient information on the decay phase. Acetate, ethanol, lactate and formate production were modeled as described by Equations 4.11-4.14.

Acetate:

$$\frac{dA}{dt} = \frac{Y_{A/PO}}{Y_{X/PO}} \frac{\mu_{max} \left(\frac{PO}{X} \right) X}{\left[K_X + \left(\frac{PO}{X} \right) \right]} \quad 4.11$$

Ethanol:

$$\frac{dE}{dt} = \frac{Y_{E/PO}}{Y_{X/PO}} \frac{\mu_{max} \left(\frac{PO}{X} \right) X}{\left[K_X + \left(\frac{PO}{X} \right) \right]} \quad 4.12$$

Lactate:

$$\frac{dL}{dt} = \frac{Y_{L/PO}}{Y_{X/PO}} \frac{\mu_{max} \left(\frac{PO}{X} \right) X}{\left[K_X + \left(\frac{PO}{X} \right) \right]} \quad 4.13$$

Formate:

$$\frac{dF}{dt} = \frac{Y_{F/PO}}{Y_{X/PO}} \frac{\mu_{max} \left(\frac{PO}{X} \right) X}{\left[K_X + \left(\frac{PO}{X} \right) \right]} \quad 4.14$$

where A, E, L and F are acetate, ethanol, lactate and formate concentrations (g COD l⁻¹) respectively. Y_{A/PO}, Y_{E/PO}, Y_{L/PO}, and Y_{F/PO}, are the products yields for acetate, ethanol, lactate and formate, respectively (g COD g⁻¹ COD substrate consumed).

b. Co-culture (*C. termitidis* and *C. beijerinckii*). No distinction in biomass measurement was done for each strain. Lactate was present at the beginning of the experiment from *C. beijerinckii* inoculum, and butyrate is a product of *C. beijerinckii*. Therefore, co-culture experiment was modeled as a single strain with the addition of lactate as substrate and butyrate as product. Consequently, biomass growth from cellulose and lactate is modeled by Equation 4.15, where PO consumption is described in Equation 4.16, and lactate consumption was considered a first order reaction (Equation 4.17).

$$\frac{dX}{dt} = \mu X + Y_{X/L} K_L L X = \frac{\mu_{max} \left(\frac{PO}{X} \right) X}{\left[K_X + \left(\frac{PO}{X} \right) \right]} + Y_{X/L} K_L L X \quad 4.15$$

$$\frac{dPO}{dt} = - \frac{1}{Y_{X/PO}} \frac{dX}{dt} = - \frac{\mu_{max} \left(\frac{PO}{X} \right) X}{Y_{X/PO} \left[K_X + \left(\frac{PO}{X} \right) \right]} \quad 4.16$$

$$\frac{dL}{dt} = -K_L L X \quad 4.17$$

where Y_{X/L} is the biomass yield from lactate (as g COD g⁻¹ COD) and K_L is the lactate consumption constant (l g⁻¹ COD biomass d⁻¹). Based on Equation 4.6, acetate production comes also from lactate. Thus acetate kinetics include both, acetate generation from lactate and directly from cellulose as shown in Equation 4.18.

$$\frac{dA}{dt} = \frac{Y_{A/PO}}{Y_{X/PO}} \frac{\mu_{max} \left(\frac{PO}{X} \right) X}{\left[K_X + \left(\frac{PO}{X} \right) \right]} + Y_{A/L} K_L L X \quad 4.18$$

where $Y_{A/L}$ is the acetate yield from lactate (g COD g⁻¹ COD).

Ethanol, formate and butyrate kinetics are shown in Equations 4.19-4.21.

Ethanol:

$$\frac{dE}{dt} = \frac{Y_{E/PO}}{Y_{X/PO}} \frac{\mu_{max} \left(\frac{PO}{X} \right) X}{\left[K_X + \left(\frac{PO}{X} \right) \right]} \quad 4.19$$

Formate:

$$\frac{dF}{dt} = \frac{Y_{F/PO}}{Y_{X/PO}} \frac{\mu_{max} \left(\frac{PO}{X} \right) X}{\left[K_X + \left(\frac{PO}{X} \right) \right]} \quad 4.20$$

Butyrate:

$$\frac{dB}{dt} = \frac{Y_{B/PO}}{Y_{X/PO}} \frac{\mu_{max} \left(\frac{PO}{X} \right) X}{\left[K_X + \left(\frac{PO}{X} \right) \right]} \quad 4.21$$

where $Y_{B/PO}$ is the butyrate yield as g COD g⁻¹ COD substrate consumed.

Kinetic parameters were estimated using MATLAB® R2014a. The solver function used to estimate numerical integration of the ordinary differential equations was Ode45, which implemented fourth/fifth order Runge–Kutta methods. Initial guesses were manually adjusted to obtain a good fit to the data, and average percentage error (APE) values were calculated.

4.3 Results and Discussion

4.3.1 Statistical analysis

Statistical analysis based on the correlation coefficients (R^2) of duplicates data were performed for all measurements, with the detailed data presented in Appendix C.

4.3.2 *C. beijerinckii* on Glucose Experiment

As depicted in Figure 4.5a, *C. beijerinckii* degraded glucose in 46 hours with an initial lag phase of 22 hours and had a yield of 2.54 mol H₂ mol⁻¹ glucose. pH dropped from 7.1 to 6.2. The same strain (*Clostridium beijerinckii* DSM 1820) produced 1.45 and 1.88 mol H₂ mol⁻¹ glucose when cultured on glucose at pH 7.3 (unregulated) and pH 6.7 (regulated), respectively [Masset et al., 2012]. Although Masset et al. [2012] used a larger reactor (18 l working volume), the difference in H₂ yields could be attributed to medium used, i.e. MDT compared to ATCC 1191 used in this study. With a 28% higher H₂ yield over *C. termitidis* for the same substrate [Gomez-Flores et al., 2015], *C. beijerinckii* was chosen to possibly enhance H₂ production when co-cultured with *C. termitidis* on cellulose.

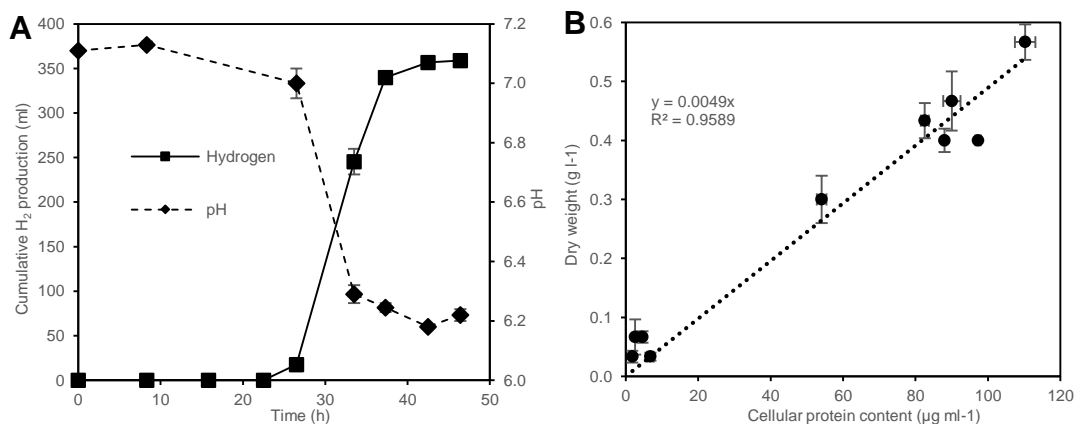


Figure 4.5: *C. beijerinckii* in 2 g l⁻¹ glucose. a pH and cumulative H₂ production profiles. b dry weight and cellular protein content correlation. Data points represent the mean values of duplicate experiments, lines above, below and to the sides represent the actual duplicates

At the same time, a correlation between dry weight and cellular protein content was developed for *C. beijerinckii* in a similar way to the correlation for *C. termitidis* [Gomez-Flores et al., 2015]. As apparent from Figure 4.5b, a 20% cellular protein content was obtained, in close agreement with the 19% obtained for *C. termitidis* in the aforementioned study.

4.3.3 Hydrogen Production

H₂ production profiles are depicted in Figure 4.6a. All four cases showed long lag phases of up to 20 days. The enhancement in H₂ production from co-culture over mono-culture is clearly visible. The following modified Gompertz model [Lay et al., 1999] has been used to describe the H₂ production with the results shown in Table 4.1.

$$H = P \exp \left\{ -\exp \left[\frac{R_{\max} e}{P} (\lambda - t) + 1 \right] \right\} \quad 4.22$$

where H is the cumulative H₂ production (ml), P is the H₂ production potential (ml), R_{max} is the maximum H₂ production rate (ml d⁻¹), λ is the lag phase time (d), t is the fermentation time, and e=exp(1)=2.718. For the agitated cultures, overall H₂ production for the co-culture compared with the mono-culture increased by 44% to 361 ml while in the non-agitated cultures the overall H₂ production increased by 30% to 326 ml. Agitation of the mono-culture had no effect on the maximum H₂ production (250 ml) but it increased the lag phase by 9 days and consequently maximum H₂ production rate was 6 ml d⁻¹ higher with agitation. Similarly, agitation increased the lag phase in co-culture by 5 days to 24 days but H₂ production rate was not affected (26-27 ml d⁻¹). The observed aforementioned longer lag phases with agitation are in agreement with Freier et al. [1988], who observed longer lag phases with *C. thermocellum* on cellulose under shaking conditions.

Figure 4.6b shows the pH profiles. During the lag phases, all cultures exhibited a marginal decrease in pH from 7.2 to around 7. Concurrent with the H₂ production, the pH dropped rapidly to around 6.2 in non-agitated co-culture fermentation, to 6.14 in non-agitated mono-culture, 6.09 in agitated mono-culture and 6.03 in agitated co-culture. As pH range for *C. termitidis* growth has been reported to be from 5 to 8.2 [Hethener et al., 1992], the pH changes observed in mono-culture fermentations were assumed not to affect the determination of the microbial kinetics. For *C. beijerinckii* DSM 1820 growth, the pH range reported is from 5.2 to 7.3, with the former reported as inhibitory [Masset et al., 2012]. As pH changes presented in co-culture fermentations were within the growth range reported for both strains, pH changes were assumed not to affect the determination of the microbial kinetics. For both the mono-culture and co-culture, the pH drop was steeper in the agitated samples than in the non-agitated cultures.

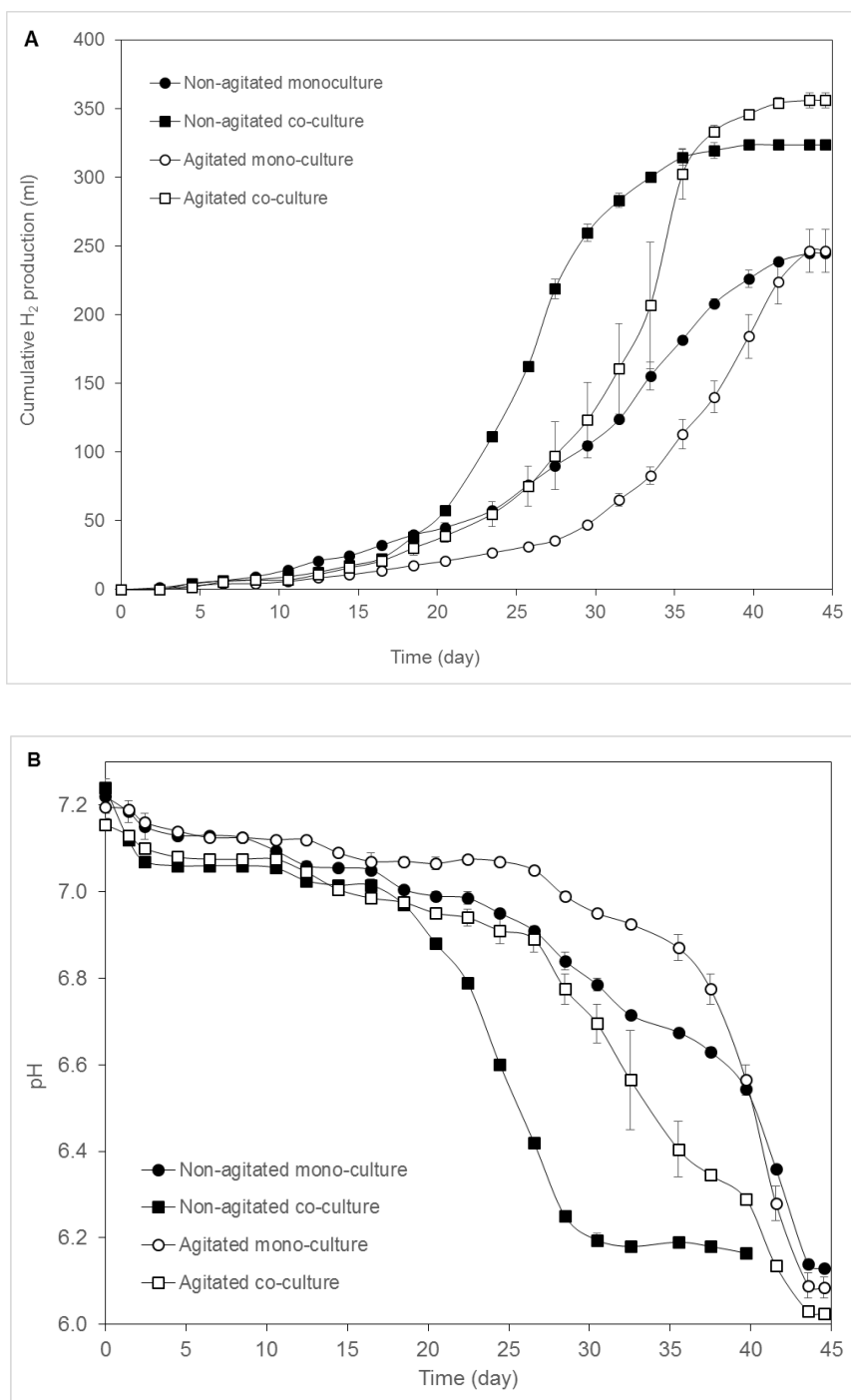


Figure 4.6: *C. termitidis* mono-cultured in 2 g l⁻¹ cellulose and co-cultured with *C. beijerinckii* 2 g l⁻¹ cellulose. a Cumulative H₂ production profiles. b pH profiles. Data points are the averages of duplicates, lines above and below represent the actual duplicates

Cellulose was not completely consumed in neither case. From the percentages of consumption shown in Table 4.1, it is evident that the co-culture enhanced the extent of cellulose utilization by 15% to about 93% but agitation had no effect.

Table 4.1: H₂ yields and Gompertz parameters of *C. termitidis* mono-cultured on 2 g l⁻¹ cellulose and co-cultured with *C. beijerinckii* on 2 g l⁻¹ cellulose

				<i>H₂ yields</i>		<i>Gompertz parameters</i>		
<i>Culture</i>		Cellulose consumed (%)	mol H ₂ mol ⁻¹ hexose eq.-added	mol H ₂ mol ⁻¹ hexose eq.-consumed	P _{max} ^a (ml)	R _m ^b (ml d ⁻¹)	λ ^c (d)	R ²
			<i>Non-agitated</i>	Mono	81	1.45	1.8	250
Co	93	1.92		2.05	326	26	19	0.99
<i>Agitated</i>	Mono	81	1.46	1.8	251	18	28	0.98
	Co	93	2.11	2.26	361	27	24	0.98

^a H₂ production potential

^b Maximum H₂ production rate

^c Lag phase

Table 4.1 also shows the H₂ yields based on hexose equivalent added and consumed. Based on hexose equivalent added, co-culture improved the H₂ yield by 45% compared to mono-culture in agitated fermentations. Nevertheless, based on hexose equivalent consumed, co-culture enhanced the H₂ yield by only 26%, due to the improvement of substrate consumption by co-culture previously mentioned. As depicted in Figures 4.8 and 4.9, lactic acid was unexpectedly present at the beginning of the co-culture fermentations and it was consumed after about 23-27 days. H₂ production from lactic acid by *Clostridium*

beijerinckii DSM 1820 when cultured on glucose has been previously reported by Masset et al. [2012].

The highest reported mesophilic H₂ yield by co-culture on cellulose is 1.31 mol H₂ mol⁻¹ hexose with *Clostridium acetobutylicum* X9 and *Ethanoigenens harbinense* B49 [Wang et al., 2008] while the highest thermophilic H₂ yield is 1.8 mol H₂ mol⁻¹ hexose with *Clostridium thermocellum* JN4 and *Thermoanaerobacterium thermosaccharolyticum* GD17 [Liu et al., 2008]. Thus, the results from this study reveal a significantly improved H₂ yield in the co-culture of *Clostridium termitidis* and *Clostridium beijerinckii* compared to the literature.

4.3.4 Microbial Products

From Figures 4.7 and 4.8, *C. termitidis* ATCC 51846 metabolites on cellulose were predominately acetate, ethanol, lactate, and formate in agreement with Ramachandran et al. [2008]. In mono-culture experiments, agitated and non-agitated, acetate and ethanol were produced with biomass growth, nevertheless, as shown in Figures 4.7b and 4.8b, formate and lactate started to be detected until day 38 simultaneously. The apparent high variation in Figure 4.8b is due to the very low scale at which the metabolites production is plotted. H₂ production peaked around day 44 for mono-culture experiments, concurrent with all metabolites peak.

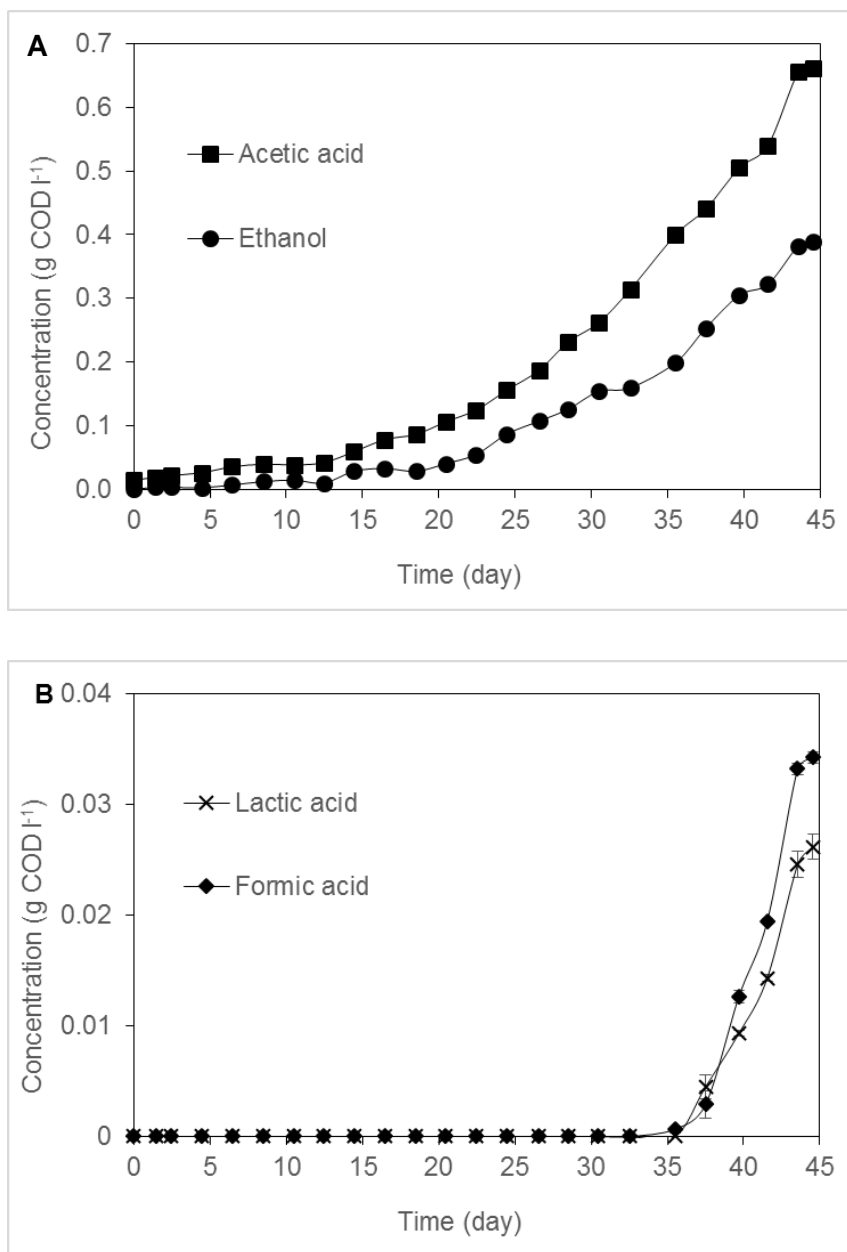


Figure 4.7: Metabolites production in non-agitated mono-culture of *C. termitidis* on 2 g l⁻¹ cellulose. a Acetic acid and ethanol. b Lactic and formic acids. Data points are the averages of duplicates, lines above and below represent the actual duplicates

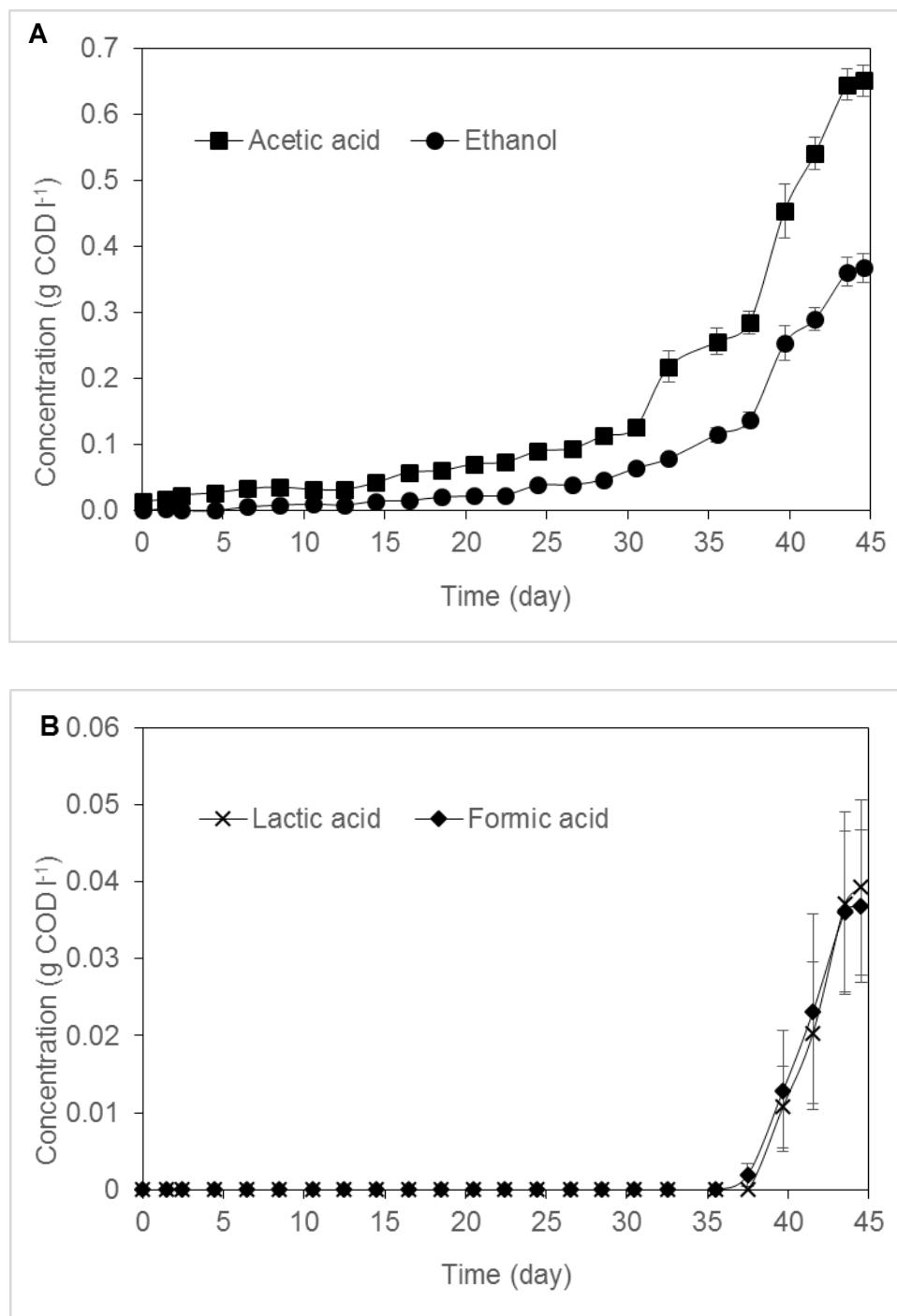


Figure 4.8: Metabolites production in agitated mono-culture of *C. termitidis* on 2 g l⁻¹ cellulose. a Acetic acid and ethanol. b Lactic and formic acids. Data points are the averages of duplicates, lines above and below represent the actual to duplicates

C. beijerinckii DSM 1820 soluble products from glucose have been reported by Masset et al. [2012] to be butyrate, acetate, formate, lactate, in addition to butanol, acetone and isopropanol by Chen and Hiu [1986], although, other strains of *C. beijerinckii* (i.e. L9 and Fanp3) have been demonstrated to produce ethanol from glucose [Lin et al., 2007; Pan et al., 2008]. Figures 4.9 and 4.10 illustrate the changes of metabolites in co-culture fermentations. The main difference between mono and co-cultures is that butyrate, which is produced only by *C. beijerinckii*, was present. In the non-agitated co-culture acetate and butyrate were produced as lactate was consumed but the exponential production of formate and ethanol started when lactate was below the detection limit of 0.005 g l^{-1} , around day 23. It should be noticed that in non-agitated co-culture only butyrate production lasted until day 40, concurrent with H_2 peak, in contrast with acetate, ethanol and formate, which production plateaued around days 27-29. In the agitated co-culture both acetate and butyrate were produced as lactate was consumed, with acetate starting the exponential production phase right after lactate was non-detect (day 27) while butyrate plateaued and started the exponential phase simultaneously with formate (day 33). It should also be noticed that in agitated co-culture only butyrate production lasted until day 44, concurrent with H_2 peak, while acetate, ethanol and formate production plateaued around day 36.

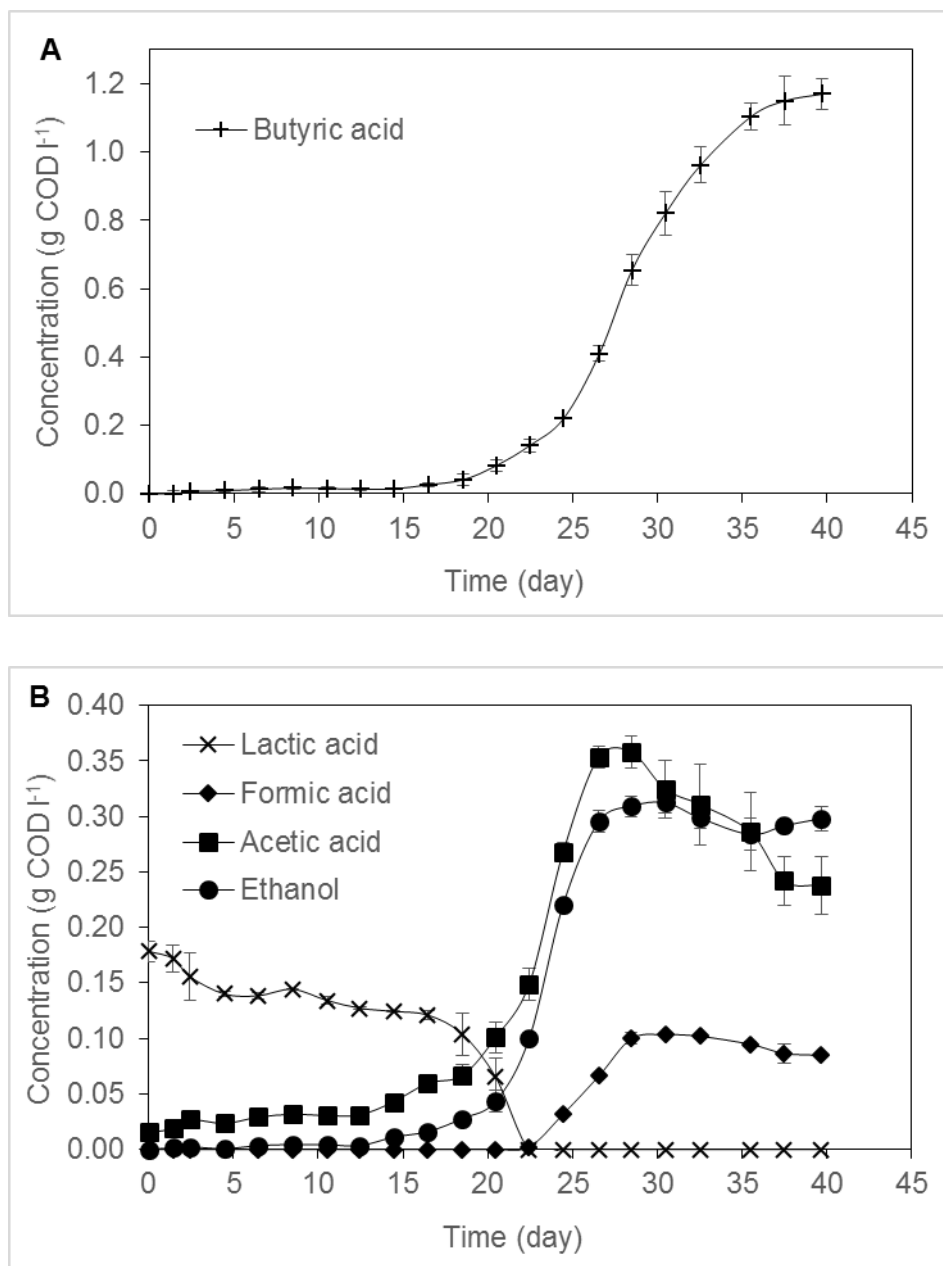


Figure 4.9: Metabolites production or consumption in non-agitated co-culture of *C. termitidis* and *C. beijerinckii* on 2 g l⁻¹ cellulose. a Butyric acid. b Ethanol, lactic, formic and acetic acids. Data points are the averages of duplicates, lines above and below represent the actual duplicates

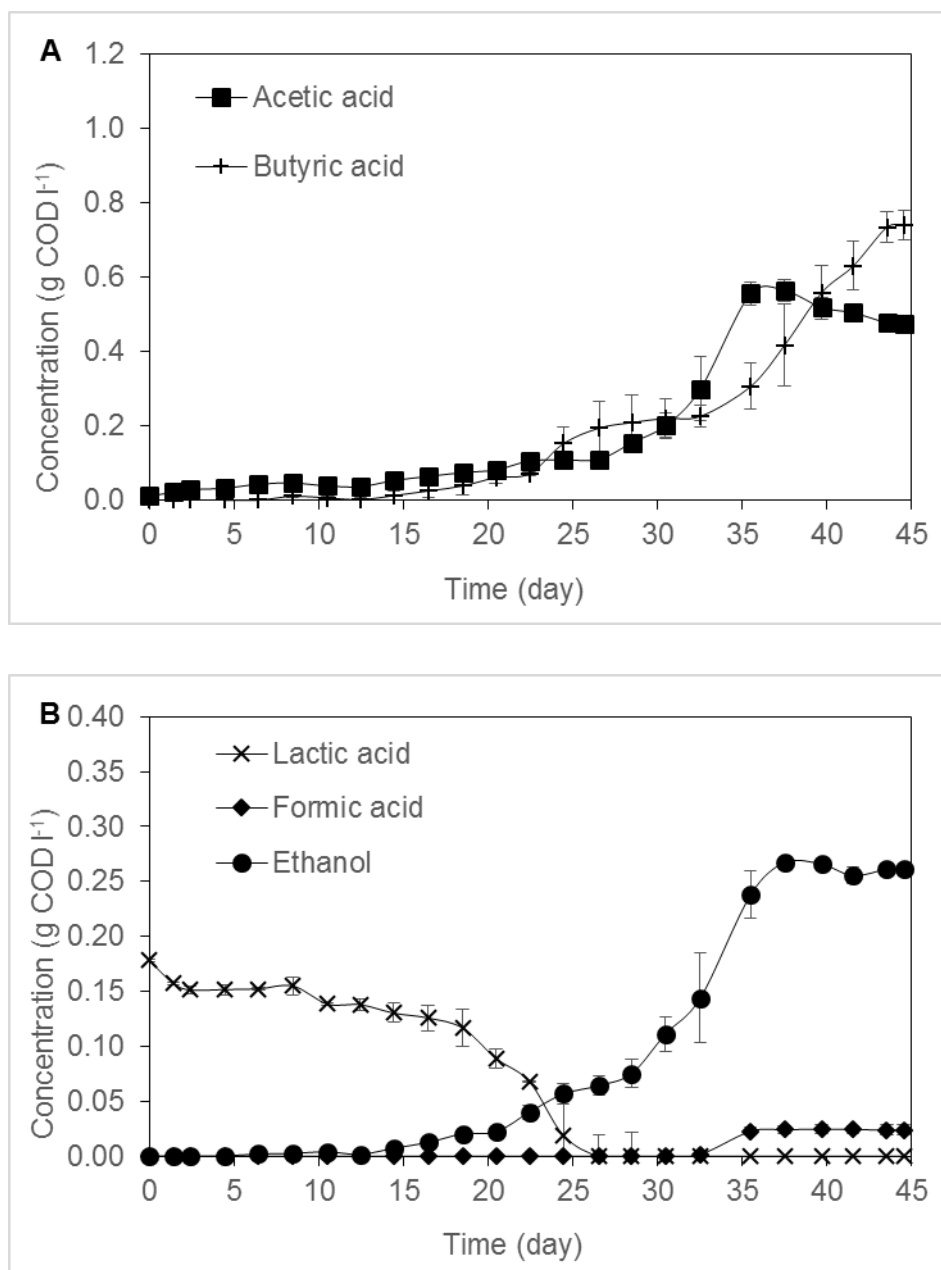
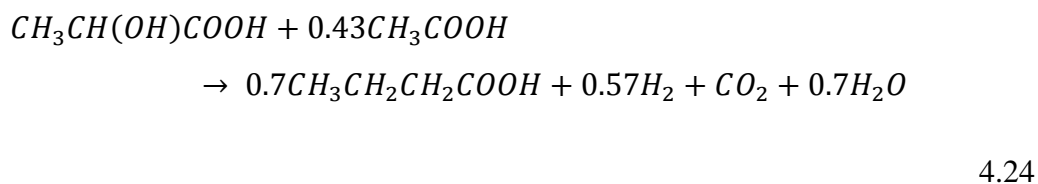
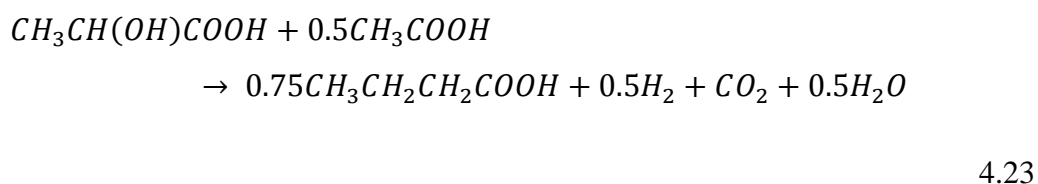


Figure 4.10 Metabolites production or consumption in agitated co-culture of *C. termitidis* and *C. beijerinckii* on 2 g l⁻¹ cellulose. a Butyric and acetic acids. b Ethanol, lactic and formic acids. Data points are the averages of duplicates, lines above and below represent the actual duplicates

Anaerobic lactate consumption has been reported by different inoculums, such as soil, kitchen waste compost, *Clostridium diolis* JPCC H-3, *Clostridium butyricum* JPCC H-1, *Clostridium acetobutylicum* P262, and also *Clostridium beijerinckii* JPCC H-4 [Grause et al., 2012; Lee et al., 2010; Matsumoto and Nishimura, 2007; Diez-Gonzalez et al., 1995]. Nevertheless, in some cases, acetate has been simultaneously consumed with lactate. The metabolic pathways reported in the literature are shown in Equations 4.6, 4.23 and 4.24 [Grause et al., 2012; Matsumoto and Nishimura, 2007; Thauer et al., 1977; Costello et al., 1991; Diez-Gonzalez et al., 1995] :



In Equation 4.6, lactate and H₂O are consumed to produce acetate, H₂ and CO₂, while in Equations 4.23 and 4.24, lactate and acetate are consumed to produce butyrate, H₂, CO₂ and H₂O. The evident lactate consumption in co-culture fermentations (agitated and non-agitated) shown in Figures 4.9b and 4.10b, could be assumed to follow Equation 4.6 since acetate was produced simultaneously.

Apparently, co-culture fermentations presented acetate consumption starting on day 29 (Figure 4.9b) and day 38 (Figure 4.10a) for agitated and non-agitated bottles, respectively, which could be explained by Equations 4.23 and 4.24, although lactate was below the detection limit during this period of time. In contrast, mono-culture fermentations (agitated and non-agitated) did not present this phenomena because *C. termitidis* does not produce butyrate, therefore acetate consumption in co-culture fermentations could be attributed to the presence of *C. beijerinckii*. Interestingly, the co-culture experiment of *C. thermocellum* JN4 and *T. thermosaccharolyticum* GD17 reported by Liu et al. [2008] also consumed

lactate whereas *C. thermocellum* JN4 in mono-culture did not. However, no explanation of this phenomena was attempted by the authors.

The maximum concentration of metabolites produced during the fermentation are presented in Table 4.2. Lactate in co-cultures experiments is negative because it was consumed. Theoretical H₂ production from acetate and butyrate shown in Table 4.2 was calculated based on 848 ml H₂ g⁻¹ acetate and 578 ml H₂ g⁻¹ butyrate (Equations 19 and 20). The theoretical values were consistent with the H₂ measured during the experiment with an average percent difference of 2% of the theoretical H₂ calculated.

Table 4.2: Metabolites production or consumption and theoretical H₂ production of *C. termitidis* mono-cultured on 2 g l⁻¹ cellulose and co-cultured with *C. beijerinckii* on 2 g l⁻¹ cellulose

<i>Culture</i>		<i>Maximum metabolites production or consumption (g l⁻¹)</i>					<i>Theoretical H₂ (ml)</i>			<i>Experimental H₂ (ml)</i>	<i>Difference (%)</i>
		Lactic acid	Formic acid	Acetic acid	Ethanol	Butyric acid	From Acetic	From Butyric	Total		
<i>Non-agitated</i>	Mono	0.02	0.1	0.58	0.18	0	247	0	247	245	1
	Co	-0.17	0.24	0.32	0.14	0.64	136	186	322	324	0
<i>Agitated</i>	Mono	0.03	0.1	0.59	0.17	0	251	0	251	246	2
	Co	-0.17	0.07	0.52	0.13	0.4	220	117	337	356	5

COD balances are electron (e^-) balances that are important in any oxidation-reduction reactions such as biological fermentations. A 100 percent COD mass balance closure indicates that the electron equivalents of the reactants are equal to the electron equivalents of the products, confirming that the oxidation-reduction reaction is balanced. COD balances calculated by summation of metabolites, H_2 , cellulose and cells as $g\ COD\ l^{-1}$ at the beginning and end of fermentations are presented in Table 4.3. The COD balances closed within 3% to 8% of the initial, thus verifying the reliability of the data.

Table 4.3: COD balance of *C. termitidis* mono-cultured on $2\ g\ l^{-1}$ cellulose and co-cultured with *C. beijerinckii* on $2\ g\ l^{-1}$ cellulose

Culture			<i>Metabolites</i> ^a	H_2 ^b	<i>Cellulose</i>	<i>Biomass</i> ^c	<i>Total COD</i>	<i>COD balance</i> ^d (%)
			($g\ COD\ l^{-1}$)	($g\ COD\ l^{-1}$)	($g\ COD\ l^{-1}$)	($g\ COD\ l^{-1}$)	($g\ COD\ l^{-1}$)	
Non-agitated	Mono	Initial	0.01	0	2.55	0.01	2.57	97
		Final	1.08	0.31	0.49	0.61	2.49	
	Co	Initial	0.19	0	2.55	0.02	2.76	108
		Final	1.79	0.41	0.17	0.63	3	
Agitated	Mono	Initial	0.01	0	2.55	0.01	2.57	99
		Final	1.08	0.31	0.48	0.66	2.54	
	Co	Initial	0.19	0	2.55	0.02	2.75	100
		Final	1.5	0.45	0.17	0.64	2.76	

^a Metabolites COD accounts for the sum of acetate, butyrate, lactate, formate and ethanol as $g\ COD\ l^{-1}$

^b Calculated based on $8\ g\ COD\ g^{-1}\ H_2$

^c Biomass COD was calculated by multiplying dry weight ($g\ l^{-1}$) $\times 0.9 \times 1.42$ ($g\ COD\ g^{-1}$ biomass)

^d COD mass balance = (Final TCOD/Initial TCOD) $\times 100\%$

4.3.5 Microbial Kinetics

As depicted in Figure 4.11, changes in biomass and cellulose over time were experimentally measured only in agitated bottles since mixing ensured homogeneity. Biomass was calculated based on the cellular protein content of *C. termitidis* in mono-culture and cellular protein content in *C. termitidis* and *C. beijerinckii* in co-culture assuming 100% viability of the cells. With the same cellular protein content for both strains (19-20%), distinction between the two microbial species on the basis of proteins is impossible. In order to estimate these profiles in non-agitated bottles, a correlation between biomass (g dry weight l^{-1}) and cumulative H_2 (ml H_2) from agitated experiments was calculated with the results shown in Figure 4.12. It is evident that for both cases i.e. mono and co-cultures biomass increased linearly with H_2 production.

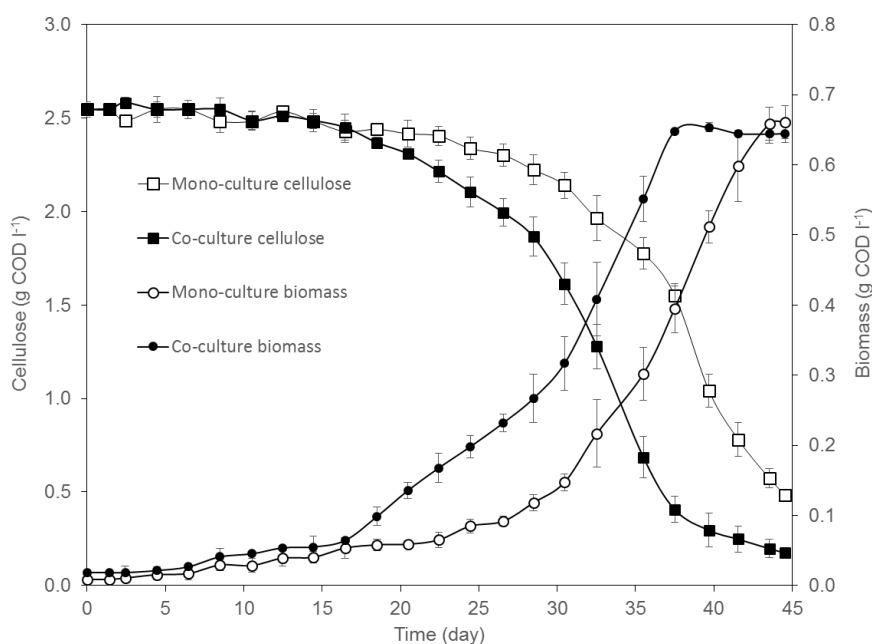


Figure 4.11: Biomass and cellulose profiles in non-agitated bottles. Data points are the averages of duplicates, lines above and below represent the actual duplicates

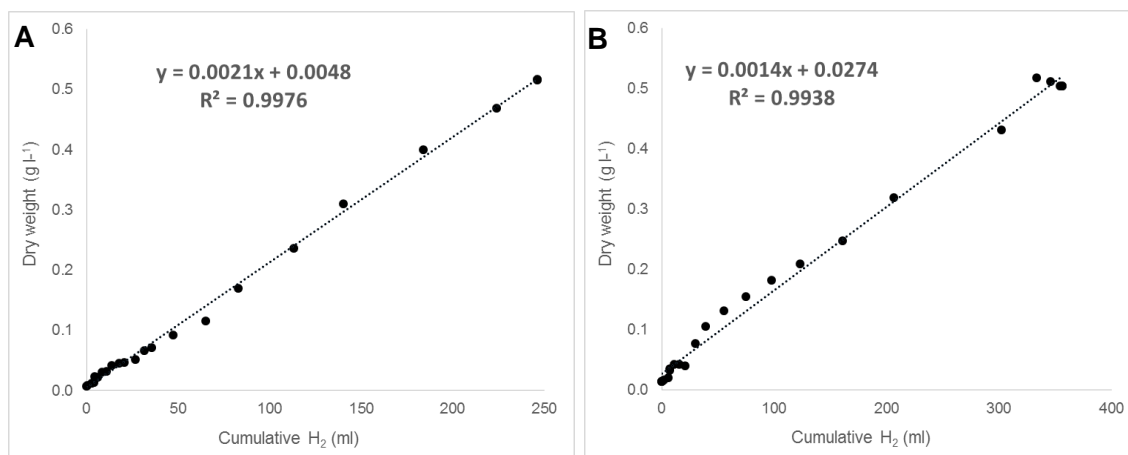


Figure 4.12: Biomass (g dry weight l⁻¹) – cumulative H₂ (ml) correlation in agitated bottles. a Mono-culture of *C. termitidis*. b Co-culture of *C. termitidis* and *C. beijerinckii*.

Cellulose concentration profile in non-agitated bottles was calculated indirectly based on Equation 4.25, all units expressed in g COD l⁻¹.

$$\text{Cellulose COD} = \text{TCOD} - (\text{metabolites COD} + \text{H}_2 \text{ COD} + \text{biomass COD})$$

4.25

Microbial kinetics were estimated from the growth phase only, ignoring the lag phase. The experimental and modeled profiles of biomass and cellulose consumption for non-agitated and agitated bottles are illustrated in Figures 4.13 and 4.15, respectively. From cellulose profiles is clear co-cultures bottles were able to utilize more cellulose than mono-cultures. Nevertheless, maximum biomass growth was similar in all cases. It may be observed in these figures that the modeled data fits experimental data quite well.

Figures 4.14 and 4.16 show the Particulate Organic to biomass (PO/X) ratio profiles for non-agitated and agitated bottles, respectively. These profiles were generated based on the experimental and modeled substrate and biomass profiles for each case. Particulate organic matter modeling approach (POM) considers the particulate substrate conversion rate as a rate-limiting process that is dependent on the particulate substrate and biomass

concentrations. The particulate degradation concentration is expressed relative to the biomass because the particulate hydrolysis is related to the relative contact area between the non-soluble organic material and the biomass [Metcalf and Eddy, 2003].

Figures 4.17-4.20 show the experimental and modeled metabolites profile. It is noteworthy that neither glucose nor cellobiose from cellulose hydrolysis were detected in any of the fermentations, meaning they were utilized by the bacteria as soon as they were generated, and making cellulose hydrolysis the rate limiting factor. It may be observed in Figures 4.17 and 4.19 that the model fits experimental data for acetate and ethanol quite well for non-agitated and agitated mono-culture experiments, nevertheless, the model failed to fit most of the experimental data for lactate and formate, and could only fit the very late stage of the fermentation. This is because the model does not account for time delays corresponding to the lag phase both metabolites showed before they started to be detected. For non-agitated co-culture experiment, it may be observed in Figure 4.18 that the model is quite good for butyrate throughout the fermentation, and also for acetate and ethanol in the early stage of the fermentation, but it deviates when both metabolites peak. As depicted in Figure 4.20, the model was in good agreement with experimental data for ethanol and lactate in agitated co-culture experiments, variations in acetate and butyrate, however, were not considered in the model. Similar to mono-culture experiments, the model does not predict the formate lag phase in co-culture experiments. Also, the observed decline of acetate in the late stage of the co-culture fermentations was not predicted by the model.

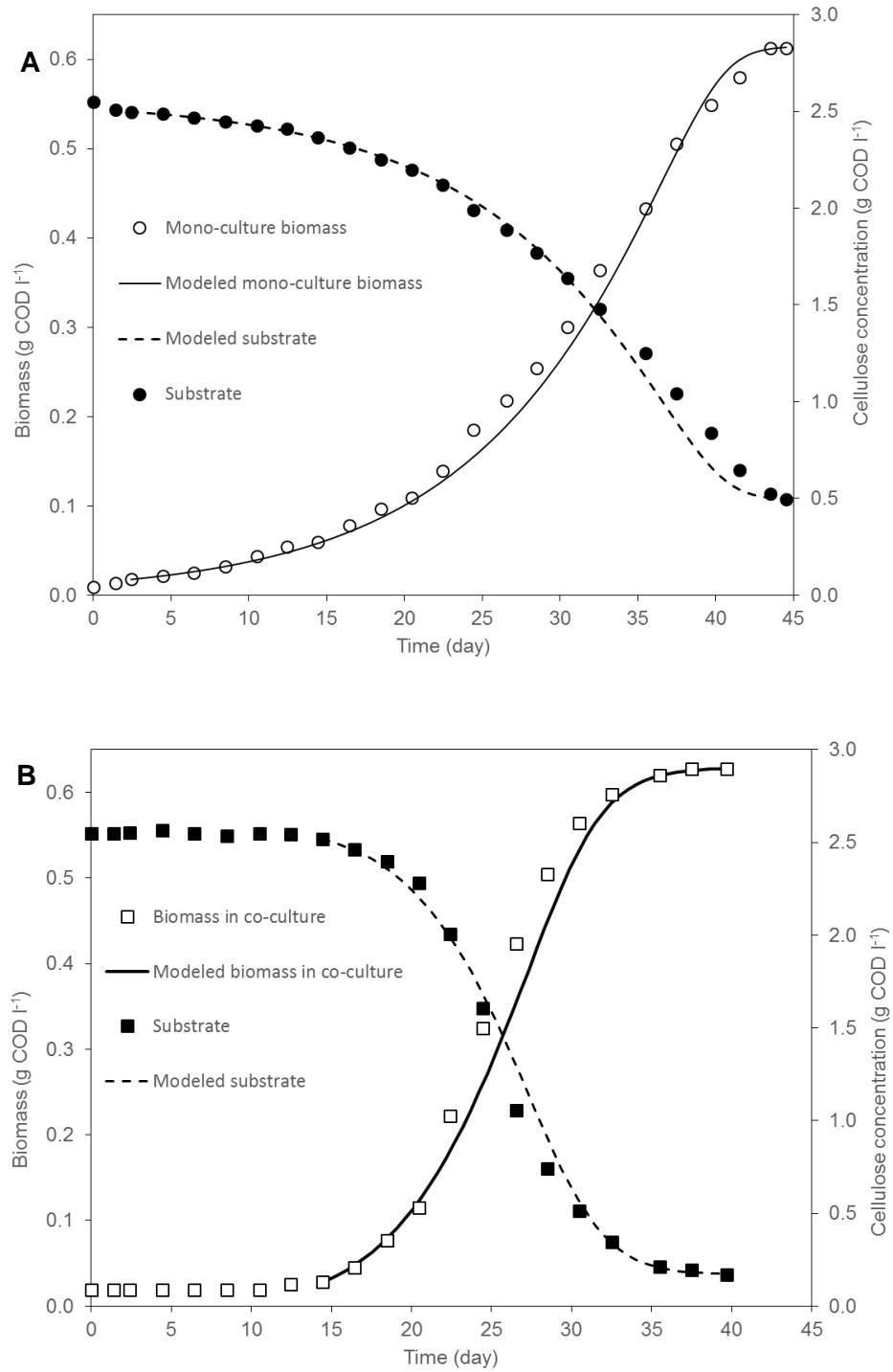


Figure 4.13: Experimental and modeled growth kinetics in non-agitated experiments. a Mono-culture. b Co-culture

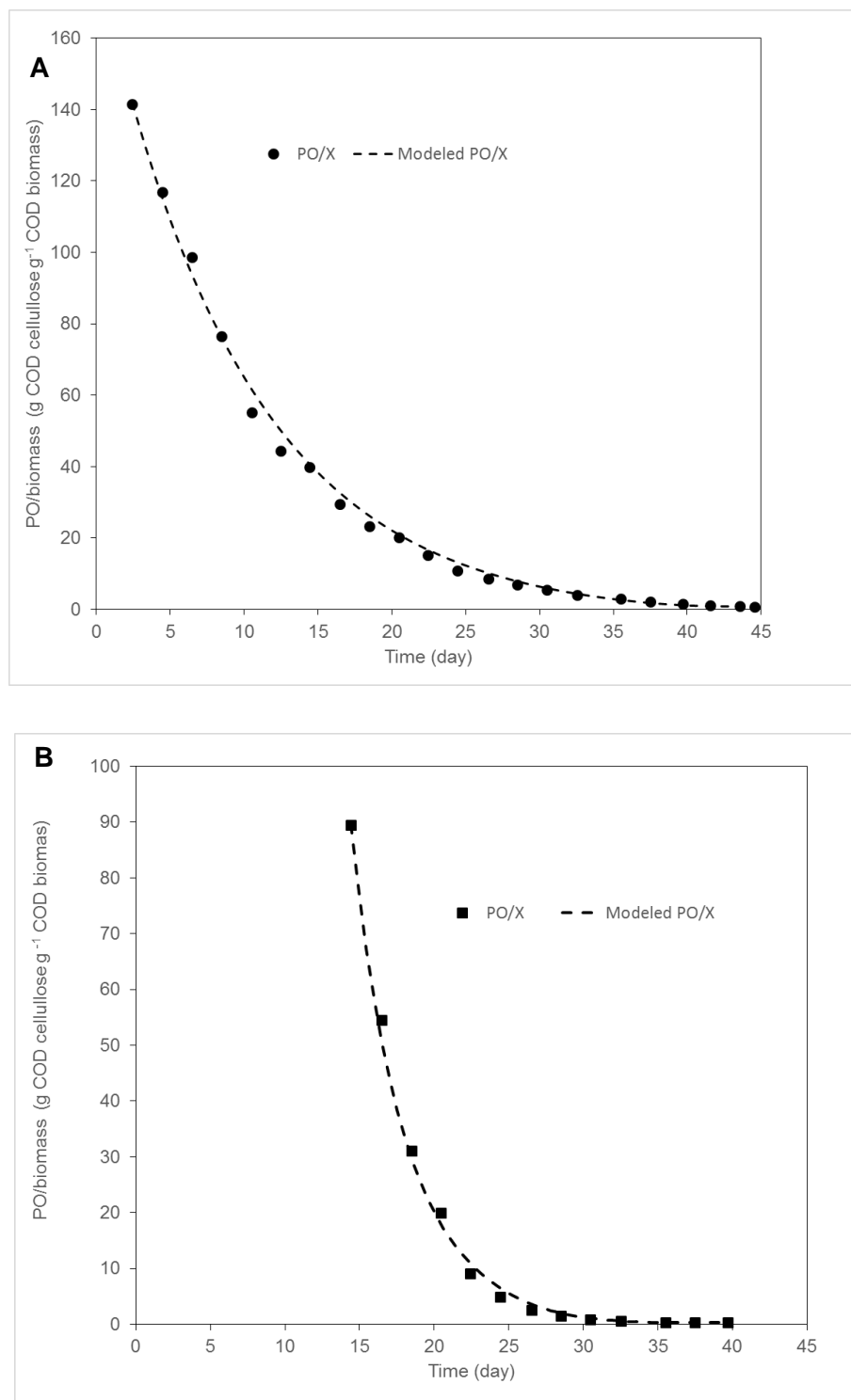


Figure 4.14: Experimental and modeled PO/biomass profiles in non-agitated experiments. a Mono-culture. b Co-culture

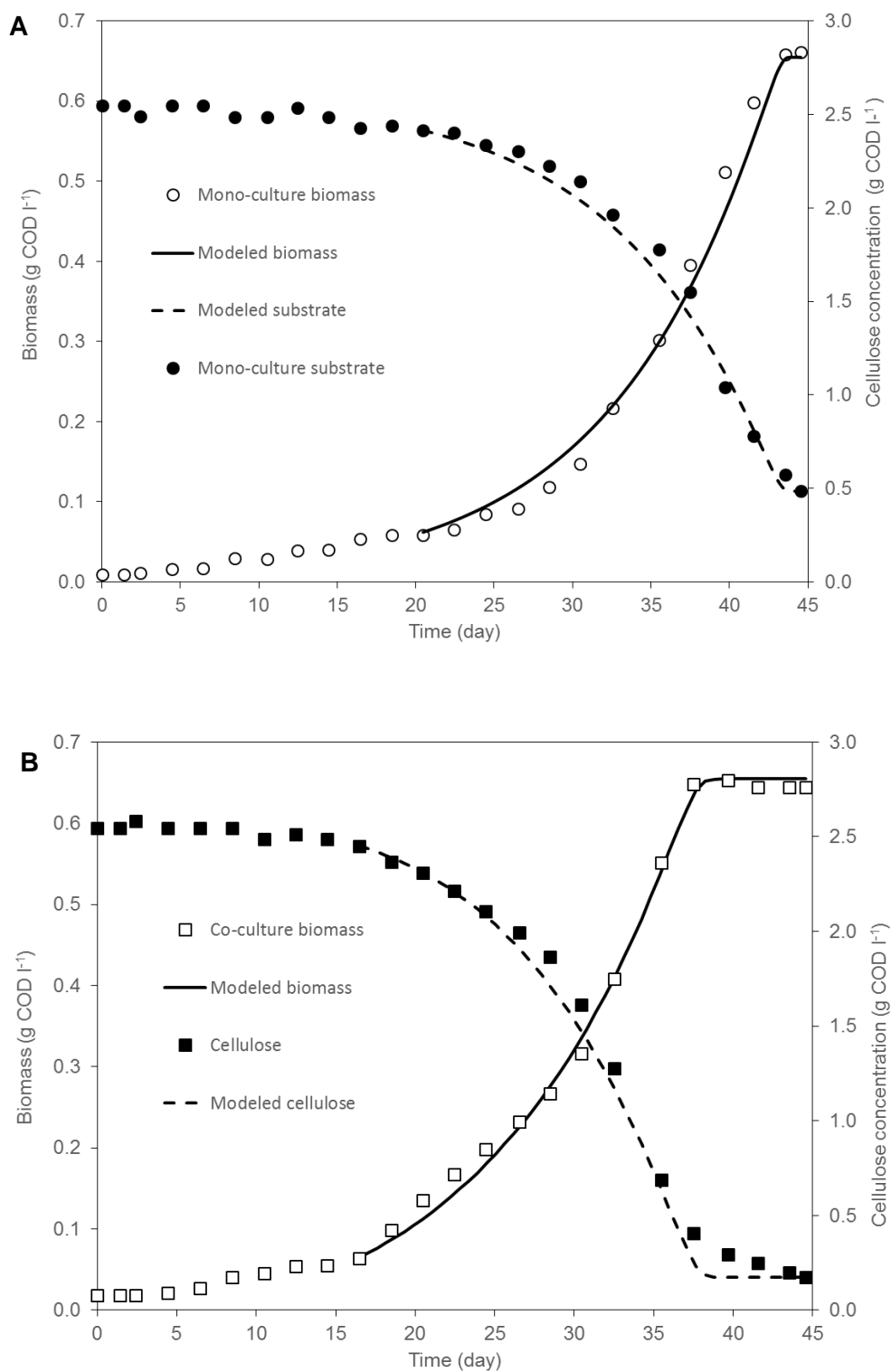


Figure 4.15: Experimental and modeled growth kinetics in agitated experiments.
a Mono-culture. b Co-culture

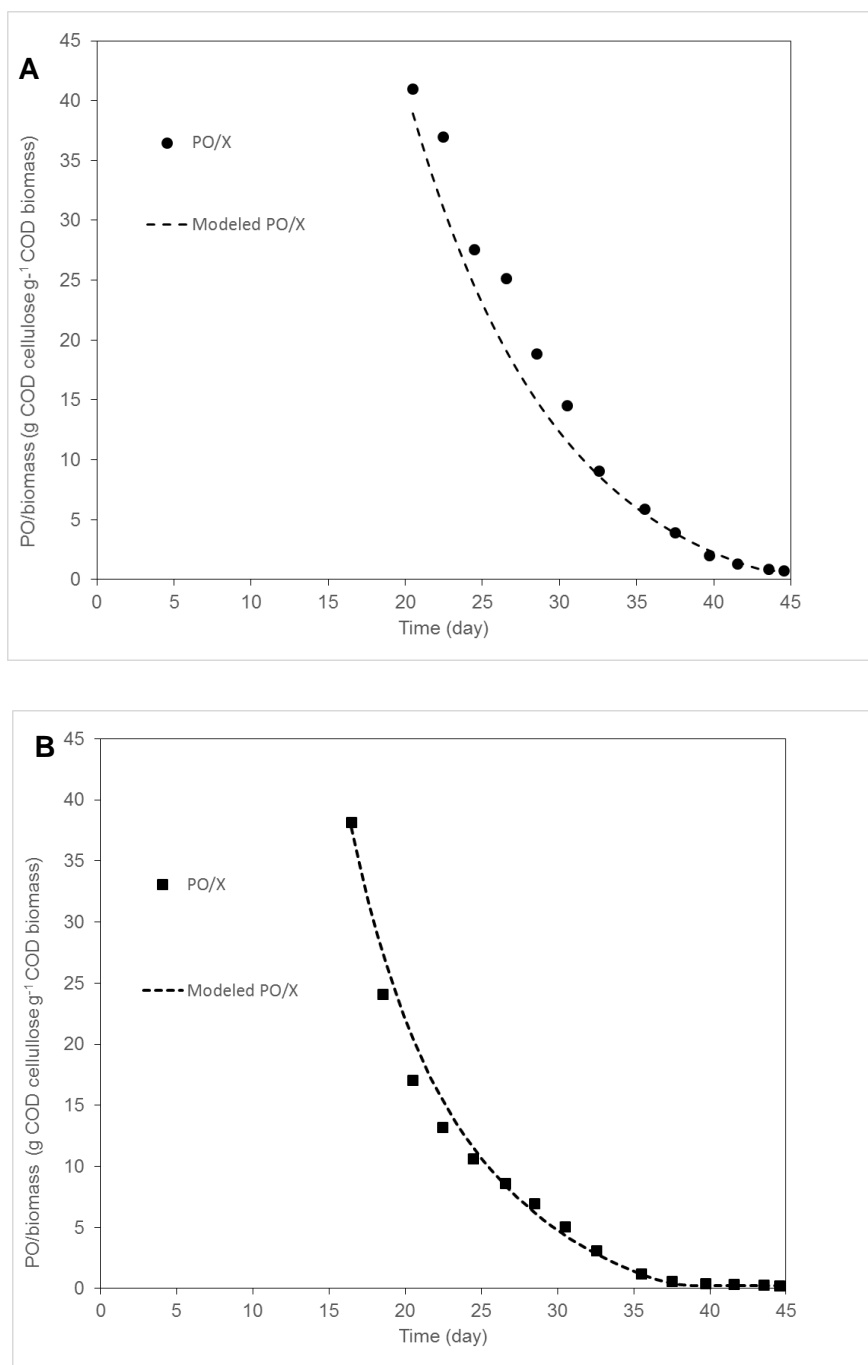


Figure 4.16: Experimental and modeled PO/biomass profiles in agitated experiments. a Mono-culture. b Co-culture

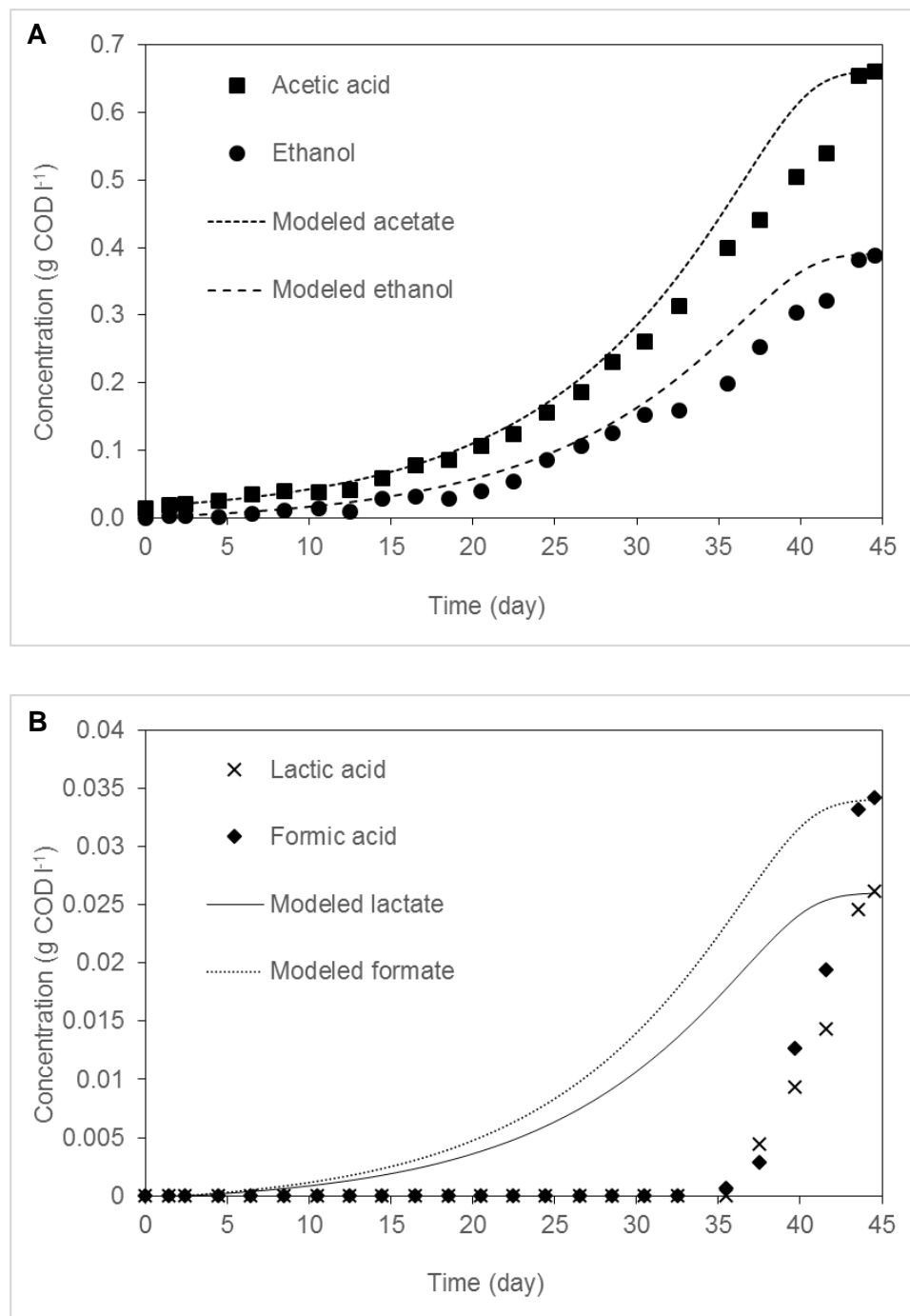


Figure 4.17: Experimental and modeled profile of metabolites in non-agitated mono-culture. a Acetic acid and ethanol. b Lactic and formic acids

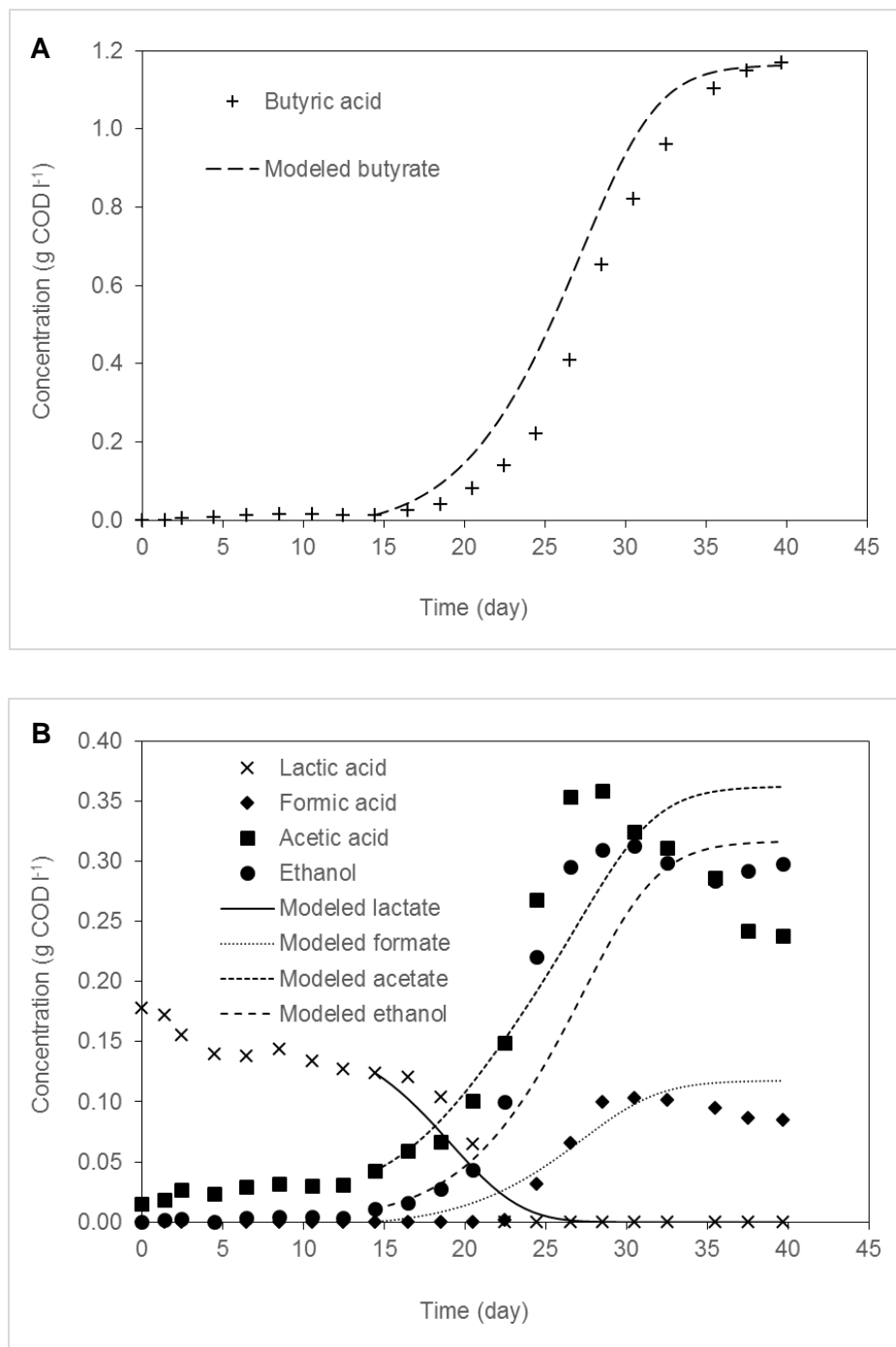


Figure 4.18: Experimental and modeled profile of metabolites in non-agitated co-culture. a Butyric acid. b Lactic, formic, acetic acids and ethanol

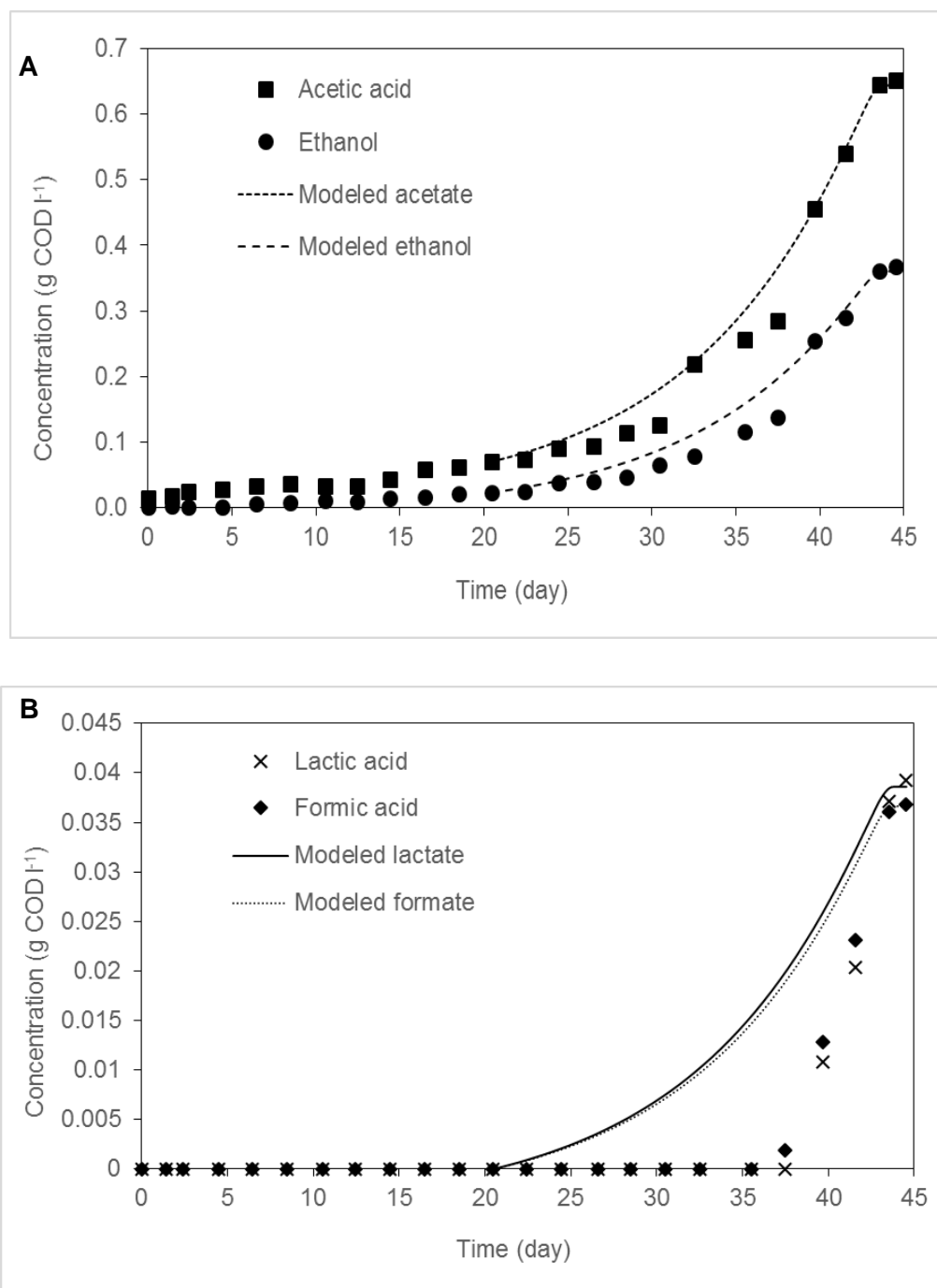


Figure 4.19: Experimental and modeled profile of metabolites in agitated mono-culture. a Acetic acid and ethanol. b Lactic and formic acids

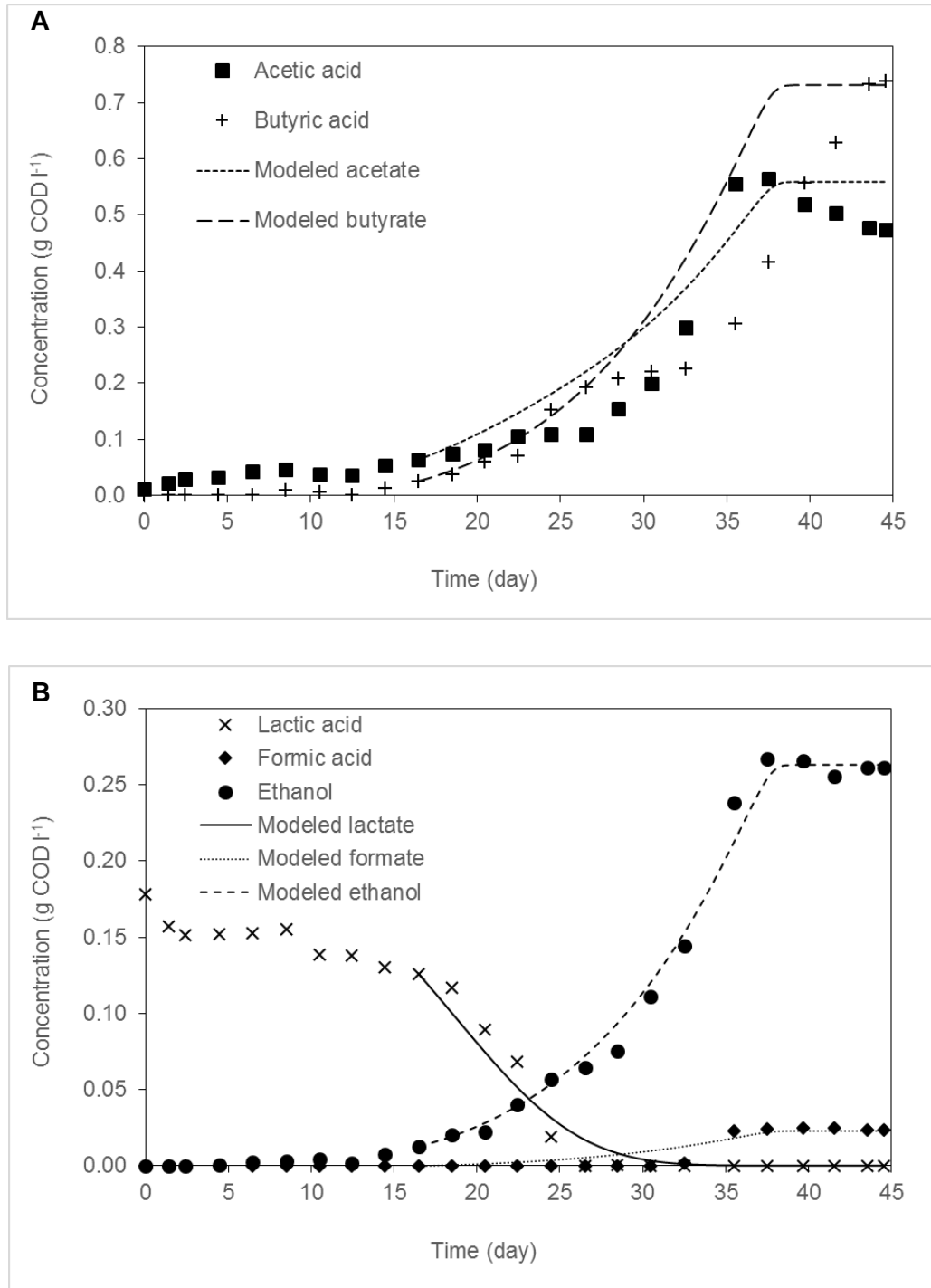


Figure 4.20: Experimental and modeled profile of metabolites in agitated co-culture.
a Butyric and acetic acids. b Lactic, formic acids, and ethanol

Mathematical models that accurately predict biochemical phenomena provide the basis for design, control, optimization and scale-up of process systems [Huang and Wang, 2010]. Kinetic parameters of the mathematical model described earlier are shown in Table 4.4. The average percentage errors (APE) and root mean square errors (RMSE) calculated for the modeled biomass, substrate and metabolites are shown in Table 4.5. Non-agitated co-culture exhibited the highest μ_{\max} (0.2 d^{-1}), thus rationalizing the end of the fermentation test before others. In this regard, the impact of the synergy in microbial kinetics was more notorious in non-agitated bottles, where μ_{\max} in co-cultures (0.2 d^{-1}) doubled the μ_{\max} in mono-cultures (0.1 d^{-1}). It is noteworthy that the maximum specific growth rates achieved on glucose and cellobiose by *C. termitidis* are more than 50 times greater than those achieved by the same strain on cellulose.

Half-saturation constant, K_x , varied between $0.04 - 1.1 \text{ g COD cellulose g}^{-1} \text{ COD biomass}$ for all fermentations. PO/X values from Figures 4.14 and 4.16 are significantly greater than these K_x values, therefore μ_{\max} values can be considered as hydrolysis rates. The recommended value for the hydrolysis rate of carbohydrates in the Anaerobic Digestion Model (ADM1) [Siegrist et al., 2002] is 0.25 d^{-1} at mesophilic conditions which is comparable to the growth rates obtained in the present study, clearly emphasizing that the biodegradation of cellulose is hydrolysis-limited.

Biomass yields were exactly the same in mono-culture ($0.3 \text{ g COD g}^{-1} \text{ COD cellulose}$) irrespective of agitation. Co-culture experiments reflected a slightly lower biomass yield than monoculture ($0.25 \text{ g COD g}^{-1} \text{ COD cellulose}$). Lactate consumption in i.e. agitated co-culture was slower than the non-agitated as reflected by K_L values of 1.5 compared to $2.5 \text{ l g}^{-1} \text{ COD biomass d}^{-1}$, which is also consistent to the higher μ_{\max} shown without agitation. Some parameters in Table 4.4 were not calculated for all cases, for example, K_L , $Y_{X/L}$ (biomass yield from lactate) and $Y_{A/L}$ (acetate yield from lactate) were only relevant in co-culture, as the mono-culture did not show lactate consumption. $Y_{X/L}$ was assumed to be the same as $Y_{X/S}$ (biomass yield from cellulose) and $Y_{A/L}$ was calculated as follows:

$$Y_{A/L} = f_{A/L}(1 - Y_{X/L}) \quad 4.26$$

where $f_{A/L}$ is the stoichiometric relationship based on Equation 4.6 of 1 mol acetate per mol lactate, calculated in g COD as 0.66. $Y_{A/L}$ was calculated to be 0.49 g COD acetate g⁻¹ COD lactate and the theoretical hydrogen production from lactate was also calculated based on Equation 4.6 and subtracted from the measured hydrogen produced. The modified H₂ yields from cellulose in non-agitated co-cultures were 1.72 mol H₂ mol⁻¹ hexose equivalent_{added} and 1.84 mol H₂ mol⁻¹ hexose equivalent_{consumed}. Similarly, the modified H₂ yields in agitated co-cultures were 1.91 mol H₂ mol⁻¹ hexose equivalent_{added} and 2.05 mol H₂ mol⁻¹ hexose equivalent_{consumed}. Upon comparison with Table 4.1, there was still an improvement of 19% and 30% of co-culture compared to mono-culture based on hexose added in non-agitated and agitated bottles, respectively. Nevertheless, the calculated H₂ from lactate may be overestimated since it is theoretical.

Biomass and cellulose exhibited the lowest average percentage errors, within the range of 4-15% in all cases, followed by PO/X with the highest value of 19% in agitated mono and co-culture. Ethanol was best fitted in agitated co-culture with an APE as low as 7%. Lactic acid consumption in co-culture had a better fit (14-23% APE) than its production in mono-culture bottles (69-81% APE) due to the lag phase observed in the latter. As depicted in Figures 4.17b, 4.18b, 4.19b and 4.20b, lag phases for lactate in mono-cultures and formate in all cases was not considered in the model, hence the high APE values (as high as 81%). The APE values excluding these lag phases are 12% and 20% for lactate in non-agitated and agitated mono-cultures, respectively. Similarly, for formate are 11% and 15% for non-agitated and agitated mono-cultures, respectively, and 14% and 8% in non-agitated and agitated co-cultures.

Desvaux et al. [2000] found a μ_{max} of 0.056 h⁻¹ with *C. cellulolyticum* grown on 2.4 g cellulose l⁻¹ with a biomass yield of 36.5 g of cells mol⁻¹ hexose equivalent. Kinetics on cellulose have been also explained by alternative models to Monod. For example, Holwerda and Lynd [2013] found that the best fit to their results on *C. thermocellum* was with a substrate utilization rate that is both first order with respect to substrate and first order in cells. Recently, Gupta et al. [2015] found a μ_{max} of 0.05 d⁻¹ on cellulose using mesophilic anaerobic digested sludge (ADS) and Ks of 2.1 g l⁻¹, which is four times lower than that achieved by *C. termitidis* in the present study.

Table 4.4: Kinetic parameters obtained in MATLAB of *C. termitidis* mono-cultured on 2 g l⁻¹ cellulose and co-cultured with *C. beijerinckii* on 2 g l⁻¹ cellulose.

		<i>Non-agitated</i>		<i>Agitated</i>	
		Mono-culture	Co-culture	Mono-culture	Co-culture
<i>Kinetic parameters</i>	S_o^a (g COD l ⁻¹)	0.49	0.17	0.48	0.17
	μ_{max} (d ⁻¹)	0.10	0.20	0.10	0.10
	Y_{XL}^b	NA	0.25	NA	0.25
	$Y_{x/PO}^c$	0.30	0.25	0.30	0.25
	K_m^d	0.33	0.80	0.33	0.40
	$Y_{L/PO}$	0.013	NA	0.02	NA
	$Y_{F/PO}$	0.017	0.05	0.019	0.01
	$Y_{A/PO}^g$	0.32	0.11	0.297	0.19
	$Y_{E/PO}^h$	0.194	0.13	0.175	0.11
	$Y_{B/PO}^i$	0	0.49	0	0.31
	$Y_{A/L}^j$	NA	0.49	NA	0.49
	K_L	NA	2.5	NA	1.5
	K_x^k	0.42	1.1	0.04	0.10

^a Non-biodegradable factor

^b Biomass yield from lactate (g COD g⁻¹ COD lactate)

^c Biomass yield (g COD g⁻¹ COD cellulose)

^d g COD substrate g⁻¹ COD biomass d⁻¹

^e Lactate yield (g COD g⁻¹ COD cellulose)

^f Formate yield (g COD g⁻¹ COD cellulose)

^g Acetate yield (g COD g⁻¹ COD cellulose)

^h Ethanol yield (g COD g⁻¹ COD cellulose)

ⁱ Butyrate yield (g COD g⁻¹ COD cellulose)

^j Acetate yield from lactate (g COD g⁻¹ COD lactate)

^k g COD cellulose g⁻¹ COD biomass

NA: Not Applicable

Table 4.5: APE and RMSE for biomass, substrate and metabolites of *C. termitidis* mono-cultured on 2 g l⁻¹ cellulose and co-cultured with *C. beijerinckii* on 2 g l⁻¹ cellulose

		<i>Non-agitated</i>		<i>Agitated</i>	
		Mono-culture	Co-culture	Mono-culture	Co-culture
<i>APE (%)</i>	Dry weight	7	8	9	5
	Cellulose	4	5	5	15
	PO/X	9	11	19	19
	Lactic acid	81	23	69	14
	Formic acid	81	41	66	56
	Acetic acid	10	19	11	21
	Ethanol	19	24	16	7
	Butyric acid	NA	25	NA	19
	Hydrogen	15	10	12	14
	<i>RMSE (g COD l⁻¹)</i>	Dry weight	0.016	0.034	0.024
Cellulose		0.062	0.088	0.076	0.086
PO/X ^a		2.42	1.39	2.91	1.46
Lactic acid		0.008	0.013	0.010	0.009
Formic acid		0.011	0.017	0.008	0.005
Acetic acid		0.042	0.069	0.033	0.071
Ethanol		0.030	0.054	0.025	0.010
Butyric acid		NA	0.115	NA	0.131
Hydrogen (ml)		9	13	8	16

APE: Average percentage error

RMSE: Root mean square error

NA: Not Applicable

^a g COD cellulose g⁻¹ biomass

Based on the modeled acetate and butyrate profiles, modeled hydrogen profiles shown in Figure 4.21 were calculated in a similar manner as the theoretical hydrogen shown in Table 4.2, with 848 ml H₂ g⁻¹ acetate and 578 ml H₂ g⁻¹ butyrate (from stoichiometry of Equations 19 and 20), and 1.067 g COD g⁻¹ acetate and 1.82 g COD g⁻¹ butyrate. For example, at time 29 day when modeled acetate concentration in non-agitated co-culture was 0.28 g COD l⁻¹ and modeled butyrate concentration was 0.8 g COD l⁻¹, modeled hydrogen produced (ml) in 500 ml was calculated as follows:

$$H_{2_{t=29d}} = \left[\frac{0.28 \text{ g COD}}{l} * \frac{0.5 \text{ l}}{1.067 \text{ g COD}} * \frac{\text{g acetate}}{\text{g acetate}} * \frac{848 \text{ ml H}_2}{\text{g acetate}} \right] + \left[\frac{0.8 \text{ g COD}}{l} * \frac{0.5 \text{ l}}{1.82 \text{ g COD}} * \frac{\text{g butyrate}}{\text{g butyrate}} * \frac{578 \text{ ml H}_2}{\text{g butyrate}} \right] = 238.29 \text{ ml H}_2$$

As shown in Figure 4.21 the modeled hydrogen profiles are very similar to the experimental hydrogen and is verified with the low APE values ranging from 10% to 15% and RMSE values (8-16 ml) included in Table 4.5.

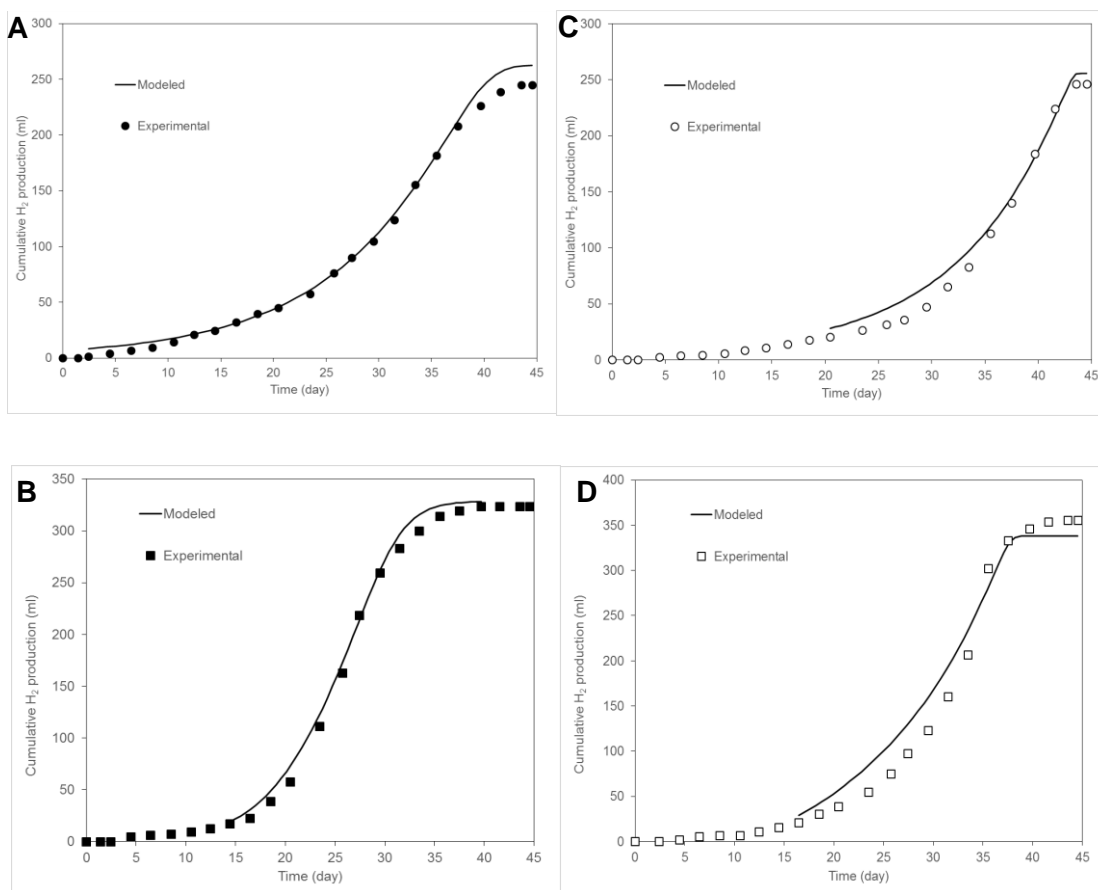


Figure 4.21: Experimental and modeled hydrogen profiles for: a Non-agitated mono-culture. b Non-agitated co-culture. c Agitated mono-culture. d Agitated co-culture

Table 4.6 shows the distribution of 1 g COD of substrate consumed in the fermentations express as yields (g COD/g COD substrate consumed). The yields from experimental data was calculated based on Tables 4.2 and 4.3, considering the maximum production of metabolites, biomass and H_2 , and cellulose and lactate consumed. Lactate and cellulose were the substrates for co-culture fermentations. The modeled yields are from Table 4.4, acetate yields for co-culture fermentations from total COD of substrate consumed were calculated based on $Y_{A/PO}$ and $Y_{A/L}$. Modeled H_2 yields were calculated based on modeled data only. As it can be seen, modeled yields are in agreement with experimental yields. Table 4.6 can also be considered a COD balance since the sum of yields should give 1. The

yields in co-culture fermentations sum more than 1 mainly because the acetate yield calculated is based on the maximum acetate concentration and does not account for the acetate consumption discussed earlier in Section 4.3.3.

Table 4.6: Distribution of 1 g COD of substrate consumed expressed as yields for all metabolites, hydrogen and biomass from experimental and modeled data

SOURCE	Culture		Lactate	Formate	Acetate	Ethanol	Butyrate	Hydrogen	Cells	Sum of yields
			Yields (g COD/g COD substrate consumed)							
EXPERIMENTAL	Non-agitated	Mono	0.012	0.016	0.312	0.186	0.00	0.151	0.294	0.97
		Co		0.033	0.134	0.117	0.458	0.16	0.237	1.14
	Agitated	Mono	0.018	0.018	0.306	0.175	0.00	0.151	0.316	0.98
		Co		0.009	0.217	0.102	0.288	0.177	0.247	1.04
MODELED	Non-agitated	Mono	0.013	0.017	0.320	0.194	0.00	0.159	0.3	1
		Co		0.050	0.128	0.13	0.49	0.160	0.25	1.2
	Agitated	Mono	0.020	0.019	0.297	0.175	0.00	0.149	0.3	0.96
		Co		0.010	0.206	0.11	0.31	0.163	0.25	1.04

4.4 Conclusion

This study is the first to model *C. termitidis* microbial kinetics on cellulose and in co-culture with *C. beijerinckii*. High H₂ yields at mesophilic temperature directly from cellulose were achieved compared to the literature. Furthermore, agitation was proved to have no significant effect on *C. termitidis* cultured alone but it impacts the metabolic pathways of co-culture. Cellulose degradation was influenced by the presence of the co-culture and not by the agitation during the fermentations, increasing by 13% its degradation. Viability of *C. termitidis* and *C. beijerinckii* producing H₂ together was evidenced, however, because of the presence of lactic acid in co-culture experiments hindered the accurate calculation of the H₂ yield from the main substrate which was cellulose.

4.5 References

- Bayer E.A., Lamed R. (1992) The cellulose paradox: pollutant par excellence and/or a reclaimable natural resource? *Biodegradation* 3:171-188
- Bayer E.A., Lamed R., Himmel M.E. (2007) The potential of cellulases and cellulosomes for cellulosic waste management. *Curr Opin Biotechnol* 18:237-245
- Bayer E.A., Morag E., Lamed R. (1994) The cellulosome — A treasure-trove for biotechnology. ENGLAND: Elsevier Ltd
- Bayer E.A., Shimon L.J., Shoham Y., Lamed R. (1998) Cellulosomes-structure and ultrastructure. *J Struct Biol* 124:221-34
- Brenner K., You L., Arnold F.H. (2008) Engineering microbial consortia: a new frontier in synthetic biology. *Trends Biotechnol* 26:483-489
- Caspi R., Altman T., Billington R., Dreher K., Foerster H., Fulcher C.A., Holland T.A., Keseler I.M., Kothari A., Kubo A., Krummenacker M., Latendresse M., Mueller L.A., Ong Q., Paley S., Subhraveti P., Weaver D.S., Weerasinghe D., Zhang P.,

- Karp P.D. (2014) The MetaCyc database of metabolic pathways and enzymes and the BioCyc collection of Pathway/Genome Databases. *Nucleic Acids Res* 42:D459
- Chen J.-S., Hiu S. (1986) Acetone-butanol-isopropanol production by *Clostridium beijerinckii* (synonym, *Clostridium butylicum*). *Biotechnol Lett* 8:371-376
- Costello D.J., Greenfield P.F., Lee P.L. (1991) Dynamic modelling of a single-stage high-rate anaerobic reactor—I. Model derivation. *Water Res* 25:847-858
- D'ippolito G., Dipasquale L., Vella F.M., Romano I., Gambacorta A., Cutignano A., Fontana A. (2010) Hydrogen metabolism in the extreme thermophile *Thermotoga neapolitana*. *Int J Hydrogen Energy* 35:2290-2295
- Desvaux M., Guedon E., Petitdemange H. (2000) Cellulose catabolism by *Clostridium cellulolyticum* growing in batch culture on defined medium. *Appl Environ Microbiol* 66:2461-2470
- Diez-Gonzalez F., Russell J.B., Hunter J.B. (1995) The role of an NAD-independent lactate dehydrogenase and acetate in the utilization of lactate by *Clostridium acetobutylicum* strain P262. *Arch Microbiol* 164:36-42
- DüRre P. (2005) Handbook on clostridia. Taylor & Francis, Boca Raton
- Eiteman M.A., Lee S.A., Altman E. (2008) A co-fermentation strategy to consume sugar mixtures effectively. *Journal of biological engineering* 2:3
- Elsharnouby O., Hafez H., Nakhla G., El Naggar M.H. (2013) A critical literature review on biohydrogen production by pure cultures. *Int J Hydrogen Energy* 38:4945-4966
- Freier D., Mothershed C.P., Wiegel J. (1988) Characterization of *Clostridium thermocellum* JW20. *Appl Environ Microbiol* 54:204-211
- Geng A., He Y., Qian C., Yan X., Zhou Z. (2010) Effect of key factors on hydrogen production from cellulose in a co-culture of *Clostridium thermocellum* and *Clostridium thermopalmarium*. *Bioresour Technol* 101:4029-4033

- Gomez-Flores M., Nakhla G., Hafez H. (2015) Microbial kinetics of *Clostridium termitidis* on cellobiose and glucose for biohydrogen production. *Biotechnol Lett*:1-7
- Grause G., Igarashi M., Kameda T., Yoshioka T. (2012) Lactic acid as a substrate for fermentative hydrogen production. *Int J Hydrogen Energy* 37:16967-16973
- Guo X.M., Trably E., Latrille E., Carrère H., Steyer J.P. (2010) Hydrogen production from agricultural waste by dark fermentation: A review. *Int J Hydrogen Energy* 35:10660-10673
- Gupta M., Gomez-Flores M., Nasr N., Elbeshbishy E., Hafez H., Hesham El Naggar M., Nakhla G. (2015) Performance of mesophilic biohydrogen-producing cultures at thermophilic conditions. *Bioresour Technol* 192:741
- Hethener P., Brauman A., Garcia J.L. (1992) *Clostridium termitidis* sp. nov., a cellulolytic bacterium from the gut of the wood-feeding termite, *Nasutitermes lujae*. *Syst Appl Microbiol* 15:52-58
- Holwerda E.K., Lynd L.R. (2013) Testing alternative kinetic models for utilization of crystalline cellulose (Avicel) by batch cultures of *Clostridium thermocellum*. *Biotechnol Bioeng* 110:2389-2394
- Kumar N., Das D. (2000) Enhancement of hydrogen production by *Enterobacter cloacae* IIT-BT 08. *Process Biochem* 35:589-593
- Kuo S., Ming Whang L., Dsaratale G., Der Chen S., Shu Chang J., Hafez H., Nakhla G., Heshamel N. (2014) Biological Hydrogen Production: Dark Fermentation. *Handbook of Hydrogen Energy*. CRC Press,
- Lay J.J., Lee Y.J., Noike T. (1999) Feasibility of biological hydrogen production from organic fraction of municipal solid waste. *Water Res* 33:2579-2586
- Lee Z.K., Li S.L., Kuo P.C., Chen I.C., Tien Y.M., Huang Y.J., Chuang C., Wong S.C., Cheng S.S. (2010) Thermophilic bio-energy process study on hydrogen fermentation with vegetable kitchen waste. *Int J Hydrogen Energy* 35:13458-13466

- Lin P.Y., Whang L.M., Wu Y.R., Ren W.J., Hsiao C.J., Chang S.L.L.S. (2007) Biological hydrogen production of the genus *Clostridium*: metabolic study and mathematical model simulation. *Int J Hydrogen Energy* 32:1728-1735
- Liu Y., Yu P., Song X., Qu Y. (2008) Hydrogen production from cellulose by co-culture of *Clostridium thermocellum* JN4 and *Thermoanaerobacterium thermosaccharolyticum* GD17. *Int J Hydrogen Energy* 33:2927-2933
- López S., Dhanoa M.S., Dijkstra J., Bannink A., Kebreab E., France J. (2007) Some methodological and analytical considerations regarding application of the gas production technique. *Anim Feed Sci Technol* 135:139-156
- Lu W., Wen J., Chen Y., Sun B., Jia X., Liu M., Caiyin Q. (2007) Synergistic effect of *Candida maltosa* HY-35 and *Enterobacter aerogenes* W-23 on hydrogen production. *Int J Hydrogen Energy* 32:1059-1066
- Masset J., Calusinska M., Hamilton C., Hiligsmann S., Joris B., Wilmotte A., Thonart P. (2012) Fermentative hydrogen production from glucose and starch using pure strains and artificial co-cultures of *Clostridium* spp. *Biotechnology for Biofuels* 5:1-15
- Matsumoto M., Nishimura Y. (2007) Hydrogen production by fermentation using acetic acid and lactic acid. *J Biosci Bioeng* 103:236-241
- Metcalf L., Eddy H.P. (2003) *Wastewater engineering : treatment and reuse*. 4th ed. McGraw-Hill, New York
- Munir R.I., Schellenberg J., Henrissat B., Verbeke T.J., Sparling R., Levin D.B. (2014) Comparative analysis of carbohydrate active enzymes in *Clostridium termitidis* CT1112 reveals complex carbohydrate degradation ability. *PLoS One* 9:e104260
- Munir R.I., Spicer V., Shamshurin D., Krokhin O.V., Wilkins J., Ramachandran U., Sparling R., Levin D.B. (2015) Quantitative proteomic analysis of the cellulolytic system of *Clostridium termitidis* CT1112 reveals distinct protein expression

profiles upon growth on α -cellulose and cellobiose. *Journal of Proteomics* 125:41-53

Munro S.A., Zinder S.H., Walker L.P. (2009) The fermentation stoichiometry of *Thermotoga neapolitana* and influence of temperature, oxygen, and pH on hydrogen production. *Biotechnol Prog* 25:1035-1042

Ngo T.A., Nguyen T.H., Bui H.T.V. (2012) Thermophilic fermentative hydrogen production from xylose by *Thermotoga neapolitana* DSM 4359. *Renewable Energy* 37:174-179

O-Thong S., Prasertsan P., Karakashev D., Angelidaki I. (2008) Thermophilic fermentative hydrogen production by the newly isolated *Thermoanaerobacterium thermosaccharolyticum* PSU-2. *Int J Hydrogen Energy* 33:1204-1214

Owen W.F., Stuckey D.C., Healy J.B., Young L.Y., Mccarty P.L. (1979) Bioassay for monitoring biochemical methane potential and anaerobic toxicity. *Water Res* 13:485-492

Pan C.M., Fan Y.T., Zhao P., Hou H.W. (2008) Fermentative hydrogen production by the newly isolated *Clostridium beijerinckii* Fanp3. *Int J Hydrogen Energy* 33:5383-5391

Pavlostathis S.G., Miller T.L., Wolin M.J. (1988) Kinetics of insoluble cellulose fermentation by continuous cultures of *Ruminococcus albus*. *Appl Environ Microbiol* 54:2660-2663

Ramachandran U., Wrana N., Cicek N., Sparling R., Levin D.B. (2008) Hydrogen production and end-product synthesis patterns by *Clostridium termitidis* strain CT1112 in batch fermentation cultures with cellobiose or α -cellulose. *Int J Hydrogen Energy* 33:7006-7012

Sabathé F., BélaïCh A., Soucaille P. (2002) Characterization of the cellulolytic complex (cellulosome) of *Clostridium acetobutylicum*. *FEMS Microbiol Lett* 217:15-22

- Shoham Y., Lamed R., Bayer E.A. (1999) The cellulosome concept as an efficient microbial strategy for the degradation of insoluble polysaccharides. LONDON: Elsevier Ltd
- Shuler M.L., Kargi F. (2002) Bioprocess engineering: basic concepts. Second ed. Prentice Hall PTR, Upper Saddle River, NJ
- Siegrist H., Rozzi A., Pavalostathis S.G., Sanders W.T.M., Keller J., Vavilin V.A., Kalyuzhnyi S.V., Angelidaki I., Batstone D.J. (2002) The IWA Anaerobic Digestion Model No 1 (ADM1). *Water Sci Technol* 45:65-73
- Taguchi F., Hang J.D., Takiguchi S., Morimoto M. (1992) Efficient hydrogen production from starch by a bacterium isolated from termites. *J Ferment Bioeng* 73:244-245
- Thauer R.K., Jungermann K., Decker K. (1977) Energy conservation in chemotrophic anaerobic bacteria. *Bacteriological Reviews* 41:100-180
- Van Niel E.W.J., Budde M.A.W., De Haas G.G., Van Der Wal F.J., Claassen P.A.M., Stams A.J.M. (2002) Distinctive properties of high hydrogen producing extreme thermophiles, *Caldicellulosiruptor saccharolyticus* and *Thermotoga elfii*. *Int J Hydrogen Energy* 27:1391-1398
- Wall J.D., Harwood C.S., Demain A.L. (2008) Bioenergy. ASM Press, Washington, D.C
- Wang A., Gao L., Ren N., Xu J., Liu C. (2009) Bio-hydrogen production from cellulose by sequential co-culture of cellulosic hydrogen bacteria of *Enterococcus gallinarum* G1 and *Ethanoigenens harbinense* B49. *Biotechnol Lett* 31:1321-1326
- Wang A.J., Ren N.Q., Shi Y.G., Lee D.J. (2008) Bioaugmented hydrogen production from microcrystalline cellulose using co-culture - *Clostridium acetobutylicum* X-9 and *Etilanoigenens harbinense* B-49. *Int J Hydrogen Energy* 33:912-917
- Xu L., Ren N., Wang X., Jia Y. (2008) Biohydrogen production by *Ethanoligenens harbinense* B49: Nutrient optimization. *Int J Hydrogen Energy* 33:6962-6967

Zhu D., Wang G., Qiao H., Cai J. (2008) Fermentative hydrogen production by the new marine *Pantoea agglomerans* isolated from the mangrove sludge. *Int J Hydrogen Energy* 33:6116-6123

Chapter 5

5 Conclusions and Recommendations

5.1 Conclusions

The following findings summarize the major outcomes of this research:

- H₂ yields of 1.99 and 1.11 mol H₂ mol⁻¹ hexose equivalent were achieved for glucose and cellobiose respectively by *Clostridium termitidis*.
- Monod microbial kinetics of *C. termitidis* on cellobiose and glucose for biohydrogen production were as follows:
 1. Maximum specific growth rates (μ_{\max}) were 0.22 and 0.24 h⁻¹ for glucose and cellobiose respectively; saturation constants (K_s) were 0.17 and 0.38 g l⁻¹ respectively and the biomass yields (Y_{X/S}) were 0.260 and 0.257 g dry weight g⁻¹ substrate.
 2. The APE for fitting the experimental biomass and substrate data were 6.7 and 8.1% for glucose and 4.2 and 8.6% for cellobiose.
 3. The RMSE for fitting the experimental biomass and substrate data were 0.025 and 0.036 g l⁻¹ for glucose and 0.02 and 0.16 g l⁻¹ for cellobiose.
- Hydrogen production and microbial kinetics of *Clostridium termitidis* in mono-culture and co-culture with *Clostridium beijerinckii* on cellulose:
 1. This study has proved the viability of co-culture of *C. termitidis* with *C. beijerinckii* for hydrogen production directly from a complex substrate like cellulose under mesophilic conditions.
 2. H₂ yield of *C. beijerinckii* only in glucose was 2.54 mol H₂ mol⁻¹ hexose.
 3. The highest hydrogen yield achieved was 2.11 mol H₂ mol⁻¹ hexose equivalent_{added} in agitated co-culture
 4. 1.46 mol H₂ mol⁻¹ hexose equivalent_{added} was achieved in agitated mono-culture.

5. Co-culture exhibited an overall 45% enhancement of hydrogen yield based on hexose equivalent added and 15% more substrate utilization.
6. Agitation did not show any significant effect on hydrogen production potential but it increased the lag phases by about 7 days.
7. The maximum specific growth rate (μ_{\max}) of *C. termitidis* with agitation on cellulose was 0.1 d^{-1} , K_x was $0.04 \text{ g COD cellulose g}^{-1} \text{ COD biomass}$ and the biomass yield ($Y_{x/s}$) was $0.3 \text{ g COD g}^{-1} \text{ COD}$, compared to 0.1 d^{-1} , $0.42 \text{ g COD cellulose g}^{-1} \text{ COD biomass}$ and $0.3 \text{ g COD g}^{-1} \text{ COD}$, respectively in non-agitated fermentation.

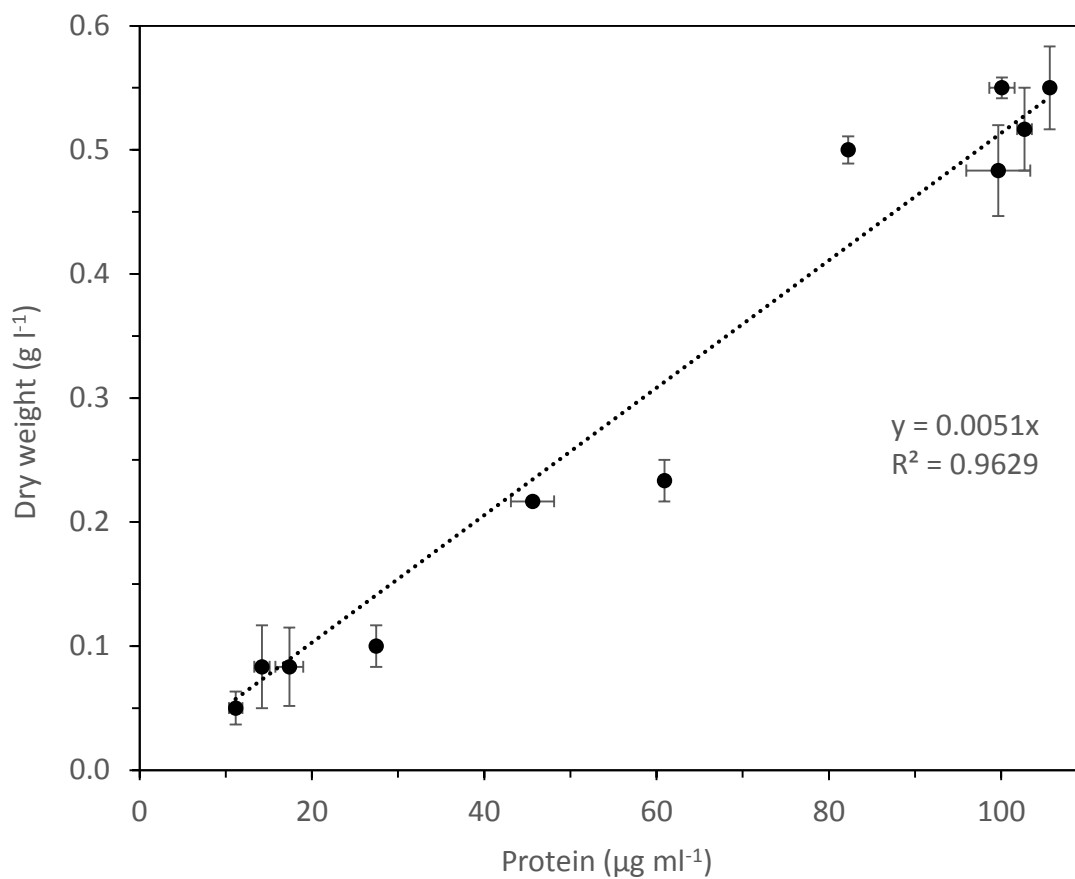
5.2 Recommendations

Based on the finding of this research, further research should address the following:

- Validate the models developed by controlling the pH or account for pH change in the modelling.
- Validate the models developed by scaling-up to fed-batch or continuous flow systems.
- Develop a mathematical model to differentiate between the hydrolysis and fermentation steps, as well as to describe the individual growth of *C. termitidis* and *C. beijerinckii* in co-cultures.
- Test real lignocellulosic wastes, such as paper waste or paper sludge as feedstocks.

Appendix A

Appendix A: Supplementary Figure 3.1 Correlation between dry weight and cellular protein content in *Clostridium termitidis*



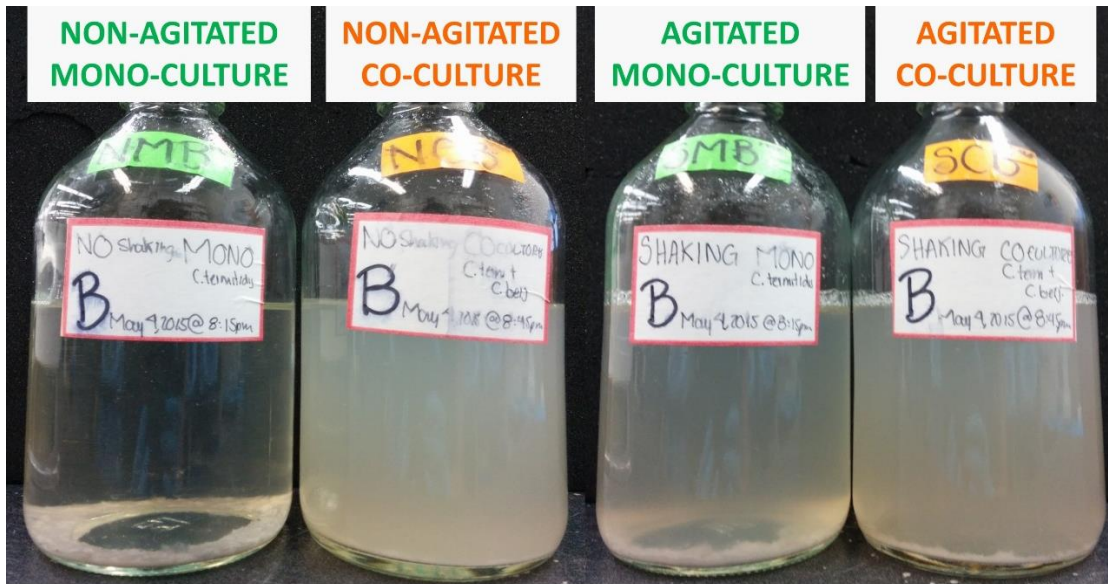
Data points are the averages of duplicates, lines above, below and to the sides represent the actual duplicates

Appendix B

Appendix B: Pictures from “Hydrogen production and Microbial Kinetics of *C. termitidis* in mono-culture and co-culture with *C. beijerinckii*” experiment (Chapter 4)



Bottles at the beginning of the experiment



Bottles almost at the end of the experiment



Different clumps exhibited by agitated bottles along the experiment

Appendix C

Appendix C: Data for duplicates and statistical analysis

Statistical analysis of duplicates were performed for all measurements in all experiments. Although the student t-test could not be used to determine statistical differences because the differences between the duplicates are not normally distributed, correlation coefficients (R^2) of the linear relationship between the two duplicates were calculated and they are shown in the last row of each table.

CHAPTER 3

Correlation between dry weight and cellular protein content in *C. termitidis*. Data shown are the mean values with the range of duplicates.

	Protein ($\mu\text{g ml}^{-1}$)	Dry weight (g l^{-1})
	11.2 \pm 0.8	0.05 \pm 0.01
	14.2 \pm 0.9	0.08 \pm 0.03
	17.4 \pm 1.6	0.08 \pm 0.03
	27.5 \pm 0.4	0.10 \pm 0.02
	45.6 \pm 2.5	0.22 \pm 0.00
	60.9 \pm 0.3	0.23 \pm 0.02
	82.3 \pm 0.1	0.50 \pm 0.01
	99.7 \pm 3.7	0.48 \pm 0.04
	100.1 \pm 1.5	0.55 \pm 0.01
	102.7 \pm 0.9	0.52 \pm 0.03
	105.6 \pm 0.5	0.55 \pm 0.03
R^2	0.9933	0.9555
Slope	0.9860	0.9362

Microbial kinetics of *C. termitidis*: dry weight, substrate, hydrogen and pH data of glucose and cellobiose experiments. Data shown are the mean values with the range of duplicates.

Glucose experiment				Cellobiose experiment				
Dry wt (g l ⁻¹)	Glucose (g l ⁻¹)	H ₂ (ml)	pH	Dry wt (g l ⁻¹)	Cellobiose (g l ⁻¹)	H ₂ (ml)	pH	
0.02±0.00	2.01±0.03	0±0	7.24±0	0.02±0.00	2.06±0.03	0.0±0.0	7.27±0.03	
0.04±0.00	1.97±0.06	5±0	7.12±0	0.02±0.00	2.04±0.02	NR	7.26±0.02	
0.09±0.00	1.80±0.05	NR	7.01±0	0.02±0.00	2.00±0.01	5±0	7.25±0.04	
0.18±0.01	1.36±0.05	NR	6.76±0	0.04±0.00	1.63±0.05	29±1	7.19±0.01	
0.28±0.01	0.70±0.01	NR	6.40±0.01	0.10±0.01	1.43±0.02	48±0	7.06±0.00	
0.44±0.01	0.15±0.01	127±2	6.03±0.02	0.25±0.01	1.00±0.07	92±0	6.68±0.02	
0.52±0.02	0.00±0.0	186±1	5.76±0.01	0.47±0.00	0.15±0.04	139±1	6.17±0.01	
0.50±0.01	0.00±0.00	225±5	5.78±0.01	0.50±0.01	0.00±0.00	139±1	6.16±0.02	
0.48±0.02	0.00±0.00	225±5	5.85±0.01	0.48±0.01	0.00±0.00	139±1	6.20±0.01	
0.45±0.02	0.00±0.00	225±5	5.85±0.01	0.46±0.01	0.00±0.00	139±1	6.16±0.00	
0.40±0.02	0.00±0.00	225±5	5.78±0.01	0.43±0.02	0.00±0.00	139±1	5.91±0.02	
R ²	0.9785	0.9993	0.9982	0.9995	0.9924	0.9964	0.9998	0.9959
Slope	0.9879	1.0481	1.0325	0.9980	0.9643	1.0241	0.9879	0.9968

NR: Not released

CHAPTER 4

Correlation between dry weight and cellular protein content in *C. beijerinckii*. Data shown are the mean values with the range of duplicates.

	Protein ($\mu\text{g ml}^{-1}$)	Dry weight (g l^{-1})
	1.8 \pm 0.3	0.03 \pm 0.01
	2.6 \pm 0.2	0.07 \pm 0.03
	4.6 \pm 0.5	0.07 \pm 0.01
	6.8 \pm 0.9	0.03 \pm 0.01
	54.1 \pm 1.3	0.30 \pm 0.04
	82.5 \pm 1.1	0.43 \pm 0.03
	88.0 \pm 0.5	0.40 \pm 0.02
	90.0 \pm 2.4	0.47 \pm 0.05
	97.3 \pm 0.7	0.40 \pm 0.00
	110.3 \pm 2.8	0.57 \pm 0.03
R ²	0.9962	0.9759
Slope	0.9898	0.8722

C. beijerinckii on glucose experiment. Data shown are the mean values with the range of duplicates.

	pH	H ₂ (ml)
	7.11 \pm 0.00	0.0 \pm 0.0
	7.13 \pm 0.01	0.0 \pm 0.0
	7.00 \pm 0.05	17.6 \pm 7.3
	6.29 \pm 0.03	245.5 \pm 14.3
	6.25 \pm 0.01	340.0 \pm 5.6
	6.18 \pm 0.00	356.9 \pm 0.8
	6.22 \pm 0.02	358.9 \pm 0.6
R ²	0.9894	0.9954
Slope	1.0032	0.9733

Cumulative hydrogen (ml) in co-culture experiment. Data shown are the mean values with the range of duplicates.

	Non-agitated		Agitated	
	Mono	Co	Mono	Co
	0±0	0±0	0±0	0.0±0
	1±0	0±0	0±0	0.1±0
	4±0	4±0	3±0	1.7±1
	7±0	6±0	4±0	5.6±0
	9±0	7±0	4±0	6.9±2
	14±1	9±0	6±1	6.9±2
	21±2	13±0	8±1	10.9±1
	24±1	17±2	11±1	15.7±2
	32±2	23±2	14±1	20.8±1
	40±1	39±1	18±2	30.2±5
	45±3	57±1	21±2	38.8±5
	57±3	111±3	27±0	55.0±9
	76±3	163±1	31±0	75.0±14
	90±0	219±7	36±1	97.3±25
	105±3	260±6	47±1	123.2±27
	124±3	283±5	65±5	160.7±33
	155±10	300±3	83±6	206.6±46
	182±2	314±6	113±11	302.3±18
	208±3	319±6	140±12	333.3±4
	226±6	324±3	184±16	345.9±1
	239±2	324±3	224±16	353.9±4
	245±2	324±3	246±16	355.9±5
	245±2	324±3	246±16	355.9±5
R ²	0.9972	0.9977	0.9961	0.9605
Slope	0.9665	1.0026	1.1449	0.9319

pH changes in co-culture experiment. Data shown are the mean values with the range of duplicates.

	Non-agitated		Agitated	
	Mono	Co	Mono	Co
	7.22±0.01	7.24±0.02	7.20±0.02	7.16±0.02
	7.19±0.02	7.12±0.01	7.19±0.00	7.13±0.01
	7.15±0.03	7.07±0.00	7.16±0.00	7.10±0.01
	7.13±0.01	7.06±0.01	7.14±0.00	7.08±0.01
	7.13±0.00	7.06±0.00	7.13±0.00	7.08±0.00
	7.13±0.00	7.06±0.01	7.13±0.00	7.08±0.00
	7.10±0.00	7.06±0.00	7.12±0.00	7.08±0.00
	7.06±0.01	7.03±0.01	7.12±0.00	7.05±0.00
	7.06±0.00	7.02±0.00	7.09±0.00	7.01±0.00
	7.05±0.00	7.02±0.02	7.07±0.02	6.99±0.00
	7.01±0.00	6.97±0.00	7.07±0.01	6.98±0.01
	6.99±0.01	6.88±0.01	7.07±0.02	6.95±0.00
	6.99±0.02	6.79±0.00	7.08±0.00	6.94±0.02
	6.95±0.01	6.60±0.01	7.07±0.00	6.91±0.03
	6.91±0.00	6.42±0.01	7.05±0.00	6.89±0.03
	6.84±0.02	6.25±0.00	6.99±0.01	6.78±0.03
	6.79±0.02	6.20±0.02	6.95±0.00	6.70±0.04
	6.72±0.00	6.18±0.01	6.93±0.00	6.57±0.12
	6.68±0.00	6.19±0.01	6.87±0.03	6.41±0.06
	6.63±0.01	6.18±0.00	6.78±0.03	6.35±0.00
	6.55±0.01	6.17±0.00	6.57±0.03	6.29±0.01
	6.36±0.00	---	6.28±0.04	6.14±0.00
	6.14±0.01	---	6.09±0.03	6.03±0.00
	6.13±0.01	---	6.09±0.03	6.03±0.00
R ²	0.9937	0.9977	0.9930	0.9768
Slope	0.9998	1.0002	0.9968	1.0044

Metabolites in non-agitated mono-culture. Data shown are the mean values with the range of duplicates.

	Lactate (g COD l ⁻¹)	Formate (g COD l ⁻¹)	Acetate (g COD l ⁻¹)	Ethanol (g COD l ⁻¹)
	0.00±0.00	0.00±0.00	0.01±0.00	0.00±0.00
	0.00±0.00	0.00±0.00	0.02±0.00	0.00±0.00
	0.00±0.00	0.00±0.00	0.02±0.00	0.00±0.00
	0.00±0.00	0.00±0.00	0.03±0.00	0.00±0.00
	0.00±0.00	0.00±0.00	0.04±0.00	0.01±0.00
	0.00±0.00	0.00±0.00	0.04±0.00	0.01±0.00
	0.00±0.00	0.00±0.00	0.04±0.00	0.01±0.00
	0.00±0.00	0.00±0.00	0.04±0.00	0.01±0.00
	0.00±0.00	0.00±0.00	0.06±0.00	0.03±0.00
	0.00±0.00	0.00±0.00	0.08±0.00	0.03±0.00
	0.00±0.00	0.00±0.00	0.09±0.00	0.03±0.01
	0.00±0.00	0.00±0.00	0.11±0.00	0.04±0.00
	0.00±0.00	0.00±0.00	0.12±0.00	0.05±0.00
	0.00±0.00	0.00±0.00	0.16±0.00	0.09±0.00
	0.00±0.00	0.00±0.00	0.19±0.00	0.11±0.00
	0.00±0.00	0.00±0.00	0.23±0.00	0.13±0.00
	0.00±0.00	0.00±0.00	0.26±0.01	0.15±0.01
	0.00±0.00	0.00±0.00	0.31±0.01	0.16±0.01
	0.00±0.00	0.00±0.00	0.40±0.00	0.20±0.00
	0.00±0.00	0.00±0.00	0.44±0.01	0.25±0.00
	0.01±0.00	0.01±0.00	0.51±0.01	0.31±0.01
	0.01±0.00	0.02±0.00	0.54±0.01	0.32±0.00
	0.02±0.00	0.03±0.00	0.66±0.00	0.38±0.00
	0.03±0.00	0.03±0.00	0.66±0.00	0.39±0.00
R ²	0.9951	0.9963	0.9983	0.9983
Slope	0.9575	1.051	0.9857	0.9938

Metabolites in non-agitated co-culture. Data shown are the mean values with the range of duplicates.

	Lactate (g COD l ⁻¹)	Formate (g COD l ⁻¹)	Acetate (g COD l ⁻¹)	Ethanol (g COD l ⁻¹)	Butyrate (g COD l ⁻¹)
	0.18±0.01	0.00±0.00	0.02±0.00	0.00±0.00	0.00±0.00
	0.17±0.01	0.00±0.00	0.02±0.00	0.00±0.00	0.00±0.01
	0.16±0.02	0.00±0.00	0.03±0.00	0.00±0.00	0.01±0.00
	0.14±0.00	0.00±0.00	0.02±0.00	0.00±0.00	0.01±0.01
	0.14±0.00	0.00±0.00	0.03±0.00	0.00±0.00	0.01±0.01
	0.14±0.00	0.00±0.00	0.03±0.00	0.00±0.00	0.02±0.01
	0.13±0.00	0.00±0.00	0.03±0.00	0.00±0.00	0.02±0.00
	0.13±0.00	0.00±0.00	0.03±0.00	0.00±0.00	0.01±0.00
	0.12±0.00	0.00±0.00	0.04±0.00	0.01±0.00	0.01±0.00
	0.12±0.00	0.00±0.00	0.06±0.00	0.02±0.00	0.03±0.00
	0.10±0.02	0.00±0.00	0.07±0.01	0.03±0.00	0.04±0.02
	0.06±0.02	0.00±0.00	0.10±0.01	0.04±0.01	0.08±0.02
	0.00±0.00	0.00±0.00	0.15±0.01	0.10±0.00	0.14±0.02
	0.00±0.00	0.03±0.00	0.27±0.01	0.22±0.00	0.22±0.00
	0.00±0.00	0.07±0.00	0.35±0.01	0.30±0.01	0.41±0.02
	0.00±0.00	0.10±0.01	0.36±0.01	0.31±0.01	0.65±0.04
	0.00±0.00	0.10±0.00	0.32±0.03	0.31±0.01	0.82±0.06
	0.00±0.00	0.10±0.00	0.31±0.04	0.30±0.01	0.96±0.05
	0.00±0.00	0.09±0.00	0.29±0.04	0.28±0.01	1.10±0.04
	0.00±0.00	0.09±0.01	0.24±0.02	0.29±0.00	1.15±0.07
	0.00±0.00	0.08±0.00	0.24±0.03	0.30±0.01	1.17±0.05
R ²	0.9522	0.9929	0.9841	0.9980	0.9971
Slope	1.0404	1.0562	1.1494	1.0601	0.9011

Metabolites in agitated mono-culture. Data shown are the mean values with the range of duplicates.

	Lactate (g COD l ⁻¹)	Formate (g COD l ⁻¹)	Acetate (g COD l ⁻¹)	Ethanol (g COD l ⁻¹)
	0.00±0.00	0.00±0.00	0.01±0.00	0.00±0.00
	0.00±0.00	0.00±0.00	0.02±0.00	0.00±0.00
	0.00±0.00	0.00±0.00	0.02±0.00	0.00±0.00
	0.00±0.00	0.00±0.00	0.03±0.00	0.00±0.00
	0.00±0.00	0.00±0.00	0.03±0.00	0.01±0.00
	0.00±0.00	0.00±0.00	0.04±0.00	0.01±0.00
	0.00±0.00	0.00±0.00	0.03±0.00	0.01±0.00
	0.00±0.00	0.00±0.00	0.03±0.00	0.01±0.00
	0.00±0.00	0.00±0.00	0.04±0.00	0.01±0.00
	0.00±0.00	0.00±0.00	0.06±0.00	0.02±0.00
	0.00±0.00	0.00±0.00	0.06±0.00	0.02±0.00
	0.00±0.00	0.00±0.00	0.07±0.00	0.02±0.01
	0.00±0.00	0.00±0.00	0.07±0.00	0.02±0.00
	0.00±0.00	0.00±0.00	0.09±0.00	0.04±0.00
	0.00±0.00	0.00±0.00	0.09±0.00	0.04±0.00
	0.00±0.00	0.00±0.00	0.11±0.00	0.05±0.00
	0.00±0.00	0.00±0.00	0.13±0.00	0.06±0.00
	0.00±0.00	0.00±0.00	0.22±0.02	0.08±0.01
	0.00±0.00	0.00±0.00	0.26±0.02	0.12±0.01
	0.00±0.00	0.00±0.00	0.28±0.02	0.14±0.01
	0.01±0.01	0.01±0.01	0.45±0.04	0.25±0.03
	0.02±0.01	0.02±0.01	0.54±0.02	0.29±0.02
	0.04±0.01	0.04±0.01	0.65±0.02	0.36±0.02
	0.04±0.01	0.04±0.01	0.65±0.02	0.37±0.02
R ²	0.9821	0.9224	0.9966	0.9965
Slope	0.5047	0.4835	0.9041	0.8764

Metabolites in agitated co-culture. Data shown are the mean values with the range of duplicates.

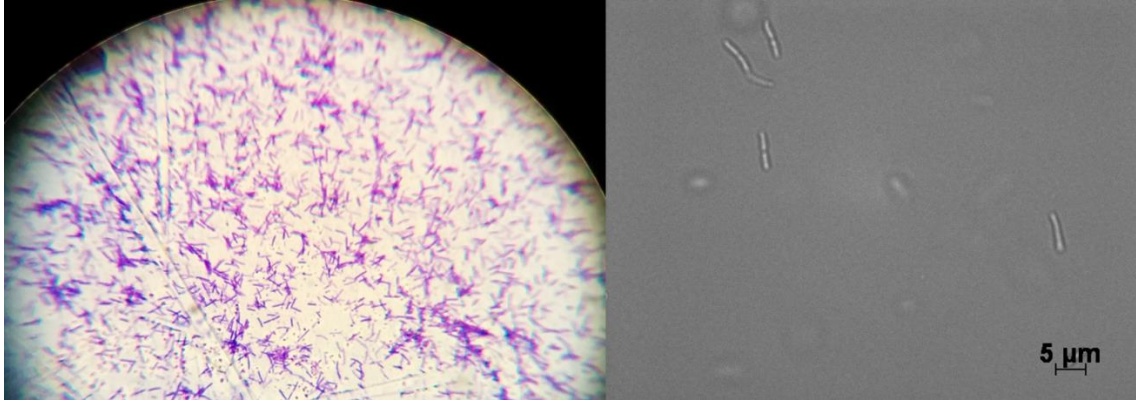
	Lactate (g COD l ⁻¹)	Formate (g COD l ⁻¹)	Acetate (g COD l ⁻¹)	Ethanol (g COD l ⁻¹)	Butyrate (g COD l ⁻¹)
	0.18±0.00	0.00±0.00	0.01±0.00	0.00±0.00	0.00±0.00
	0.16±0.00	0.00±0.00	0.02±0.00	0.00±0.00	0.00±0.00
	0.15±0.00	0.00±0.00	0.03±0.00	0.00±0.00	0.00±0.00
	0.15±0.00	0.00±0.00	0.03±0.00	0.00±0.00	0.00±0.00
	0.15±0.00	0.00±0.00	0.04±0.00	0.00±0.00	0.00±0.00
	0.16±0.01	0.00±0.00	0.05±0.00	0.00±0.00	0.01±0.00
	0.14±0.00	0.00±0.00	0.04±0.00	0.00±0.00	0.01±0.00
	0.14±0.01	0.00±0.00	0.04±0.00	0.00±0.00	0.01±0.01
	0.13 ±0.01	0.00±0.00	0.05±0.00	0.01±0.00	0.01±0.01
	0.13±0.01	0.00±0.00	0.06±0.01	0.01±0.00	0.02±0.02
	0.12±0.02	0.00±0.00	0.07±0.01	0.02±0.00	0.04±0.02
	0.09±0.01	0.00±0.00	0.08±0.01	0.02±0.01	0.06±0.01
	0.07±0.00	0.00±0.00	0.11±0.01	0.04±0.01	0.07±0.00
	0.03±0.03	0.00±0.00	0.11±0.00	0.06±0.01	0.15±0.05
	0.02±0.02	0.00±0.00	0.11±0.01	0.06±0.01	0.19±0.07
	0.02±0.02	0.00±0.00	0.15±0.00	0.08±0.01	0.21±0.07
	0.00±0.00	0.00±0.00	0.20±0.03	0.11±0.02	0.22±0.05
	0.00±0.00	0.00±0.00	0.30±0.09	0.14±0.04	0.23±0.03
	0.00±0.00	0.02±0.00	0.56±0.03	0.24±0.02	0.31±0.06
	0.00±0.00	0.02±0.00	0.56±0.03	0.27±0.00	0.42±0.11
	0.00±0.00	0.02±0.00	0.52±0.03	0.27±0.00	0.56±0.07
	0.00±0.00	0.02±0.00	0.50±0.02	0.26±0.01	0.63±0.07
	0.00±0.00	0.02±0.00	0.48±0.01	0.26±0.00	0.73±0.04
	0.00±0.00	0.02±0.00	0.47±0.01	0.26±0.00	0.74±0.04
R ²	0.9056	0.9283	0.9445	0.9695	0.9500
Slope	0.9752	1.2362	0.9864	0.9138	0.7774

Biomass and cellulose in agitated cultures. Data shown are the mean values with the range of duplicates.

	Biomass (g COD l ⁻¹)		Cellulose (g COD l ⁻¹)	
	Mono	Co	Mono	Co
	0.01±0.00	0.02±0.00	2.55±0.01	2.55±0.04
	0.01±0.00	0.02±0.00	2.55±0.03	2.55±0.02
	0.01±0.00	0.02±0.01	2.49±0.03	2.58±0.03
	0.02±0.01	0.02±0.01	2.55±0.04	2.55±0.07
	0.02±0.01	0.03±0.00	2.55±0.01	2.55±0.05
	0.03±0.01	0.04±0.01	2.48±0.06	2.55±0.06
	0.03±0.01	0.05±0.00	2.48±0.05	2.49±0.05
	0.04±0.01	0.05±0.00	2.53±0.00	2.51±0.02
	0.04±0.01	0.05±0.02	2.48±0.04	2.49±0.06
	0.05±0.01	0.06±0.00	2.43±0.06	2.45±0.07
	0.06±0.01	0.10±0.01	2.44±0.01	2.37±0.03
	0.06±0.00	0.14±0.01	2.42±0.07	2.31±0.02
	0.07±0.01	0.17±0.02	2.40±0.05	2.21±0.06
	0.08±0.01	0.20±0.02	2.34±0.06	2.11±0.08
	0.09±0.01	0.23±0.01	2.30±0.06	2.00±0.08
	0.12±0.01	0.27±0.03	2.22±0.08	1.87±0.11
	0.15±0.01	0.32±0.04	2.14±0.07	1.61±0.11
	0.22±0.05	0.41±0.05	1.96±0.12	1.28±0.12
	0.30±0.04	0.55±0.03	1.78±0.09	0.69±0.11
	0.40±0.04	0.65±0.00	1.55±0.05	0.41±0.07
	0.51±0.02	0.65±0.01	1.04±0.09	0.29±0.09
	0.60±0.05	0.64±0.00	0.78±0.09	0.25±0.07
	0.66±0.02	0.64±0.01	0.57±0.05	0.20±0.05
	0.66±0.02	0.64±0.01	0.48±0.03	0.17±0.03
R ²	0.9797	0.9785	0.9880	0.9903
Slope	1.0962	0.9636	0.9577	0.9495

Appendix D

Appendix D: *C. termitidis* on cellobiose under Optical and Electronic Microscopy.



Curriculum Vitae

Name: Maritza Gomez-Flores

Post-secondary Education and Degrees: Benemerita Universidad Autonoma de Puebla
Puebla, Puebla, Mexico
2006-2011 B.Sc.

The University of Western Ontario
London, Ontario, Canada
2013-2015 M.E.Sc.

Honours and Awards: Scholarship recipient
Consejo Nacional de Ciencia y Tecnologia de Mexico (CONACyT) and Alianza para la Formacion e investigacion en Infraestructura para el Desarrollo de Mexico
2013-2015

Credentials: Leadership in Energy and Environmental Design (LEED) Green Associate
Green Building Certification Institute
2014 - Present

Related Work Experience

Environmental Engineer, Intern
State Commission of Water and Sanitation of Puebla
2011-2012

Health, Safety and Environment, Trainee
Faurecia Interior Systems
2012-2013

Research Assistant
The University of Western Ontario
2013-2015

Publications:

- Gomez-Flores M.**, Nakhla G., Hafez H. (2015) Microbial kinetics of *Clostridium termitidis* on cellobiose and glucose for biohydrogen production. *Biotechnol Lett*:1-7
- Gupta M., **Gomez-Flores M.**, Nasr N., Elbeshbishy E., Hafez H., Hesham El Naggar M., Nakhla G. (2015) Performance of mesophilic biohydrogen-producing cultures at thermophilic conditions. *Bioresour Technol* 192:741